Effects of Aneuploidy on Growth And Cell Cycle Progression

by

Christian Gonzalez Rubio

B.S. Chemistry
City College of New York, 2003

SUBMITTED TO THE DEPARTMENT OF BIOLOGY IN PARTIAL FULFILLMENT OF THE REQUIREMENTS FOR THE DEGREE OF

DOCTOR OF PHILOSOPHY IN BIOLOGY
AT THE
MASSACHUSETTS INSTITUTE OF TECHNOLOGY

APRIL 2010
[JUNE 2010]

Signature of the Author: _____
Department of Biology
30 April 2010

Certified by: _____
Angelika Amon
Professor of Biology
Thesis Supervisor

Accepted by: _____
Stephen P. Bell
Professor of Biology
Chair, Committee for Graduate Students

Effects of Aneuploidy on Growth And Cell Cycle Progression

by

Christian Gonzalez Rubio

Submitted to the Department of Biology
On April 30, 2010 in Partial Fulfillment of the
Requirements for the Degree of Doctor of Philosophy in Biology

ABSTRACT

In budding yeast, aneuploidy has a detrimental effect in cell growth and proliferation. The work presented here shows that most aneuploid yeast strains delay cell cycle entry by increasing the critical size for budding and by decreasing the rate of volume accumulation during the G1 phase of the cell cycle. This increase in the critical size for budding is due to in a delay in CLN2 mRNA accumulation and can be suppressed by supplying cells with high levels of this cyclin. Deletion of the cell cycle entry inhibitor *WHI5* only partially suppressed the G1 delay of aneuploid cells. These two results combined point to the possibility that aneuploidy might be interfering through a parallel pathway with the activation of the transcription factors Swi4 and Swi6. The growth defect seen in aneuploid cells is not due to gross defects in the translational machinery or lack of nutrients. Instead, yeast cells respond to aneuploidy by altering the translational efficiency of a number of genes. The results presented here indicate that aneuploidy affects entry into the cell cycle in at least two ways. The condition elicits a growth defect during the G1 phase of the cell cycle and increases the critical size for budding.

Thesis Supervisor: Angelika Amon
Title: Professor of Biology

Dedicated to Alexander Rosenzweig and Crystal Suri, two of the most wonderful people that I have ever met.

Y a mis padres, siempre.

Acknowledgements:

I would like to thank Angelika for all of her support, advice, and encouragement during my graduate career. Advisors like her are very difficult to find.

I would also like to thank the members of my thesis committee meeting. Thank you to Steve Bell and Jackie Lees for all of their insightful suggestions. Thank you to Wendy Gilbert and Frederick Cross for joining my committee prior to my defense.

I would also like to thank all the member of the Amon Lab – past and present - for making the lab such a wonderful place to work.

The work presented here would not have been made possible without the never ending support of my family.

And I have to thank all my dear friends – you know who you are!

Table of Contents

Chapter 1: Introduction

Every time a cell divides it must accurately duplicate its genome and partition it evenly between the daughter cells. Cells have evolved mechanisms to ensure that this happens properly. However, once in a while these mechanisms fail. As a result, one cell ends up losing a chromosome while the other one gains at least a full chromosome: it becomes aneuploid. Aneuploidy is characterized by an uneven number of chromosomes – uneven being "a number that is not the exact multiple of the haploid karyotype (Torres et al., 2008)." The cell that has lost a chromosome content usually dies, but what happens to the cell that has survived and now become aneuploid? The work presented here explores some of the consequences of being aneuploid. While all of the experiments in this thesis were carried out using the yeast *Saccharomyces cerevisiae*, the conclusions reached can be extended to higher organisms.

As the work presented in this thesis will show, aneuploidy has a profound effect on cell proliferation. More specifically, aneuploidy interferes with growth and cell cycle progression during the G1 phase of the cell cycle. This chapter is divided into two main parts. The first part is a general introduction to aneuploidy: its definition, causes and developmental consequences. The second part is an overview of cell cycle progression and growth in yeast focusing on the G1 phase of the cell cycle. Finally, the effects that aneuploidy has specifically on growth and cell cycle progression are briefly discussed and further developed in Chapter 2.

I. Whole Chromosome Aneuploidy.

Aneuploidy is a condition characterized by having an unbalanced number of chromosomes (reviewed in Torres et al. 2008). The first systematic analysis of this condition was carried out by Theodor Boveri using sea urchin embryos that had been fertilized by two sperms and resulted in a tripolar mitosis and hence in aneuploid cells. The aneuploid embryos that resulted from this faulty fertilization had many developmental problems and died. This led Boveri to conclude that being aneuploid leads to abnormal development and in some cases lethality. Similar observations have been made in fruit flies, mice, yeast, and humans.

Origins of aneuploidy

Whole chromosome aneuploidy in yeast and in mammalian cells is often caused by errors in chromosome segregation during mitosis. Holland and Cleveland (2005) propose several causes for these segregation errors:

1. Weak mitotic checkpoint:

   The mitotic checkpoint is the major regulatory mechanism that prevents chromosome missegregation during mitosis (Rieder et al. 1995). This checkpoint delays progression into anaphase in response to a single unattached kinetochore. If checkpoint signaling is weakened, cells will initiate

anaphase before all of the chromosomes have been properly attached to the spindle thus leading to aberrant segregation.

2. Defects in chromosome cohesion or spindle attachment:

Data from studies of aneuploid colorectal cancers indicate that defects in the machinery that controls sister chromatid cohesion might promote aneuploidy. Overexpression of separase or securin, two proteins essential for sister chromatid separation, leads to aneuploidy in mammalian cells.

Chromosome missegregation also arises from faulty chromosome-microtubule attachment during mitosis. For proper chromosome segregation, microtubules from each of the opposing spindle poles must attach to kinetochores on opposite sides of the sister chromatids and create tension. On occasion, two microtubules emanating from the same spindle pole attach to a pair of sister chromatids leading to what is called a merotelic attachment. If this faulty attachment persist during anaphase then aneuploid cells are formed.

3. Assembly of multipolar mitotic spindles:

If a mammalian cell containing multiple centrosomes enters mitosis it can form multiple spindles. If a multipolar anaphase occurs, it will result in aneuploid daughter cells. Cells acquire multiple centrosomes by several

mechanisms including centrosome overduplication, cell fusion, or an abortive mitosis.

Polyploidization is another mechanism that has been proposed to lead to aneuploidy. No cytokinesis leading to a tetraploid cell might be a very common way in which a cell, and specifically a tumor cell, acquires extra chromosomes (Storchova and Pellman 2004). This has led to the proposal that aneuploidy develops from a tetraploidization event leading to subsequent aberrant division.

Aneuploidy and disease

The aneuploid state is intimately linked with human disease. Theodor Boveri was the first scientist to postulate a connection between aneuploidy and tumor formation. He proposed that some aneuploid cells could proliferate better than wild type cells and lead to abnormal growth. Today we know that many solid tumors are aneuploid (Storchova and Kuffer 2008). Aneuploidy is also the cause of several developmental syndromes. Down syndrome (trisomy 21), Patau's syndrome (trisomy 13), and Edward's syndrome (trisomy 18) are caused by the presence of extra chromosomes.

Aneuploidy and cancer

Aneuploidy is a hallmark of cancer – most solid tumors are aneuploid (Rajagopalan and Lengauer 2004). Whether aneuploidy is a cause or a consequence of cancer is a very heavily debated issue. There are two views of cancer causation: the genetic view and the chromosomal view.

In 1971 in a paper published by Knudson, retinoblastoma was postulated to be a cancer caused by two mutational events (Knudson 1971). He concluded that this cancer could be inherited and formulated the "two-hit theory" to explain this disease. He also explained that there are two forms of the disease: one dominantly inherited form with one mutation inherited and the second occurring in somatic cells, and a nonhereditary form where both mutations occur in somatic cells. Today we refer to the Rb (retinoblastoma) gene as a tumor suppressor gene whose normal function is to repress G1-S phase genes. Loss of the retinoblastoma protein in a cell leads to aberrant cell cycle progression and eventually to cancer.

Cancer is thought to be a disease caused by mutations in genes involved in cell cycle progression as well as growth (Sherr, 2004). These genes are called proto-oncogenes if, when mutated, they promote tumorigenesis or tumor suppressors if, when mutated, they lead to unregulated proliferation, as in the case of Rb. In most cases cancer-promoting mutations arise in somatic cells spontaneously as a consequence of faulty

DNA replication or the effect of environmental factors such as exposure to ultraviolet radiation. Once a tumor starts evolving, it can acquire genetic instability: an increase in the rate at which genes are mutated and chromosomes are gained, lost or rearranged (Rajagopalan et al., 2003). This leads to disease progression.

The alternate view of tumor formation is based on the observation that many cancers are aneuploid. As already mentioned, in 1902 Boveri proposed that aneuploid cells produced from defective mitosis lead to tumor formation. The idea is that a chromosome missegregation event leads to aneuploid cells that now have genetic imbalances that make them prone to tumor formation. This idea has been tested in mice extensively. Indeed, aneuploidy caused by weakening the mitotic checkpoint by reducing its components Mad2, Bub3 or Bub1 has been linked to tumorigenesis (Rao et al., 2004). Weaver et al. (2006) used mice with reduced levels of the kinetochore -linked motor protein CENP-E , involved in maintaining the interactions between chromosomes and the microtubules of the mitotic spindle, to show that aneuploidy drives an elevated level of spontaneous lymphomas and lung tumors in old animals. In a more recent study, Li et al (2009) generated mice carrying a Cdc20 allele with three residues important for the interaction with Mad2 were mutated to alanine. This mutation renders the spindle checkpoint dysfunctional as Mad2 is unable to bind Cdc20 and prevent APC^{cdc20} activity. They found that mice heterozygous for this mutation developed spontaneous tumors at very fast rates. This mutation decreased spindle checkpoint activity thus increasing the degree of chromosomal instability leading to aneuploidy and eventually cancer.

Despite studies like the ones described above, the role of aneuploidy in driving tumorigenesis is still not clear. Additional studies have shown that in fact aneuploidy can prevent tumorigenesis. Jeganathan et al. (2007) showed that while a reduction of Bub1 levels can increase chromosome missegregation it can also reduce the incidence of spontaneous liver tumors in mice. In another study Rao et al. (2005) showed that reduction of BubR1 suppresses tumor formation in the small intestine of mice. More recently, work by Williams et al. (2008) demonstrated that trisomic mouse cells had decreased rates of proliferation as well as increased cell size and metabolic rates. This work is consistent with the view that having an abnormal number of chromosomes is initially disadvantageous for a cell and does not bring about an instantaneous ability to become tumorigenic.

It is clear that the role of aneuploidy in tumorigenesis is very complex. It is not yet known whether aneuploidy is a cause or a consequence of tumor formation. It is possible that mutations in tumor suppressor genes and proto-oncogenes lead to abnormal growth and increased genomic instability which in turn leads to chromosome missegregation events and aneuploid cells. On the other hands, the possibility exists that errors in mitosis lead to aneuploid cells and that this aneuploid state contributes to tumorigenesis by unbalancing genes requires for proper growth and development.

Aneuploidy and developmental syndromes in humans

Down syndrome, or trisomy 21, is probably the best known of human developmental syndromes caused by aneuploidy. It is also the only one that does not lead to early death (reviewed in Dierssen et al., 2009). The aneuploidy present in Down Syndrome results as an error in chromosome segregation during meiosis. Down syndrome causes many physiological and cognitive alterations whose exact genetic mechanisms have not been elucidated. This specific type of aneuploidy presents with many brain development phenotypes that lead to problems in language development and learning, among others. Trisomy 21 affects brain and central nervous system development in humans.

Aneuploidy in yeast

Yeast is an excellent model organism to study the effects of aneuploidy on cell physiology and division. Some of the earliest studies were carried out by Campbell et al. (1975) in *S. cerevisiae* and used triploids to recover aneuploids of composition n+1 from meiotic segregants. Newer methods have used aborted matings to create stable aneuploids (Torres et al. 2007). Niwa et al. (2006) also used triploid meiosis to generate aneuploids in *S. pombe*.

Torres et al. (2007) generated a collection of haploid yeasts harboring one extra copy of almost all the yeast chromosomes. The results of this study show that aneuploidy causes a transcriptional response. In other words, these aneuploid cells not only had increased levels of mRNA produced from the extra chromosome but also showed an increase in the transcription of genes involved in the environmental stress response (ESR). These strains also showed a G1 delay when released from α-factor arrest, and greater sensitivity to protein synthesis inhibitors and high temperature. Torres et al. (2007) also showed that these phenotypes are due to the presence of additional copies of yeast genes and not due to the presence of additional DNA in the nucleus. This study showed that aneuploidy actually causes a proliferative disadvantage in *S. cerevisiase*.

In a similar study, Niwa et al. (2006) showed that aneuploidy also has a negative impact on the proliferative capacity of *S. pombe* cells. They showed that all types of aneuploidies except for chromosome 3 are unstable. They also showed that aneuploid *S. pombe* strains grow more slowly than haploid.

II. Cell cycle entry in yeast

The G1 to S transition in yeast

The major cell cycle transition where the decision to enter the cell cycle is made is called START (Hartwell et al., 1974). START has also been defined as the point at which a yeast cell acquires resistance to mating pheromone, a secreted factor that arrests

cells at the beginning of the cell cycle (Hereford et al., 1974). It is also the stage at which cell growth and division are coupled (Singer and Johnston, 1981). If conditions are not ideal for cell cycle entry and progression, cells arrest at this point. Past this point, cells are irreversibly committed to finishing the cell cycle.

The series of molecular events that lead to cell cycle entry has been well characterized in yeast. External factors such as size and nutritional status activate the cyclin-dependent kinase Cln3 bound to Cdc28 which then phosphorylates Whi5, a transcription inhibitor, leading to activation of the transcription factors Swi4 and Swi6 and transcription of the cyclin-dependent kinases *CLN1* and *CLN2*, which drive entry into S phase (Figure 1).

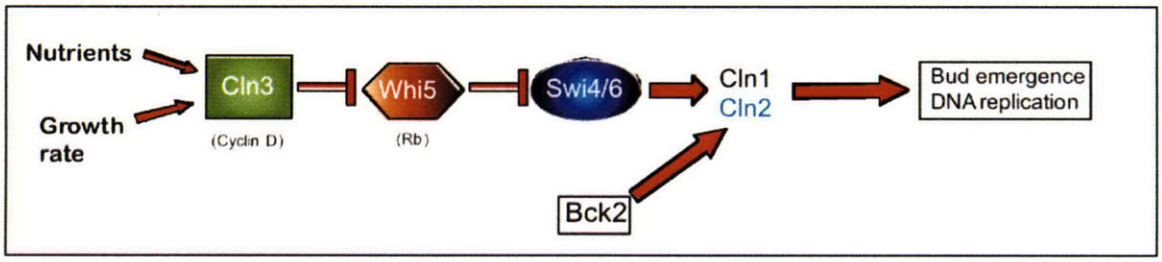

Figure 1: Molecular events that lead to the G1 to S transition in yeast.

Signals such as nutritional status and cell size are thought to activate the Cln3-Cdc28 complex. Whi5 then gets phosphorylated and Swi4/Swi6 repression is relieved. The cyclins encoded by the *CLN1* and *CLN2* genes then get transcribed and translated and cells enter the cell cycle.

Cln3, as the first cyclin to activate Cdc28 during the G1 phase of the cell cycle, plays a very important role in progression through START and cell cycle entry (Wijnen

et al., 2002). It is thought that several factors such as size, nutritional status, and growth rate affect activation of the Cln3-Cdc28 complex. As already mentioned, once active, this complex phosphorylates and inactivated the G1-S inhibitor Whi5 (Costanzo et al., 2004 and de Bruin et al., 2004). Consistent with a role in G1-S promotion, deletion of *CLN3* leads to a delayed cell cycle entry.

Whi5 is the yeast equivalent of the metazoan retinoblastoma tumor suppressor protein (Rb) (Costanzo et al., 2004 and de Bruin et al., 2004). Its discovery explained how Cln3-Cdc28 activity is able to activate Swi4/Swi6-dependent transcription (SBF-dependent transcription). Whi5 physically associates with Swi4 and Swi6. Costanzo et al. (2004) immunoprecipitated Whi5 and used tandem mass spectrometry to identify proteins that bound to it. They found that Swi4 and Swi6 co-immunoprecipitated with Whi5. Whi5 also shows a cell cycle regulated nuclear localization: upon its phosphorylation, it exits the nucleus. However, nuclear exit is not a requirement for its inactivation given that an allele that lacks all six C-terminal CDK sites does not disrupt cell cycle kinetics but is unable to localize to the cytoplasm.

Once Whi5 is phosphorylated and exits the nucleus, Swi4 and Swi6 drive G1 progression. Many of the genes that are activated at START have multiple binding sites for SBF in their promoters (Spellman et al., 1998). Swi4 is transcribed in a cell cycle-specific manner whereas Swi6 shows a different pattern of regulation (Sidorova et al., 1995). Swi6 enter the nucleus late in M phase and remains there throughout G1. The

localization of Swi6 is regulated by phosphorylation. This phosphorylation, however, is not required for activation or repression of Swi6-regulated genes. For a long time it remained a mystery how these two transcription factors were activated. The characterization of Whi5 answered this question.

The identification and characterization of Whi5 was very important because it explained for the first time how activation of Cln3 can lead to cell cycle entry. Whi5 is essentially an inhibitor of G1-specific transcription. Accordingly, its overexpression delays cell cycle entry whereas its deletion accelerates cell cycle entry. Deletion of *CLN3* leads to a delay in cell cycle entry (Cross, 1988). Surprisingly, deletion of both *CLN3* and *WHI5* leads to accelerated cell cycle entry (like a *whi5*Δ single mutant) showing that *WHI5* functions downstream of *CLN3*. Thus, deletion of *WHI5* abolishes the need for *CLN3*-dependent activation of SBF-regulated genes.

Once Cln3 is activated and Whi5 is inhibited, Swi4/Swi6 activates transcription of the cyclins *CLN1* and *CLN2*. The major role of these two cyclins is to trigger the activation of the S-phase cyclins by promoting the destruction of Sic1 (Verma et al., 1997). Sic1 is an inhibitor S-phase CDKs. During late G1, and with the increase of Cln1 and Cln2-CDK activity, Sic1 is phosphorylated on multiple sites and is targeted for degradation and S phase entry (Nash et al., 2001). Another important event that takes place in late G1 and is driven by Cln1 and Cln2 is the inactivation of the ubiquitin-protein ligase APC^{Cdh1} involved in protein degradation (Amon et al., 1994). This prevents CLB cyclins from accumulating before CLN cyclins (Huang et al., 2001).

There is another pathway that can lead to cell cycle entry that acts in parallel to *CLN3*. *BCK2* was isolated as a suppressor of *cln* deficiency (Epstein and Cross. 1994). Deletion of *BCK2* leads to large cells and a delay in SBF transcription. Deletion of both *CLN3* and *BCK2* is lethal resulting in a G1 arrest. This arrest can be rescued by overexpression of *CLN2* (Wijnen and Futcher, 1999). It seems then that Bck2, like Cln3, can activate SBF-dependent genes. However, di Como et al. (1995) showed that Bck2 is also able to activate SBF-target genes in the absence of Swi4 and Swi6 suggesting that Bck2 might also act through other promoter-bound proteins. *BCK2* is thus the key player in a pathway that is parallel to the *CLN3*, *CLN2*, *CLN1* pathway and important for cell cycle entry and critical size setting.

Cell Size Control in Yeast.

Growing cells must carefully regulate their size. Any defects in this regulation can lead to cells with abnormally large or small sizes. It is thought that there are two ways in which a cell can regulate its size. Either a cell divides before reaching a certain size, at the critical size, which is postulated to be measured by some sort of sizer. Alternatively cell growth and proliferation are regulated independently and the size at budding is simply the net result of this coordination (Rupes, 2002). This later view is not as popular or widely accepted as the former.

Many studies have shown that yeast cells must reach a critical size before entering the cell cycle. Johnston (1977) restricted nutrients in yeast cells and showed that cells that had initiated the cell cycle were able to complete it but that their daughters arrested in G1. He also showed that these daughter cells, once supplied with nutrients, were not able to reenter the cell cycle until reaching a specific size. The machinery that controls the critical size includes the G1 cyclins Cln1, Cln2, and Cln3. In other words, the sizer or any other property that determines cell size, has to somehow communicate this to the cyclins which then initiate cell cycle entry. Overexpression of any of the cyclins Cln3, Cln2 or Cln1, leads to small size phenotypes, whereas deletion of any of them leads to abnormally large sizes (Tyers et al., 1993 and Jorgensen and Tyers, 2004). In addition, deletion of *WHI5* also leads to premature cell cycle entry as cells bud at a much smaller volume. Independent of the reasons behind it, any signal that interferes with the timely execution of the G1 cyclin cascade results in an abnormal cell size – an altered critical size.

The critical size is defined as the minimum volume that a yeast cell must reach before it enters the cell cycle (Hartwell and Unger, 1977). The critical size is not necessarily a fixed volume but can change depending on many factors. For instance, ploidy has a great effect on cell volume (Murray et al., 1977). In general, the greater the DNA content, the greater the critical size for budding. Johnston et al. (1979) showed that the cell volume at bud initiation varied with the cell's growth rate as well. Indeed, growth rate is perhaps one of the most important factors that controls the critical size. In general, cells that grow slowly bud at smaller volumes than cells that grow faster (Rupes, 2002).

For instance, cells grown in raffinose are much smaller than cells grown in glucose and their doubling time is much higher. However, it is important to note that these cells grown in raffinose have a lengthened G1 – in other words, they spend a longer amount of time or a longer fraction of their cell cycle at that stage (Figure 2). They, however, accelerate cell cycle entry when compared to cells grown in glucose in that they bud at a much smaller volume.

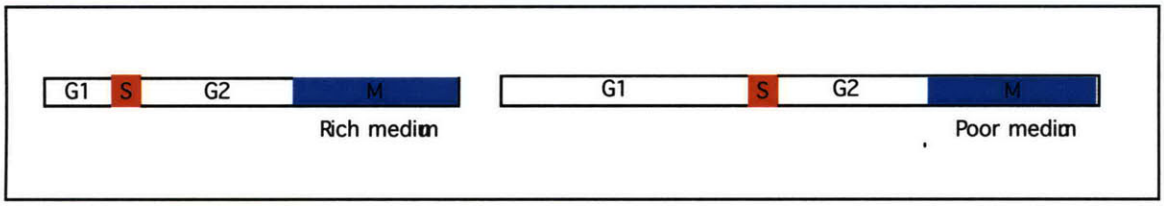

Figure 2: Carbon source affects the cell cycle.

The nature of the carbon source in which a cell grows has a profound effect on cell cycle entry and doubling time. Cells grown in a rich carbon source such as glucose have a relatively short G1 period and a shorter doubling time. On the other hand, cells grown in a poor carbon source such as raffinose have a longer doubling time and spend more time in G1.

The abundance of Cln1 and Cln2 mRNA and proteins increases as cells grow during G1 (Dirick et al., 1995). However, because these mRNAs and proteins are unstable, their abundance is in equilibrium with their rate of synthesis (Scheneider et al., 1998). This fact, however, poses a problem for slow growing cells since these cells will never be able to attain the same level of Clns than faster growing cells. In other words, if a certain level of Cln activity is required for entry into the cell cycle, slow growing cells will have a much harder time reaching this level. How can a slow growing cell then proceed through START? The answer is that slow growing cells lower the threshold level of cyclin-CDK activity required for START (Figure 3). Schneider et al. (2004) showed

that Cln1 and Cln2 protein levels are regulated by the rate of growth in that slow growing cells express less Cln1 and Cln2. These cells enter the cell cycle at a smaller volume because they are able to lower the threshold of cylin activity required for cell cycle entry.

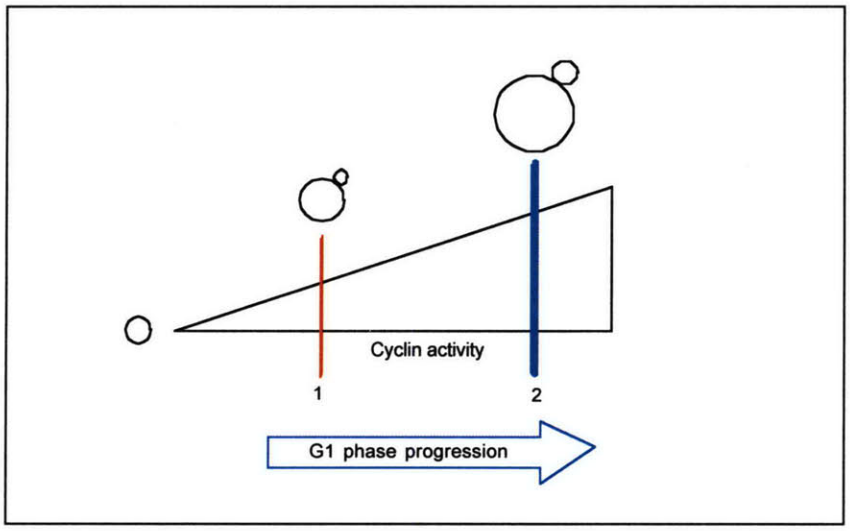

Figure 3 : Variability of the cyclin-CDK activity threshold required for Start.

Cell cycle entry requires a specific level of cyclin activity. When cells grow in a poor carbon source they enter the cell cycle at a smaller size indicating that they have lowered their threshold for G1 cyclin activity (1). Cells grown in a good carbon source have a much higher threshold for cell cycle entry and can grow to a much larger size (2).

Exactly how carbon source controls cell size is not known. Cells grown in glucose are larger than cells grown in any other carbon source. They also grow faster thus decreasing their doubling time. A number of studies have shown that the cAMP pathway regulates cell size. Glucose activates the Ras-cAMP pathway to cause increased cAMP

production. Two components of this pathway, *CDC25* and *CYR1*, when inactivated produce a phenotype closely resembling nutrient-starved G1 arrested cells (Hall et al., 1998). Also, when glucose is added to a culture grown in raffinose, the cells transiently delay cell cycle progression and increase in size before budding (Flick et al., 1998). Tokiwa et al. (1994) showed that addition of glucose to a slow growing culture causes a severe but temporary drop in *CLN1* mRNA and protein levels. Similarly, Flick et al. (1998) showed that the glucose-associated delay in cell cycle entry is associated specifically with transcriptional repression of *CLN1*. Interestingly, these two groups were not able to detect any changes in *CLN2* expression upon glucose addition. Hall et al (1998) also showed that glucose and cAMP can regulate Cln3-Cdc28 kinase activity. They found that Cln3 protein levels were highest in glucose and lower in glycerol and ethanol. This is consistent with their observation that Cln3 protein levels were much higher in cells growing in medium containing cAMP than cells without cAMP.

There is another way in which Cln3 regulation can affect cell size. Wang et al. (2004) have proposed a mechanism involving the spatial regulation of the Cln3-Cdc28 complex. They showed that Whi3 regulates the localization of Cdc28 in the cell as *whi3*Δ cells show higher nuclear concentrations of Cdc28 and are smaller. Also, overexpression of Whi3 causes Cdc28 to be excluded from the nucleus. They also show that both Cln3 and Cdc28 accumulate in the nucleus in late G1 in a regulated manner that shows a requirement for Whi3. Another study shows that Cln3 associates to the endoplasmic reticulum through Whi3 (Colomina et al., 2008).

Cell growth.

When cells divide, they must grow and double their size and biomass. The bulk of cell growth involves protein synthesis. Nutritional status also affects translational status and growth capacity. The key to understanding cell growth and its regulation is to understand how cells respond to nutrients or stresses and how this affects the translation machinery. Three important networks are involved in this regulation: the TOR network, the Ras/PKA network, and *GCN4*.

Yeast has two different TOR genes, *TOR1* and *TOR2*, whose proteins promote growth (reviewed in Zaman et al. 2008). Both proteins encoded by these genes play a very important role in translation initiation and also in cell cycle progression in response to nutrients (Barbet et al. 1996). Tor1 and Tor2 are protein kinases that together with five other proteins compromise the TORC1 and TORC2 complexes. TORC1, but not TORC2, is inhibited by the macrolide drug rapamycin. This inhibition mimics the effects of nitrogen deprivation on transcription, development and metabolism. TORC1 directly phosphorylates the essential protein Tap42 to promote its binding to the catalytic subunit of the Ser/Thr protein phosphatase 2A (PP2A) and PP2A-like phosphatases. Tap42 in its phosphorylated form inhibits PP2A activity to promote growth. TORC1 also has other targets. Urban et al. (2007) showed that TORC1 directly regulates Sch9, a protein kinase necessary for ribosome biogenesis, by phosphorylating it. Furthermore, loss of TOR function in yeast leads to a decrease in translation initiation. Treatment with rapamycin

results in eIF4G degradation (Berset et al., 1998). This initiation factor interacts with eIF4E and is important for the assembly of other initiation factors onto mRNA.

Protein kinase A (PKA) also plays a very important role in cellular growth (reviewed in Zaman et al. 2008). It is a heterotetramer composed of two catalytic subunits and two regulatory subunits. Targets of this kinase include proteins involved in the carbohydrate metabolism, enzymes involved in glycolysis, and ribosome biogenesis. The regulatory subunit is encoded by *BCY1*. Binding of cyclic AMP (cAMP) to Bcy1 alleviates this protein's inhibitory activity. The levels of cAMP in the cell in turn are regulated by its synthesis catalyzed by adenylyl cyclase and its degradation by phosphodiesterases. Adenylyl cyclase is regulated by the small GTP-binding proteins Ras1 and Ras2. Glucose addition to cells results in a rapid Ras-dependent cAMP increase and subsequent PKA activation.

When yeast cells are deprived of amino acids or subjected to certain stresses they increase translation of an mRNA coding for *GCN4* (reviewed in Hinnebusch, 2005). *GCN4* is a transcriptional activator of genes involved in amino acid synthesis. The induction of *GCN4* is controlled by four short open reading frames in the leader of the mRNA. These four uORFs prevent scanning ribosomes from reaching the *GCN4* start codon. Under starvation conditions approximately half of the scanning ribosomes will be able to scan beyond these four uORFs and reach the start codon of the gene. *GCN4* translation is induced by phosphorylation of eIF2α by Gcn2. Gcn2 is a protein kinase that phosphorylates eIF2α when cells are starved. This phosphorylation prevents formation of

the eIF2*GTP*Met-tRNA^{met} ternary complex. The reduction in ternary complex formation leads to a global decrease in translation initiation while selectively stimulating *GCN4* mRNA translation (Dever, 1997).

Growth and Cell cycle Progression.

Growth and cell cycle progression are two independent processes that are coupled at START (Mitchison 1970). Exactly how this occurs has been widely debated. Polymenis and Schmidt (1997) showed that *CLN3* expression is regulated at the level of translation by a short uORF in the 5'-end of its mRNA. Furthermore they concluded that Cln3 synthesis is achieved via a leaky scanning mechanism from ribosomes that bypass the uORF thus linking protein synthesis and cell cycle entry. When the cell is growing under favorable conditions, this uORF prevents translation of Cln3 and allows cells to grow more prior to cell cycle entry. Jorgensen et al. (2004) have also provided a link between ribosome synthesis and cell cycle entry. They show that Sfp1 and Sch9, both activators of the ribosomal protein (RP) and ribosome biogenesis (Ribi) regulons, respond rapidly to nutrient conditions. They further show that Sfp1 nuclear localization is regulated by the Ras/PKA and TOR signaling pathways. Starvation or the nuclear absence of Sfp1 in turn causes Hfl1 and Ifh1, two proteins which normally bind to RP promoters, to localize to nucleolar regions. Cells lacking Sfp1 or Sch9 are also very small, with a smaller critical size than wild type cells, so in a way these proteins provide a link between cell size and nutritional status.

III. Aneuploidy, cell growth, and cell cycle progression in yeast.

The work presented in this thesis explores the relationship between aneuploidy, cell growth and cell cycle progression in yeast. Since growth and cell cycle entry are coordinated during the G1 phase of the cell cycle, most of the experiments carried out here explore progression through G1. The data presented show that aneuploid yeast cells delay entry into the cell cycle in two ways: by increasing the critical size for budding and by decreasing the rate of volume accumulation (i.e. growth). The increased critical size is due to a delay in *CLN2* transcription. In addition, expression of *CLN2* at an earlier time leads to cell cycle entry indicating that the observed delay is suppressed by overexpression of *CLN2*. In addition, deletion of *WHI5* and *BCK2* did not rescue the observed increase in volume in agreement with the idea that aneuploidy is disrupting events at least at the level of Swi4/Swi6 transcription.

Aneuploidy also causes cells to accumulate volume at a slower rate. The data presented here show that for the most part the translational machinery in aneuploid cells is intact. This means that these cells do not seem to have gross defects in ribosome biogenesis. It also means that these cells are able to translate most of the extra transcripts present. Why then are these cells growing more slowly? The ribosome footprinting data shows that while translation of some transcripts becomes more efficient, it becomes less efficient for others. These changes are subtle but could be synergistic. Metabolomic studies presented here show that aneuploid cells have excess Krebs cycle intermediates, suggesting that aneuploidy is interfering with the cell's ability to produce energy. This could be directly related to growth.

What is clear from the data presented in this work is that aneuploidy decreases the proliferative capacity of cells. If these results hold true for human cells they would imply that becoming aneuploid does not directly lead to cancer and tumor formation. To become tumorigenic an aneuploid cell will then have to overcome the proliferative barriers imposed by being aneuploid.

References:

Amon A, Irniger S, Nasmyth K. 1994. Closing the cell cycle circle in yeast: G2 cyclin proteolysis initiated at mitosis persists until the activation of G1 cyclins in the next cycle. Cell. 77(7):1037-50.

Barbet NC, Schneider U, Helliwell SB, Stansfield I, Tuite MF, Hall MN. 1996. TOR controls translation initiation and early G1 progression in yeast. Mol Biol Cell. 7(1):25-42.

Berset C, Trachsel H, Altmann M. 1998. The TOR (target of rapamycin) signal transduction pathway regulates the stability of translation initiation factor eIF4G in the yeast Saccharomyces cerevisiae. Proc Natl Acad Sci U S A. 95(8):4264-9.

Colomina N, Ferrezuelo F, Wang H, Aldea M, Garí E. 2008. Whi3, a developmental regulator of budding yeast, binds a large set of mRNAs functionally related to the endoplasmic reticulum. J Biol Chem. 2008 283(42):28670-9.

Campbell DA, Fogel S, Lusnak K. 1975. Mitotic chromosome loss in a disomic haploid of Saccharomyces cerevisiae. Genetics. 79(3):383-96.

Costanzo M, Nishikawa JL, Tang X, Millman JS, Schub O, Breitkreuz K, Dewar D, Rupes I, Andrews B, Tyers M. CDK activity antagonizes Whi5, an inhibitor of G1/S transcription in yeast. 2004. Cell.;117(7):899-913.

Cross FR. 1988. DAF1, a mutant gene affecting size control, pheromone arrest, and cell cycle kinetics of Saccharomyces cerevisiae. Mol Cell Biol. 1988 November; 8(11): 4675–4684.

de Bruin RA, McDonald WH, Kalashnikova TI, Yates J 3rd, Wittenberg C. 2004. Cln3 activates G1-specific transcription via phosphorylation of the SBF bound repressor Whi5. Cell. 117(7):887-98.

Dever TE. 1997. Using GCN4 as a reporter of eIF2 alpha phosphorylation and translational regulation in yeast. Methods. 11(4):403-17.

Di Como CJ, Chang H, Arndt KT. 1995. Activation of CLN1 and CLN2 G1 cyclin gene expression by BCK2. Mol Cell Biol. 15(4):1835-46.

Dierssen M, Herault Y, Estivill X. 2009. Aneuploidy: from a physiological mechanism of variance to Down syndrome. Physiol Rev. 89(3):887-920. Review.

Dirick L, Böhm T, Nasmyth K. 1995. Roles and regulation of Cln-Cdc28 kinases at the start of the cell cycle of Saccharomyces cerevisiae. EMBO J. 14(19):4803-13.

Epstein CB, Cross FR. 1994. Genes that can bypass the CLN requirement for Saccharomyces cerevisiae cell cycle START. Mol Cell Biol. 14(3):2041-7.

Flick K, Chapman-Shimshoni D, Stuart D, Guaderrama M, Wittenberg C. 1998. Regulation of cell size by glucose is exerted via repression of the CLN1 promoter. Mol Cell Biol. 18(5):2492-501.

Hall DD, Markwardt DD, Parviz F, Heideman W. 1998. Regulation of the Cln3-Cdc28 kinase by cAMP in Saccharomyces cerevisiae. EMBO J. 17(15):4370-8.

Hartwell LH, Culotti J, Pringle J. R, Reid B. J. 1974. Genetic control of the cell division cycle in yeast. Science. 183: 46–5.

Hartwell LH, Unger MW. 1977. Unequal division in Saccharomyces cerevisiae and its implications for the control of cell division. J Cell Biol. 75(2 Pt 1):422-35.

Hereford LM, Hartwell LH. 1974. Sequential gene function in the initiation of Saccharomyces cerevisiae DNA synthesis. J Mol Biol 84: 445–46.

Hinnebusch AG. 2005. Translational regulation of GCN4 and the general amino acid control of yeast. Annu Rev Microbiol. 59:407-50.

Holland AJ, Cleveland DW. 2009. Boveri revisited: chromosomal instability, aneuploidy and tumorigenesis. Nat Rev Mol Cell Biol. 10(7):478-87.

Huang JN, Park I, Ellingson E, Littlepage LE, Pellman D. 2001. Activity of the APC(Cdh1) form of the anaphase-promoting complex persists until S phase and prevents the premature expression of Cdc20p. J Cell Biol. 154(1):85-94.

Jeganathan K, Malureanu L, Baker DJ, Abraham SC, van Deursen JM. 2007. Bub1 mediates cell death in response to chromosome missegregation and acts to suppress spontaneous tumorigenesis. Cell Biol. 179(2):255-67. Epub 2007 Oct 15.

Johnston GC, Ehrhardt CW, Lorincz A, Carter BL. 1979. Regulation of cell size in the yeast Saccharomyces cerevisiae. J Bacteriol.137(1):1-5.

Johnston GC. 1977. Cell size and budding during starvation of the yeast Saccharomyces cerevisiae. J Bacteriol. 132(2):738-9.

Jorgensen P, Rupes I, Sharom JR, Schneper L, Broach JR, Tyers M. 2004. A dynamic transcriptional network communicates growth potential to ribosome synthesis and critical cell size. Genes Dev. 18(20):2491-505.

Jorgensen P, Tyers M. 2004. How cells coordinate growth and division. Curr Biol. 14(23):R1014-27.

Knudson AG Jr. 1971. Mutation and cancer: statistical study of retinoblastoma. Proc Natl Acad Sci U S A. 68(4):820-3.

Li M, Fang X, Wei Z, York JP, Zhang P. 2009. Loss of spindle assembly checkpoint-mediated inhibition of Cdc20 promotes tumorigenesis in mice. J Cell Biol. 185(6):983-94.

Mitchison JM. 1970. The biology of the cell cycle. Cambridge University Press, Cambridge, England.

Murray LE, Veinot-Drebot LM, Hanic-Joyce PJ, Singer RA, Johnston GC. 1987. Effect of ploidy on the critical size for cell proliferation of the yeast Saccharomyces cerevisiae. Curr Genet. 11:591-594.

Nash P, Tang X, Orlicky S, Chen Q, Gertler FB, Mendenhall MD, Sicheri F, Pawson T, Tyers M. 2001. Multisite phosphorylation of a CDK inhibitor sets a threshold for the onset of DNA replication. Nature. 414(6863):514-21.

Niwa O, Tange Y, Kurabayashi A. 2006. Growth arrest and chromosome instability in aneuploid yeast. Yeast. 23(13):937-50.

Polymenis M, Schmidt EV. 1997. Coupling of cell division to cell growth by translational control of the G1 cyclin CLN3 in yeast. Genes Dev.11(19):2522-31.

Rajagopalan H, Lengauer C. 2004. Aneuploidy and cancer. Nature. 432(7015):338-41. Review.

Rajagopalan H, Nowak MA, Vogelstein B, Lengauer C. 2003. The significance of unstable chromosomes in colorectal cancer. Nat Rev Cancer. 3(9):695-701.

Rao CV, Yang YM, Swamy MV, Liu T, Fang Y, Mahmood R, Jhanwar-Uniyal M, Dai W. 2005. Colonic tumorigenesis in BubR1+/-ApcMin/+ compound mutant mice is linked to premature separation of sister chromatids and enhanced genomic instability. Proc Natl Acad Sci U S A. 102(12):4365-70.

Rieder CL, Cole RW, Khodjakov A, Sluder G. 1995. The checkpoint delaying anaphase in response to chromosome monoorientation is mediated by an inhibitory signal produced by unattached kinetochores. J Cell Biol. 130(4):941-8.

Rupes I. 2002. Checking cell size in yeast. Trends Genet. 18(9):479-85.

Schneider BL, Patton EE, Lanker S, Mendenhall MD, Wittenberg C, Futcher B, Tyers M. 1998. Yeast G1 cyclins are unstable in G1 phase. Nature. 395(6697):86-9.

Schneider BL, Zhang J, Markwardt J, Tokiwa G, Volpe T, Honey S, Futcher B. 2004. Growth rate and cell size modulate the synthesis of, and requirement for, G1-phase cyclins at start. Mol Cell Biol. 24(24):10802-13.

Sherr CJ. 2004. Principles of tumor suppression. Cell. 116(2):235-46.
Sidorova JM, Mikesell GE, Breeden LL. 1995. Cell cycle-regulated phosphorylation of Swi6 controls its nuclear localization. Mol Biol Cell. 6(12):1641-58.

Singer RA, Johnston GC. 1981. Nature of the G1 phase of the yeast Saccharomyces cerevisiae. Proc Natl Acad Sci U S A. 78(5):3030-3.

Spellman PT, Sherlock G, Zhang MQ, Iyer VR, Anders K, Eisen MB, Brown PO, Botstein D, Futcher B. 1998. Comprehensive identification of cell cycle-regulated genes of the yeast Saccharomyces cerevisiae by microarray hybridization. Mol Biol Cell.9(12):3273-97.

Storchova Z, Kuffer C. 2008. The consequences of tetraploidy and aneuploidy. J Cell Sci. 121(Pt 23):3859-66.

Storchova Z, Pellman D. 2004. From polyploidy to aneuploidy, genome instability and cancer. Nat Rev Mol Cell Biol. 5(1):45-54.

.
Tokiwa G, Tyers M, Volpe T, Futcher B. 1994. Inhibition of G1 cyclin activity by the Ras/cAMP pathway in yeast. Nature. 371(6495):342-5.

Torres EM, Sokolsky T, Tucker CM, Chan LY, Boselli M, Dunham MJ, Amon A. 2007. Effects of aneuploidy on cellular physiology and cell division in haploid yeast. Science. 317:916-24.

Torres EM, Williams BR, Amon A. 2008. Aneuploidy: cells losing their balance. Genetics. 179(2):737-46.

Tyers M, Tokiwa G, Futcher B. 1993. Comparison of the Saccharomyces cerevisiae G1 cyclins: Cln3 may be an upstream activator of Cln1, Cln2 and other cyclins. EMBO J. 12(5):1955-68.

Urban J, Soulard A, Huber A, Lippman S, Mukhopadhyay D, Deloche O, Wanke V, Anrather D, Ammerer G, Riezman H, Broach JR, De Virgilio C, Hall MN, Loewith R. 2007. Sch9 is a major target of TORC1 in Saccharomyces cerevisiae. Mol Cell. 26(5):663-74.

Verma R, Annan RS, Huddleston MJ, Carr SA, Reynard G, Deshaies RJ. 1997. Phosphorylation of Sic1p by G1 Cdk required for its degradation and entry into S phase. Science. 278(5337):455-60.

Wang H, Garí E, Vergés E, Gallego C, Aldea M. 2003. Recruitment of Cdc28 by Whi3 restricts nuclear accumulation of the G1 cyclin-Cdk complex to late G1. EMBO J. 23(1):180-90.

Weaver BA, Silk AD, Montagna C, Verdier-Pinard P, Cleveland DW. Aneuploidy acts both oncogenically and as a tumor suppressor. 2007. Cancer Cell. 11(1):25-36.

Wijnen H, Landman A, Futcher B. 2002. The G(1) cyclin Cln3 promotes cell cycle entry via the transcription factor Swi6. Mol Cell Biol. 22(12):4402-18.
Williams BR, Prabhu VR, Hunter KE, Glazier CM, Whittaker CA, Housman DE, Amon A. 2008. Aneuploidy affects proliferation and spontaneous immortalization in mammalian cells. Science. 322(5902):703-9.

Zaman S, Lippman SI, Zhao X, Broach JR. 2008. How Saccharomyces responds to nutrients. Annu Rev Genet. 42:27-81.

Chapter 2 : The effects of aneuploidy on cell growth and START in yeast.

Foot printing experiments were performed by Gloria Brar and Christian Gonzalez at UCSF. Nicholas Ingolia assisted with the data analysis. Figure 7C-D. Tables 2 and 3.
The CLN2 northern experiments were performed by Thomas Carlile and Christian Gonzalez at MIT. Figure 10.
The metabolomic analysis was carried out by Stephan Christen and Uwe Sauer at ETH in Zurich. Figure 6.
Eduardo Torres contributed the microarray data for disome XVI. Figure 7B.
All other experiments were performed by Christian Gonzalez.

The effects of aneuploidy on cell growth and START in yeast.

Christian Gonzalez, Gloria A. Brar, Stefan Christen, Thomas Carlile, Nicholas Ingolia, Eduardo M. Torres, Uwe Sauer, Jonathan Weissman and Angelika Amon*

David H. Koch Institute for Integrative Cancer Research
Howard Hughes Medical Institute
Massachusetts Institute of Technology, E17-233
40 Ames Street
Cambridge, MA 02139
USA

Abstract

In budding yeast, aneuploidy delays cells cycle entry from a mating factor arrest suggesting that the G1 cycling program is misregulated in these cells. Here we show that most aneuploid yeast strains delay cell cycle entry. This increase in the critical size for budding is due to a delay in *CLN2* mRNA accumulation and can be suppressed by supplying cells with high levels of this cyclin. Surprisingly, deletion of the cell cycle entry inhibitor *WHI5* only partially suppressed the G1 delay of aneuploid cells indicating that aneuploidy interferes with the cell cycle machinery either downstream of Whi5 inactivation or through parallel pathways. The growth defect seen in aneuploid cells is not due to gross defects in the translational machinery. Instead, yeast cells respond to aneuploidy by altering the translational efficiency of a number of genes. Our results indicate that aneuploidy affects entry into the cell cycle in at least two ways. The condition elicits a growth defect during the G1 phase of the cell cycle and increases the critical size for budding.

Introduction

Aneuploidy, defined as a genetic complement that is not a multiple of the haploid genome, is detrimental in all organisms analyzed to date (reviewed in Torres et al., 2008). The condition leads to developmental abnormalities and death. A systematic study of 20 different aneuploid budding yeast strains revealed that in this organism too, aneuploidy antagonizes cell proliferation (Torres et al., 2007). Analysis of cell cycle progression of aneuploid yeast strains released from a pheromone-induced G1 arrest furthermore showed that most aneuploid cells exhibit a delay in entry into the cell cycle. The basis for this G1 delay however, was not determined.

The molecular events governing cell cycle entry – a transition known as START - are well characterized in *Saccharomyces cerevisiae*. During early G1, Cln3-CDK complexes are activated in a manner that is coordinated with signals such as nutrient availability, growth rate and the presence of mating pheromone. Cln3-CDKs then phosphorylate the transcriptional inhibitor Whi5 (Costanzo et al. 2004 and de Bruin et al. 2004). Also, during early G1, Whi5 localizes to the nucleus where it inhibits the SBF transcription factor complex. SBF, which is composed of Swi4 and Swi6, activates the transcriptional program essential for DNA replication and bud formation. Key among its targets are the two G1 cyclin encoding genes *CLN1* and *CLN2*. Phosphorylation of Whi5 by Cln3-CDKs triggers the export of this transcriptional inhibitor from the nucleus. SBF - dependent transcription then commences and Cln1/2-CDKs accumulate. Once sufficient

Cln-CDK activity is achieved, cells enter the cell cycle by phosphorylating proteins critical for bud formation and the initiation of DNA replication (Morgan 1997).

Activation of the CDK - transcription cascade governing entry into the cell cycle is tightly controlled by macromolecule biosynthesis rates and cell size. Cell cycle entry only occurs when cells have reached a certain size, known as the critical cell size (reviewed in Rupes 2002). In general, cells that grow at a slow rate bud at smaller volumes than cells that grow at higher rates (Jorgensen and Tyers 2004). In other words, higher growth rate leads to an increase in critical cell size. How growth rate controls the G1 cell cycle machinery is poorly understood but it is clear that Cln-CDKs must be the target because modulating Cln-CDK activity affects the critical cell size. For example, overexpression of any of the cyclins Cln3, Cln2 or Cln1, leads to small size phenotypes, while their deletion leads to cells growing abnormally large (Tyers et al. 1993 and Jorgensen and Tyers 2004).

Polymenis and Schmidt (1997) described a mechanism that links growth rate to cell cycle control. The CLN3 transcript contains a short upstream open reading frame (uORF) that acts as a translational control element. When protein synthesis rates are low, *CLN3* message is poorly translated, hence slowing progression through G1. Inactivation of this uORF shortened G1 by decreas ing the critical size in cells grown in a poor carbon source. In effect, the presence of the uORF prevents cells from accumulating sufficient CLN3 mRNA to pass Start when growth conditions are not adequate.

Although it is known that aneuploidy delays cell cycle entry from a pheromone block and release, it is not known whether the condition affects cell growth, the cell cycle machinery governing cell cycle entry, or both. We show here that of 15 aneuploid yeast strains examined, 12 strains exhibit a G1 growth defect. This growth defect correlates with the size of the additional chromosome raising the possibility that production of genes located on the additional chromosome proportionally interferes with macromolecule biosynthesis and hence cell volume increase. Furthermore we show that aneuploidy not only interferes with cell growth but also with the cell cycle machinery governing cell cycle entry. 12 aneuploid strains exhibited cell cycle entry defects as judged by an increase in critical cell size. This cell cycle entry defect manifests itself in a delay in *CLN2* mRNA accumulation and can be suppressed by supplying cells with high levels of Cln2. Surprisingly, deletion of *WHI5* only partially suppresses the increase in critical cell size of aneuploid cells indicating that aneuploidy inhibits the cell cycle machinery either downstream of Whi5 inactivation or through parallel pathways. Our results indicate that aneuploidy interferes with the regulatory program controlling cell cycle entry in multiple ways.

Results

Disomic yeast cells exhibit a cell cycle entry delay.

We previously generated 20 budding yeast strains containing one or two additional chromosomes (henceforth referred to as disomic yeast strains; Torres et al., 2007). These strains share a number of phenotypes, prominent among them a cell cycle

entry delay after release from an α-factor pheromone-induced G1 arrest. 16 out of 20 aneuploid yeast strains exhibited a delay in bud formation and initiation of DNA replication, with most strains showing a delay ranging from 10-20 minutes. Treatment of cells with pheromone inhibits cell cycle progression but not cell growth, thus disrupting the co-ordination of cell growth and division and making it impossible to delineate whether cell growth or cell cycle entry (or both) are impaired in aneuploid yeast cells.

To characterize the effects of aneuploidy on cell growth and cell cycle entry, we isolated small unbudded daughter cells using centrifugal elutriation and examined their growth and cell cycle entry properties. For this analysis we chose two aneuploid yeast strains that did not exhibit a G1 delay upon pheromone release (yeast strains disomic for chromosome II or V) and 10 strains that showed significant cell cycle entry defects after release from an α-factor arrest (strains disomic for chromosome IV, VIII, XI, XII, XIII, XIV, XV, XVI, VIII+XIV, XI+XVI; Figure 1). Consistent with our previous studies, strains disomic for chromosome II or V did not exhibit a cell cycle entry defect as judged by their ability to form buds. In fact it appeared that cells disomic for chromosome V entered the cell cycle slightly earlier than wild-type cells (Figure 1C). In contrast, cell cycle entry was delayed in all other aneuploid yeast strains. The delays ranged from ~120 min for disome IV to ~25 min for disome VIII. We conclude that most aneuploid yeast strains are delayed in cell cycle entry.

The critical cell size is increased in most aneuploid strains.

A defect in cell cycle entry can be caused either by a cell cycle defect that culminates in a delay in the accumulation of Cln-CDK activity or by slowed growth. A delay in entry into the cell cycle caused by defects in the cell cycle machinery result in an increase in critical cell size (reviewed in Rupes 2002). We find that, out of fifteen aneuploid strains analyzed, twelve showed an increase in critical cell size as defined by the average cell size at the time when 50% of the cells had formed a bud (Figure 2 A – N, Table 1). This increase in critical size ranged from as little as ~3fL for disome XIV to as much as ~54 fL for disome 2N-1-9. Although the cell cycle entry defect was generally more severe the larger the additional chromosome (Figure 2O), a strict correlation between chromosome size and cell cycle entry delay was not observed.

Aneuploid yeast strains exhibit a growth defect.

Slow growth also delays entry into the cell cycle. For example, cells lacking the transcription factor Sfp1, which is required for ribosome biogenesis (Fingerman et al. 2003) exhibit a severe G1 delay. *sfp1Δ* cells obtained by centrifugal elutriation take much longer to enter the cell cycle than wild-type cells as judged by bud formation (Jorgensen et al. 2004, Figure 5D). Growth rate measurements during G1 and size at the time of bud formation show that this cell cycle entry defect is due to a growth defect and not cell cycle defects, because the critical size is smaller rather than larger (Figure 3A – C).

To determine whether a growth defect could also contribute to the G1 delay observed in aneuploid cells, we examined the volume increase of aneuploid and wild type cells during G1.We isolated small daughters cells using centrifugal elutriation, cultured them in rich medium at 30°C and monitored cell volume as a function of time. To measure growth rates of cells during G1, we analyzed time points when fewer than 10% of cells bore a bud. Of the 15 strains that we analyzed, we found that 12 aneuploid strains exhibit a growth defect (Figure 3A – H, Figure 4). This is best seen when one compares the size distribution of wild-type and aneuploid cells at the time of elutriation with that after growth in rich medium for 60 minutes (Figure 3B, D, F, H). To quantify the growth defect we fitted the quantifications to exponential functions and established growth rate constants (Table 1). The average rate constant for wild type was 0.0075 ± 0.0005/min. Growth rates were reduced in the aneuploid cells ranging from rate constants as low as 0.0030/min for disome XII to 0.0061/min for disome XIV. Growth rates were not affected in strains disomic for chromosome X, in fact growth appeared slightly accelerated in this strain (Figure 4D). It is also worth noting that the cell cycle entry defect of cells disomic for chromosome XVI is entirely due to a growth defect. Critical cell size was not affected in the strain, yet budding was delayed for almost 40 minutes (Table 1; Figure 2K; Figure 1J). Growth rate analysis demonstrated that growth was severely impaired in disome XVI cells (Figure 3G, H), providing an explanation for the delay in bud formation.

In summary, our results indicate that most aneuploid yeast strains exhibit a growth defect. Comparison of growth rates with the size of the additional chromosome(s)

present in the aneuploid strain showed that the parameters correlated well (r^2=0.51, Figure 3I). This finding raises the interesting possibility that the presence of additional active chromosomes interferes with macromolecule biosynthesis.

Decreased growth rates are not due to gross amino acids biosynthesis defects.

Our results show that aneuploidy interferes with both the cell cycle program governing the G1 – S phase transition and growth. We first decided to examine the effects of aneuploidy on growth. To determine the basis for this growth defect we first measured the intracellular amino acid levels of aneuploid cells. We hypothesized that aneuploidy, by its potential need for increased protein synthesis due to the presence of extra mRNA from the extra chromosome, could be depleting amino acid pools. Lower amino acid pools would in turn decrease total protein synthesis leading to decreased growth. This hypothesis assumes that the cell has no capacity to deal with a putative increase in free amino acid requirements. It is also possible that when we measure free amino acid levels that these be the same for wild type and aneuploid cells and even that they be higher for aneuploid cells than for wild type. In both of these situations, amino acid availability would not be limiting factor affecting protein synthesis or growth.

To measure intracellular amino acid pools we grew cells in medium that was only supplemented with amino acids cells failed to make on their own (lysine, leucine, tryptophane, methionine) and levels of the amino acids histidine, serine, glycine, phenylalanine, tyrosine, proline, valine, alanine, isoleucine, threonine, asparagine and aspartate as well the intermediates of the TCA cycle were quantified using ToF mass

spectrometry. Glutamine, glutamate and arginine were not measured due to technical limitations. We found that intracellular amino acid pools were not lower in strains disomic for chromosomes IV, VIII, XI, XIII, XV, or XVI (Figure 6) indicating that free amino acid pools (at least of the amino acids whose levels we determined) were not depleted in aneuploid yeast strains. Consistent with this conclusion is the observation that aneuploid cells do not exhibit a starvation response. *GCN4* encodes a transcription factor that controls the expression of 30 amino acid biosynthetic genes (reviewed in Hinnebusch 2005). Its abundance is translationally regulated. Upon amino acid starvation, *GCN4* translation is increased. We examined translation of a *GCN4-LacZ* reporter construct in the absence or presence of amino acid starvation induced by the addition of the toxic histidine intermediate 3-AT. Translation of the *GCN4-LacZ* reporter was neither increased in the presence or absence of 3-AT in disomes IV, VIII, XI, XV, or XVI cells (Figure 7), confirming that general amino acid starvation was not responsible for the growth defect observed in aneuploid yeast strains.

Unexpectedly, our metabolomic analysis of aneuploid yeast strains showed that intermediates of the TCA cycle, especially malate, were increased in a large number of aneuploid cells (Figure 6A). We do not know why these intermediates accumulate in aneuploid strains but it is likely a consequence of the cell growth defect these strains experience, because cells carrying a deletion of *SFP1* show a very similar increase in the levels of these biosynthetic intermediates (Figure 6B). It thus appears that a slowing of growth rate leads to a decrease in flow through the TCA cycle, causing intermediates to accumulate. These findings raise the very interesting possibility that growth rates affect

the TCA cycle in these cells. Understanding the molecular mechanisms underlying this feedback control will be essential if we want to understand how cell growth and metabolism are coordinated. We note that these findings also demonstrate that metabolism is altered in aneuploid cells.

Effects of aneuploidy on translation.

Given that in aneuploid cells free amino acid pools are not depleted, yet they still growing slow, we hypothesized that translation could be impaired in these strains. To further characterize the translational status of these cells we examined polysome formation by sucrose gradient fractionation (Baim et al. 1985). Although the size of the 40S, 60S, and 80S peaks were somewhat variable even between replicas of wild-type cells perhaps due to technical problems, polyribosomal peaks were similar between repeat experiments (data not shown) and revealed no significant differences between wild-type cells and cells disomic for chromosomes IV, X, XI, or VIII+XIV (Figure 9A-F) – only in disome XVI did polysomes seem lower. Disome XII is a special case because our polysomal profiles seem to show that this strain exhibits a translation initiation defect. S^{35}-Methionine incorporation studies did not reveal any significant differences between wild-type and disome XVI cells either, yet we were able to detect defects in S^{35}-Methionine incorporation in *sfp1Δ* cells, which exhibit a severe growth defect (Fingerman et al. 2003, data not shown, Figure 8A). These results indicate that disomic strains do not suffer from dramatic translation defects (i.e. they seem to be able to

synthesize ribosomal subunits and assemble them onto mRNA), which is consistent with the observation that the growth defects in aneuploid strains are subtle.

The fact that aneuploid cells exhibit a reduced growth rate and the observation that this reduced growth rate correlates well with the size of the additional chromosome(s) (Figure 3I) raises two interesting points. First, provided that the chromosome is active and produces proteins as efficiently as the other chromosomes, simply making more proteins does not increase growth rate but in fact slows growth. Second, the fact that protein synthesis coming from the additional chromosome interferes proportionally with growth as measured by the rate of volume accumulation

suggests that either protein production and/or energy necessary for macromolecule synthesis are rate-limiting. An essential aspect of these hypotheses is that the genes present on the additional chromosome are not only transcribed, as we have shown earlier (Torres et al., 2007) but are also translated. To test this, we measured the translation rates of most genes in cells disomic for XVI using the method developed by Ingolia et al. (2009) for ribosomal footprinting. We picked disome XVI for this analysis because it did not have a significant increase in critical size but it did significantly decrease volume accumulation during the G1 phase of the cell cycle making sure that we only analyzed growth defects and not cell cycle defects. Consistent with previous studies (Torres et al., 2007), this analysis revealed that disome XVI cells have twice the amount of mRNA of genes located on chromosome XVI than wild type (Figure 8B). These additional RNAs are translated as judged by their association with ribosomes (Figure 8C) and the analysis of translation efficiencies across the genome (Figure 8D). We conclude

that the additional copy of chromosome XVI is as efficiently translated as all other chromosomes. We also noted that the overall distribution of ribosomes on transcripts was similar between wild-type and disome XVI cells (data not shown), again indicating that large-scale changes in translation efficiency are not detectable in disome XVI cells, which, by cell volume measurements, have one of the more severe growth defects among the disomic strains (Table 1).

An interesting additional aspect of this analysis is that it identifies genes that show decreased or increased translation in disome XVI cells compared to wild-type. We observe decreased translation of well over 500 genes (Table 3). Among these genes are some whose products are involved in phosphate metabolism (*PHO89*, *PHO5, PHO12, GIT1* and *SPL2*) and some ribosomal proteins (including *RPS12*, *RPL16A, RPL35A, RPS23A, RPS20, RPS5, RPS6B, RPL35B* , among others) and ribosomal biogenesis related genes (including *ESF1, RRP8, NSR1, EBP2* and others). The low-abundance of these factors could contribute to the growth defect we observe in disome XVI cells. Interestingly, *FAR1* was also down regulated. It has been shown that deletion of *FAR1* leads to a small size and accelerated cell cycle entry, exactly what is seen in disome XVI (Alberghina et al. 2004). Among the genes that were up-regulated we found two interesting clusters of genes (Table 2). First, we identified a number of protein folding factors (*SSA1, HSP31, HSP104, SSE2, HSP78, HSP42* and *HSP82*). This observation is consistent with our previous observation that aneuploid yeast cells experience significant proteotoxic stress (Torres et al., 2007). Intriguing was also the observation that the locus encoding ubiquitin, *UBI4*, was translationally more active in disome XVI cells than in

wild-type. This could be a response to increased proteotoxic stress and reduced growth rates seen in disomic strains given that this gene is the major stress-inducible ubiquitin gene (Hanna et al. 2003). Increased translation of a large number of genes involved in cell wall structure/formation such as *PST1, SED1, CWP1, YGP1, SRL1* and *PIR3* was also observed. The significance of this up-regulation is at present unknown, but perhaps points to increased cell wall stress.

In summary, our data indicate that aneuploid cells exhibit a subtle growth defect. Given the fact that the additional chromosomes are efficiently translated and that a good correlation exists between growth defect and size of additional chromosome, we propose that increased protein production does not automatically lead to an increase in growth rate. Furthermore, the production of proteins from the additional chromosome contributes to the growth defect of disomic cells perhaps by causing a subtle decrease in overall translation. In other words, since overall protein synthesis as determine by ^{35}S-methionine incorporation does not seem to be significantly affected by aneuploidy, yet the transcripts from the extra chromosomes are being translated, only a decrease in the translation of all other transcript can reconcile these two observations. That is just making any protein does not equal cell growth.

Aneuploid cells are delayed in *CLN2* expression

In addition to exhibiting a growth defect most aneuploid cells are delayed in entry into S phase (Table 1). The genetic program governing entry into the cell cycle

culminates in the expression of the G1 cyclins *CLN1* and *CLN2* (Dirick et al. 1995). To determine whether the cell cycle entry delay of aneuploid cells was due to a defect in *CLN1* and *CLN2* expression we examined *CLN2* RNA levels in two disomic strains with intermediate cell cycle entry defects, disome IV and disome XI strains. Cells were isolated by centrifugal elutriation and *CLN2* RNA levels were measured as a function of cell volume. These analyses showed that transcription of *CLN2* occurs at a larger volume in the two disomic strains than in wild-type (Figure 10). Maximal *CLN2* transcription occurred at 42 and 50 fL in disome IV and XI strains, respectively whereas *CLN2* levels were maximal in wild type cells with a volume of 26 fL.

Since maximal *CLN2* levels are detected at a larger volume in disomic cells than in wild type, we conclude that *CLN2* transcription is impaired in disome IV and XI strains. Previous studies of *CLN2* expression in disomic strains released from a pheromone-induced G1 arrest revealed similar results (Torres et al., 2007). If maximal *CLN2* transcription had occurred at the same volume in disomic and wild type cells, then we would have concluded that aneuploidy is not interfering with SBF-dependent transcription but rather with events downstream of it. The possibility does exist that aneuploidy is interfering both with *CLN2* transcription and with other events downstream. To address this possibility we examined whether overexpression of *CLN2*, which is known to accelerate entry into the cell cycle, suppressed the START delay of cells disomic for chromosome IV, VIII or XI. We overexpressed *CLN2* from the galactose inducible *GAL1-10* promoter for 1 hour and then isolated small daughter cells using centrifugal elutriation. Because cells were grown in medium supplemented with

raffinose and galactose as the carbon source, cells expressing wild-type levels of *CLN2* budded at the smaller critical size of ~28 fL (Figure 11A). Wild-type cells overexpressing *CLN2* exhibited a critical size of 20 fL (Figure 11A). Overexpression of *CLN2* completely suppressed the cell cycle entry defect of cells disomic for chromosomes IV, VIII, or XI (Figure 11B-D). Disomes containing high levels of *CLN2* showed 50% budding at around 18, 20, and 25 fL respectively whereas those not overexpressing *CLN2* exhibited a critical size of 35, 44, and 48 fL respectively. We conclude that the increase in critical size in aneuploid cells is due to defects in Cln-CDK activity caused by a delay in *CLN2* transcription.

Deletion of *WHI5* partially suppresses the cell cycle entry defect of disomic yeast strains.

Next, we wished to look at the regulation of the transcription factors responsible for *CLN2* transcription. Both *CLN1* and *CLN2* transcription is controlled by the transcription factor complex SBF that is negatively regulated by the transcription inhibitor Whi5 (Costanzo et al. 2004, de Bruin et al. 2004). Once Cln3-CDKs are sufficiently active, they phosphorylate Whi5 thereby promoting its export out of the nucleus. To determine whether disomic yeast strains delayed cell cycle entry by interfering with Whi5 inactivation we examined the consequences of deleting the gene encoding this transcription repressor on critical size. Wild type cells bud at around 37 fL but when *WHI5* is deleted the critical size decreases to ~28 fL (Figure 12A). Disome IV cells bud at ~49 fL. When *WHI5* is deleted in these cells the cell volume when cultures

are 50% budded decreases to 42 fL (Figure 12B). Similarly, Disome VIII buds at around ~45 fL. Deletion of *WHI5* brings this volume down to 34 fL (Figure 12C). Finally, Disome XI exhibits a critical size of ~58 fL. This volume decreases to ~51 fL when *WHI5* is deleted in these cells (Figure 12D). Thus, deletion of *WHI5* affects wild-type and disomic cells to a similar degree, decreasing the critical size of these cells by 7-11 fL. If we look at this decrease in critical size relative to the critical size itself (i.e. volume decrease cause by deletion of *WHI5* divided by the actual critical size) we see that for the larger disomes this fraction of "rescue" is much smaller. In other words, deletion of *WHI5* has a much larger effect on critical size in wild type than in aneuploid cells, suggesting that aneuploid cells are not larger because they fail to inactivate Whi5 and that instead there are other mechanisms affecting the critical size. If deletion of *WHI5* had decreased the critical size of both wild type and aneuploid cells to the same volume of ~28 fL, then we could have concluded that aneuploid cells delay transcription of *CLN2* because they fail to inactivate Whi5. Since Cln3-CDK activity has been shown to directly phosphorylate Whi5 and inhibit it, we conclude that disomy interferes with cell cycle entry at least in part by affecting events downstream or parallel to Whi5 inactivation.

To investigate a pathway parallel to Whi5 inactivation. Cln3-CDK activity is not essential for cell cycle entry indicating that other pathways exist that activate Cln1/2-CDKs. *BCK2* is one such factor (Epstein et al. 1994). Cells with *BCK2* deleted are large and delay *CLN1* and *CLN2* transcription. In addition, deletion of the gene causes lethality in cells lacking Cln3. To determine whether disomes interfere with cell cycle entry through *BCK2*, we examined the size of disomic cells lacking this gene. If aneuploidy

were inhibiting *BCK2* activity, then we would expect that wild type and aneuploid cells lacking this gene will be of the same size (and assuming that deletion of *BCK2* does not affect progression through other stages of the cell cycle). By the same argument, if deletion of *BCK2* leads to an additive increase in cell volume, this would indicate that aneuploidy is not acting through this pathway. Disomes VIII, XI, and XVI cells lacking *BCK2* exhibited an increased and additive cell size compared to disomic cells wild type for the gene (Figure 12E). This result is consistent with that idea that aneuploidy is not necessarily delaying cell cycle entry by interfering with Bck2 activity.

Discussion

Our studies indicate that aneuploidy delays entry into the cell cycle in two ways: it inhibits growth and it increases the critical size for budding. As a result aneuploid cells spend more time in G1 than euploid cells.

The growth defect of aneuploid cells.

Most of the aneuploid strains we examined show a growth defect during G1. This growth defect is not nearly as dramatic as that seen in mutants impaired in ribosome biogenesis or protein synthesis, but the defect is nevertheless readily observable by careful cell volume measurements. Why have we not seen this defect however using methods to assess protein synthesis activity? It is possible that aneuploid cells are defective in cell volume accumulation but not protein synthesis, with the implication that

aneuploid cells must be much denser than euploid cells. We favor the idea that the defect in cell volume accumulation reflects an overall defect in macromolecule biosynthesis, but the defect is too subtle to be detected by methods such as ^{35}S-methionine incorporation and polyribosome quantification.

What is the basis for the cell volume accumulation defect of aneuploid yeast strains? Our analyses indicate that it does not stem from diminished amino acid pools or a constitutive active amino acid starvation response. Rather we propose that macromolecule biosynthesis is hampered in aneuploid cells. Two, not mutually exclusive scenarios, can explain this defect. Changes in the expression level of key regulators of macromolecule biosynthesis, vesicle fusion, protein sorting and/or energy production are altered in aneuploid cells, which in turn leads to a slowing of growth. In this scenario the reason for the growth defect would be different in every single disomic strains. The analysis of genes whose translation is up- or down-regulated could provide evidence for such a scenario. We observe decreased translation of over 500 genes in disome XVI cells compared to wild-type cells. Among these genes are some whose products are involved in phosphate metabolism (*PHO89, PHO5, PHO12, GIT1* and *SPL2*) and some ribosomal proteins (including *RPS12, RPL16A, RPL35A, RPS23A, RPS20, RPS5, RPS6B, RPL35B*, among others) and ribosomal biogenesis related genes (including *ESF1, RRP8, NSR1, EBP2* and others). The low-abundance of these factors could contribute to the growth defect we observe in disome XVI cells.

It is also possible that an increased burden on the translation machinery hampers cell growth. Our data indicate that the additional chromosomes are actively transcribed and translated. The number of ribosomes associated with chromosome XVI encoding RNAs is, overall, twice that of the other chromosomes. The method we employed to measure translation however does not allow us to assess whether the translation of the additional chromosome is associated with a concomitant overall decrease in translation. Furthermore, this hypothesis makes two assumptions that we have not yet tested. (1) the protein production machinery is rate limiting and (2) the proteins that are produced from the additional chromosome are not able to contribute to cell mass increase in the same manner as do proteins that are produced from genomes with balanced karyotypes. Although we do not know whether these two assumptions are accurate, we nevertheless favor the protein synthesis limitation idea over the idea that changes in the gene dosage of individual proteins are responsible for the observed growth defect. The reason for this preference is the observation that a remarkably good inverse correlation exists between the size of the additional chromosome and the growth defect of aneuploid cells. Specific genes interfering with different aspects of growth would not be expected to result in such a correlation.

Aneuploidy interferes with the cell cycle machinery governing START.

Of the fifteen aneuploid strains studied, twelve showed defects in entry into the cell cycle. Analysis of a subset of these, disome IV and XI, showed a delay in *CLN2* mRNA accumulation and the cell cycle entry delay of three disomic strains, disome IV,

VIII or XI, were suppressed by high levels of Cln2. These results suggest that aneuploidy interferes with Cln2 accumulation at least in these three aneuploids strains and we assume in other aneuploid yeast strains also.

As with the effects of aneuploidy on cell growth, we must ask whether aneuploidy interferes with the G1 – S phase transition because changes in the expression level of individual proteins interfere with cell cycle entry or whether some general property of aneuploid cells brings about this cell cycle delay? Can we obtain evidence for the first possibility from our translation analysis of disome XVI cells? As already mentioned, *FAR1* is under translated in disome XVI cells. We cannot exclude the possibility that yet to be identified Cln-CDK regulators exist. For example, *SFG1* is under-translated relative to wild-type cells in disome XVI cells. Sfg1 has been shown to play a role in cell cycle progression in G1 (White et al. 2008).

While it is possible that selective genes interfere with cell cycle entry we favor the idea that the cell cycle entry delay of aneuploid cells reflects a response to some aspect of the aneuploid state. For example it is known that an increase in ploidy leads to an increase in cell size. Given that the cell cycle entry delay of aneuploid cells is not very well correlated with the size of the additional chromosome, we do not consider this possibility likely. Instead we speculate that the protein stoichiometry imbalances caused by aneuploidy not only lead to an increased burden on the protein folding and degradation machinery but also provoke a transient G1 delay as is seen in so many other

stress responses. Indeed proteotoxic stress induced by heat shock, for instance, causes a transient G1 delay (Li and Cai 1999).

Most signals controlling cell cycle entry interfere with the accumulation of Cln3-CDK activity. It was therefore surprising that the cell cycle entry defect of aneuploid strains was only partially suppressed by the deletion of *WHI5*. In fact, the degree by which deletion of this cell cycle inhibitor decreased the critical size of aneuploid cells was less than in wild-type cells, suggesting that if at all, aneuploidy affected Cln3-CDK control of Whi5 in a minor way. *BCK2* also regulates SBF transcription. However, deletion of this gene increased the size of aneuploid cells thus excluding the possibility that aneuploidy interfered with cell cycle entry by interfering with *BCK2* function. Aneuploidy could interfere directly with SBF's ability to promote transcription of *CLN1* and *CLN2* or the recruitment of the basic transcription machinery. Finally, it is possible that yet to be discovered pathways exist that promote the accumulation of *CLN1/2* transcription, which aneuploidy interferes with.

The effects of aneuploidy on cell cycle progression in other systems.

Our studies of aneuploid yeast and mouse cells revealed that in both systems, aneuploidy causes proteotoxic stress. Aneuploid yeast cells exhibit sensitivity to translation and protein folding inhibitors as well as high temperature (Torres et al. 2007). The finding that translation of the protein folding factors *SSA1, HSP31, HSP104, SSE2, HSP78, HSP42* and *HSP82* is increased in disome XVI cells (this study) further supports

this idea. Is there evidence for a conserved effect on cell cycle progression? Aneuploid primary MEFs exhibit cell proliferation defects (Williams et al. 2008) but the basis of this defect has not been explored. A study of different aneuploid fission yeast cells created by triploid meioses, however showed that these cells also exhibit a G1 delay (Niwa et al. 2006). It thus appears that in this organism too, aneuploidy interferes with the cell's ability to enter the cell cycle. Whether aneuploidy elicits a growth defect in this yeast has not been explored. Determining the molecular mechanisms underlying this effect of aneuploidy on progression through G1 will be an important aspect of understanding how aneuploidy impacts cell physiology.

Materials and methods

Yeast strains, plasmids, and growth conditions

All yeast strains are derivatives of W303 and are described in Table 4. Yeast strains were generated and manipulated as described previously (Gutherie and Fink 1991). The *GCN4-LacZ* construct described in Hinnebusch (1985) was integrated at the *URA3* locus. Cells were grown at 30°C in either YEP supplemented with 2% raffinose or glucose and synthetic media containing G418.

Elutriation

Cells were grown in 1 or 2 L of synthetic media supplemented with 2% raffinose at 30°C to an OD_{600} less than 2. Cells were collected by centrifugation and resuspended in 30 ml of cold YEP. The resuspended cells were then sonicated and kept at 4°C for the duration of the elutriation. A Beckman elutriation rotor JE 5.0 was chilled to 4°C and equilibrated with YEP at 4000 rpm. Cells were then loaded at a pump speed of around 20 ml/min and

allowed to equilibrate for 15-20 minutes. Pump speed was then increased until small unbudded cells exited the elutriation chamber. Cells were then concentrated and resuspended in YEP supplemented with glucose at 30°C.

Cell volume determination

To determine the cell volume of elutriated cells, 50-100 uL of culture were collected and diluted into Isoton II solution (Beckman) to give <10% saturation when processed with a Beckman Coulter Multisizer 3. For each timepoint, 50,000 cells were counted and sized. Cell volume distributions were smoothed with a rolling window of 3 bins. From these distributions we obtained median, mean, and mode statistical descriptions for the population. The modal values were used for the plots.

Protein synthesis analysis

Cells were grown to exponential phase in YEP supplemented with 2% glucose that was supplemented with 12 μL of S35-Cys (120 μCi final) and 12 μL of S35-Met (120 μCi final) and incubated at room temperature. Radiactively labeled amino acids were obtained from Perkin Elmer at 10 mCi/mL stock concentrations. Time points were collected every 30 minutes by collecting two 250 μL aliquots per sample. Aliquots were immediately mixed with 250 μL of cold 10% trichloroacetic acid (TCA) and incubated for at least 20 min at 4°C. 100 μL glass beads were added to each sample and cells lysed using a

Biopulverizer 101. Samples were then incubated at 95°C for 10 min to destroy charged amino acids. Samples were cooled, extracts cleared, and the supernatant spotted on a glass filter. Samples were washed with ~10 ml of 5% TCA followed by 100% ethanol. Filters were then air dried and mixed with scintillation fluid. Incorporation was determined with a scintillation counter. The two duplicate aliquots were averaged and reported. Cell number was also determined for each sample and used to normalized radioactive incorporation.

Polyribosome profile analysis

Polyribosome preparation was performed as described before (Baim et al. 1985). 100 ml cultures were grown at 30°C to an OD_{600} of 0.5-0.7. Cycloheximide was then added to a final concentration of 0.1 mg/ml, cultures incubated for about 5 minutes, and then ice was added directly. Cells were pelleted by centrifugation and washed once in 15 ml of cold lysis buffer and resuspended in 0.5 ml of cold lysis buffer. Glass beads were then added and the cells lysed in a fast-prep machine. The lysates were then centrifuged fours times at 12,000 x g and 4°C until clear. OD_{260} was then measured and samples normalized. Lysates were then layered onto a 11 ml linear sucrose gradient. The gradients were centrifuged in a Beckam SW41 rotor at 30,000 rmp for 3 h and fractionated.

Polysomal footprinting

Polysomal footprinting was carried out as described (Ingolia et al. 2009). In short, 1 L cultures were grown at 30°C to an OD_{600} of 0.7. Cells were collected by filtration and frozen in liquid nitrogen. Extracts were prepared using a mixer mill.Polysomes were isolated and digested with RNase to yield the RNA footprints. These were then isolated using sucrose gradients, purified, reverse transcribed, repurified, and subjected to deep sequencing. Total mRNAs as reference were also isolated and subjected to the same procedures.

Metabolomic analysis

All strains were grown in shake flasks at 30°C and 250 rpm in defined minimal medium containing per liter (adapted from Verduyn et al. 1992): 5 g KH_2PO_4, 0.5 g $MgSO_4$*7 H_2O, 2 g MSG, 1.5 mg EDTA, 4.5 mg $ZnSO_4$ * 7 H_2O, 0.3 mg $CoCl_2$, 1 mg $MnCl_2$*4 H_2O, 0.3 mg CuSO4*5 H2O, 4.5 mg $CaCl_2$ * 2 H2O, 3 mg $FeSO_4$ * 7 H_2O, 0.4 mg $NaMoO_4$ * 2 H_2O, 1mg H_3BO_3, 0.1 mg KI. Filter-sterilized vitamins were added separately to a final concentration per liter of: 0.005 mg biotin, 0.1 mg Ca-pantothenate, 0.1 mg nicotinic acid, 2.5 mg inositol, 0.1 mg pyridoxine, 0.02 mg p-aminobenzoic acid, 0.1 mg thiamine. The medium was buffered with 100 mM KH-phtalate at a pH of 5. Due to the genetic markers the medium was supplemented with the following compounds per liter: 0.031 g lysine, 0.02 g uracil, 0.24 g leucine, 0.08 g adenine, 0.02 g tryptophane, 0.021 g methionine, 0.2 g geneticin (G-418). Cells were grown to an OD_{600} between 0.7 and 1.5 when metabolism of 1 ml culture was arrested by quenching in -40°C methanol 10 mM ammonium acetate. After centrifugation at -9°C (3 min, 5000 rpm) the samples

were stored at -80°C. Intracellular metabolites were extracted by incubation in 75% ethanol 10 mM ammonium acetate for 3 min at 80°C . The supernatant was dried using a vacuum centrifuge. For quantification the dried extracts were derivatized with TBDMS (N-tert-butyldimethylsilyl-N-methyltrifluoroacetamide). The metabolites were separated by gas chromatography and injected to a ToF spectrometer as described in Ewald et al. 2009 .

Liquid beta-galactosidase assay

Cell extracts and activity measurements were carried out as described previously (Dever, T 1997). Cells were grown in –His synthetic media supplemented with 2% glucose overnight to saturation. 35 ml cultures were then inoculated with 700 uL of the saturated cultures and grown for 2 hours at 30°C. After these two hours, each culture was supplemented with 1 M 3-aminotriazole to a final concentration of 100 mM. Cells not supplemented with 3-AT were grown for an additional 6 hours at 30°C while those supplemented with 3-AT for an additional 8 hours. Cells were then centrifuged and resuspended in lysis buffer, and lysed using glass beads. The lysate was cleared by centrifugation and the total protein content determined using the method of Bradford. Beta-galactosidase activity was then measured

Northern blot analysis

Total RNA was isolated as described in Cross and Tinkelenberg (1991). Northern blots were performed as described in Hochwagen et al. (2005). Cells were grown at 30°C in synthetic media supplemented with 2% raffinose until OD_{600} <2. Cells were then elutriated as described and released into the cell cycle. Time points were taken right until after the critical size had been reached. Blots were probed for *CLN2* and *ACT1* served as loading control.

Figure 1

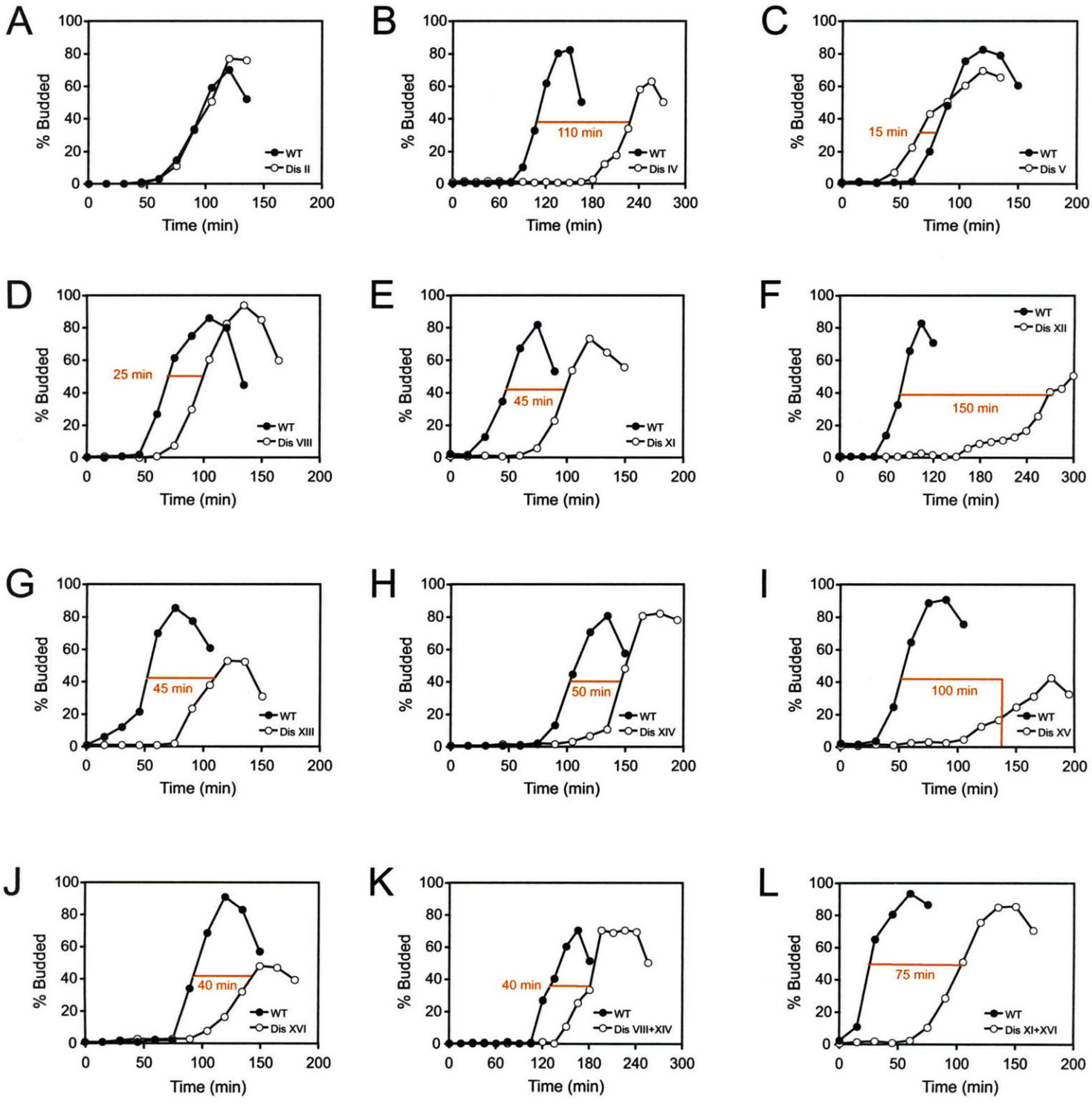
A
% Budded
Time (min)
WT
Dis II
B
110 min
Dis IV
C
15 min
Dis V
D
25 min
Dis VIII
E
45 min
Dis XI
F
150 min
Dis XII
G
45 min
Dis XIII
H
50 min
Dis XIV
I
100 min
Dis XV
J
40 min
Dis XVI
K
40 min
Dis VIII+XIV
L
75 min
Dis XI+XVI

Figure 1. Cells carrying an extra chromosome delay budding.
(A-L) Wild type ([A-O], A11311, closed symbols), disome II ([A], A6863, open symbols), disome IV ([B], A12687, open symbols), disome V ([C], A14479, open symbols), disome VIII ([D], A13628, open symbols), disome XI ([E], A13771, open symbols), disome XII ([F], A15566, open symbols), disome XIII ([G], A15567, open symbols), disome XIV ([H], A13979, open symbols), disome XV ([I], A12697, open symbols), disome XVI ([J], A12700, open symbols), disome VIII + XIV ([K], A15615, closed symbols), and disome XI + XVI ([L], A12699, closed symbols) were grown at 30°C in synthetic media supplemented with 2% glucose. Small daughter cells were then isolated by centrifugal elutriation and released into the cell cycle at 30°C in YEP supplemented with 2% glucose. Time points were taken every 15 minutes and the percentage of budded cells determined.

Figure 2

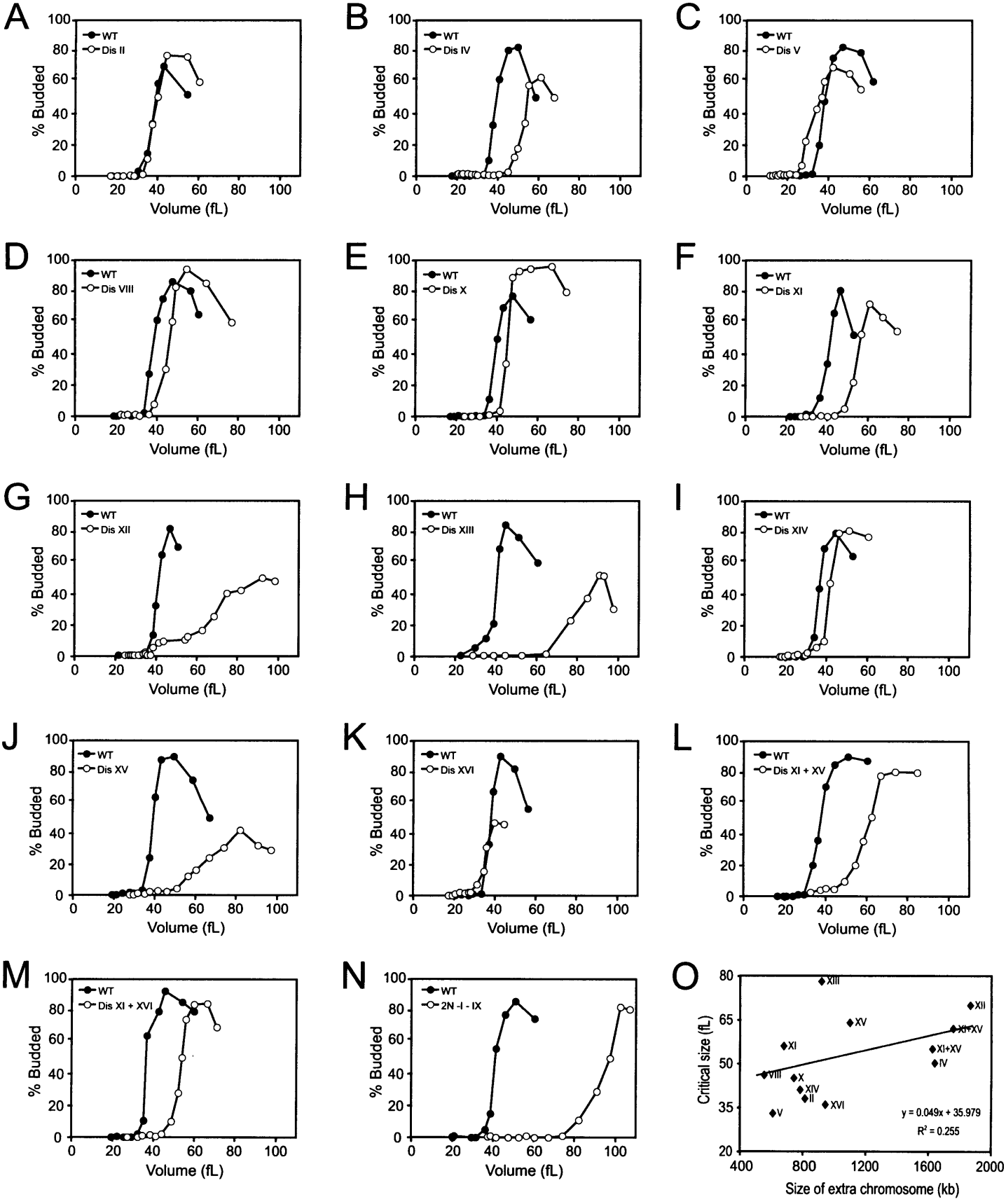
A
WT
Dis II
B
WT
Dis IV
C
WT
Dis V
D
WT
Dis VIII
E
WT
Dis X
F
WT
Dis XI
G
WT
Dis XII
H
WT
Dis XIII
I
WT
Dis XIV
J
WT
Dis XV
K
WT
Dis XVI
L
WT
Dis XI + XV
M
WT
Dis XI + XVI
N
WT
2N -I - IX
% Budded
Volume (fL)
O
Critical size (fL)
Size of extra chromosome (kb)
XIII
XII
XV
XI+XV
XI
XI+XV
IV
VIII
X
XIV
II
XVI
V
y = 0.049x + 35.979
R² = 0.255

Figure 2. Cells carrying an extra chromosome delay entry into the cell cycle by increasing the critical size for budding.
(A-O) Wild type ([A-O], A11311, open symbols), disome II ([A], A6863, closed symbols), disome IV ([B], A12687, closed symbols), disome V ([C], A14479, closed symbols), disome VIII ([D], A13628, closed symbols), disome X ([E], A12689, closed symbols), disome XI ([F], A13771, closed symbols), disome XII ([G], A15566, closed symbols), disome XIII ([H], A15567, closed symbols), disome XIV ([I], A13979, closed symbols), disome XV ([J], A12697, closed symbols), disome XVI ([K], A12700, closed symbols), disome XI + XV ([L], A12691, closed symbols), disome XI + XVI ([M], A12699, closed symbols), and disome 2N – I - IX ([N], A15245, closed symbols) were grown at 30°C in synthetic media supplemented with 2% glucose. Small daughter cells were then isolated by centrifugal elutriation at 4°C and released into the cell cycle at 30°C in YEP supplemented with 2% glucose. Time points were taken every 15 minutes, cell size measured with a Coulter counter, and the percentage of budded cells determined. Graphs represent volume versus budding. The critical size is defined as the volume at which 50% of the cells are budded. (O) Correlation between the critical size for budding and the size of the extra chromosome in the disome. In general, as the size of the extra chromosome increases, so does the critical size for budding.

Figure 3

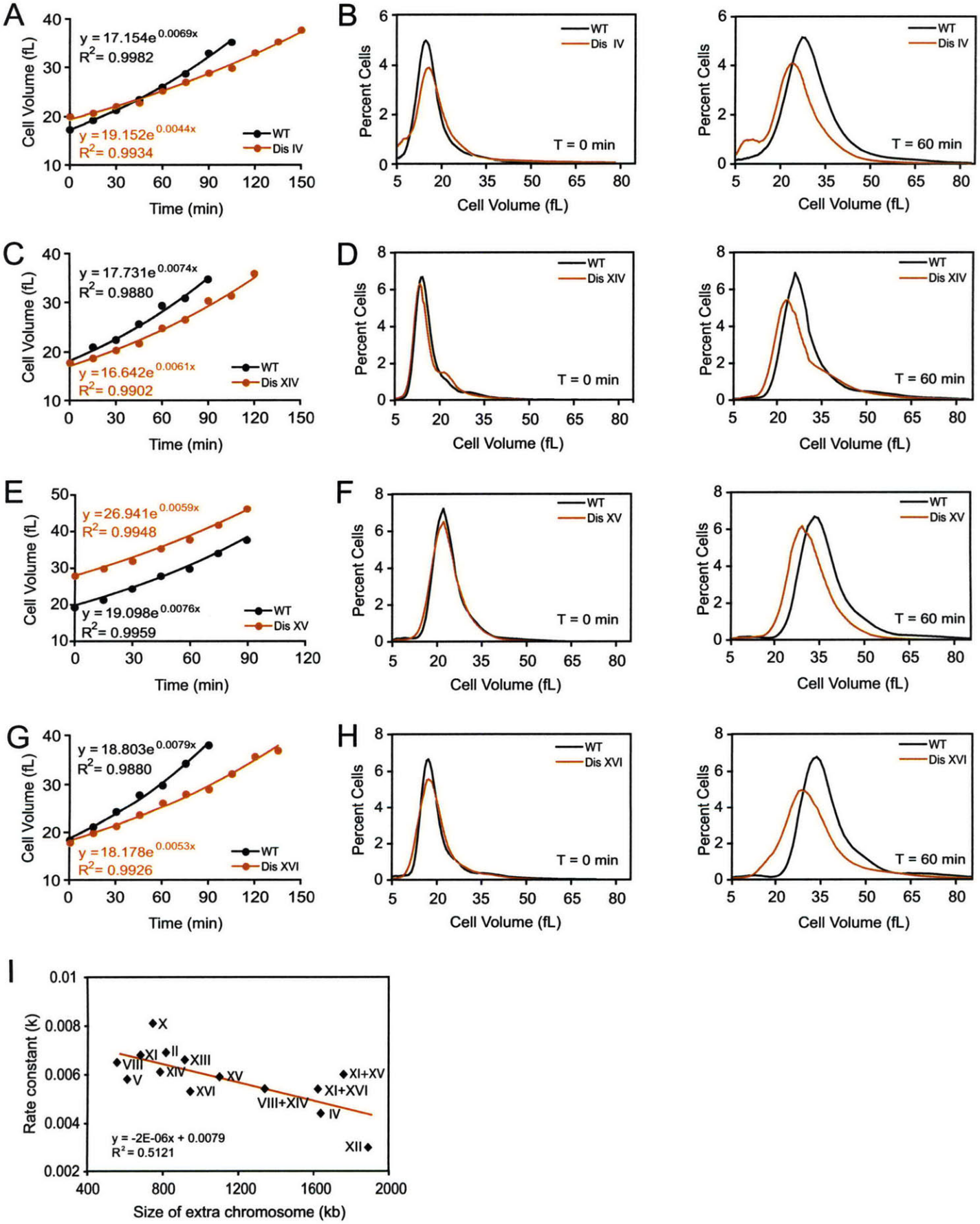
A
y = 17.154e^0.0069x
R² = 0.9982
y = 19.152e^0.0044x
R² = 0.9934
WT
Dis IV
Cell Volume (fL)
Time (min)
B
WT
Dis IV
T = 0 min
Percent Cells
Cell Volume (fL)
WT
Dis IV
T = 60 min
Percent Cells
Cell Volume (fL)
C
y = 17.731e^0.0074x
R² = 0.9880
y = 16.642e^0.0061x
R² = 0.9902
WT
Dis XIV
Cell Volume (fL)
Time (min)
D
WT
Dis XIV
T = 0 min
Percent Cells
Cell Volume (fL)
WT
Dis XIV
T = 60 min
Percent Cells
Cell Volume (fL)
E
y = 26.941e^0.0059x
R² = 0.9948
y = 19.098e^0.0076x
R² = 0.9959
WT
Dis XV
Cell Volume (fL)
Time (min)
F
WT
Dis XV
T = 0 min
Percent Cells
Cell Volume (fL)
WT
Dis XV
T = 60 min
Percent Cells
Cell Volume (fL)
G
y = 18.803e^0.0079x
R² = 0.9880
y = 18.178e^0.0053x
R² = 0.9926
WT
Dis XVI
Cell Volume (fL)
Time (min)
H
WT
Dis XVI
T = 0 min
Percent Cells
Cell Volume (fL)
WT
Dis XVI
T = 60 min
Percent Cells
Cell Volume (fL)
I
Rate constant (k)
Size of extra chromosome (kb)
y = -2E-06x + 0.0079
R² = 0.5121
X
XI
II
XIII
VIII
XIV
XV
XI+XV
V
XVI
XI+XVI
VIII+XIV
IV
XII

Figure 3. Cells carrying an extra chromosome decrease the rate of volume accumulation during the G1 phase of the cell cycle.
(A, C, E, G) Wild type ([A-I], A11311, black), disome IV ([A], A12687, red), disome XIV ([C], A13979, red), disome XV ([E], A12697, red), disome XVI ([G], A12700, red), were grown at 30°C in synthetic media supplemented with 2% glucose. Small daughter cells were then isolated by centrifugal elutriation and released into the cell cycle at 30°C in YEP supplemented with 2% glucose. Time points were taken every 15 minutes and cell size measured with a Coulter counter. Curves were fitted to a simple exponential. (B, D, F, H) Comparison of the cell size distributions for wild-type and disomic cells after 1 hour of growth. Wild type ([B-H], A11311, black), disome IV ([B], A12687, red), disome XIV ([D], A13979, red), disome XV ([F], A12697, red), disome XVI ([H], A12700, red) cells were grown and G1 cells isolated as before. Time points were taken every 15 minutes, cell size measured with a Coulter counter, and the percentage of budded cells determined. (I) Correlation between the growth rate constant k and the size of the extra chromosome present the particular disome. In general, as the size of the extra chromosome increases, the rate constant decreases.

Figure 4

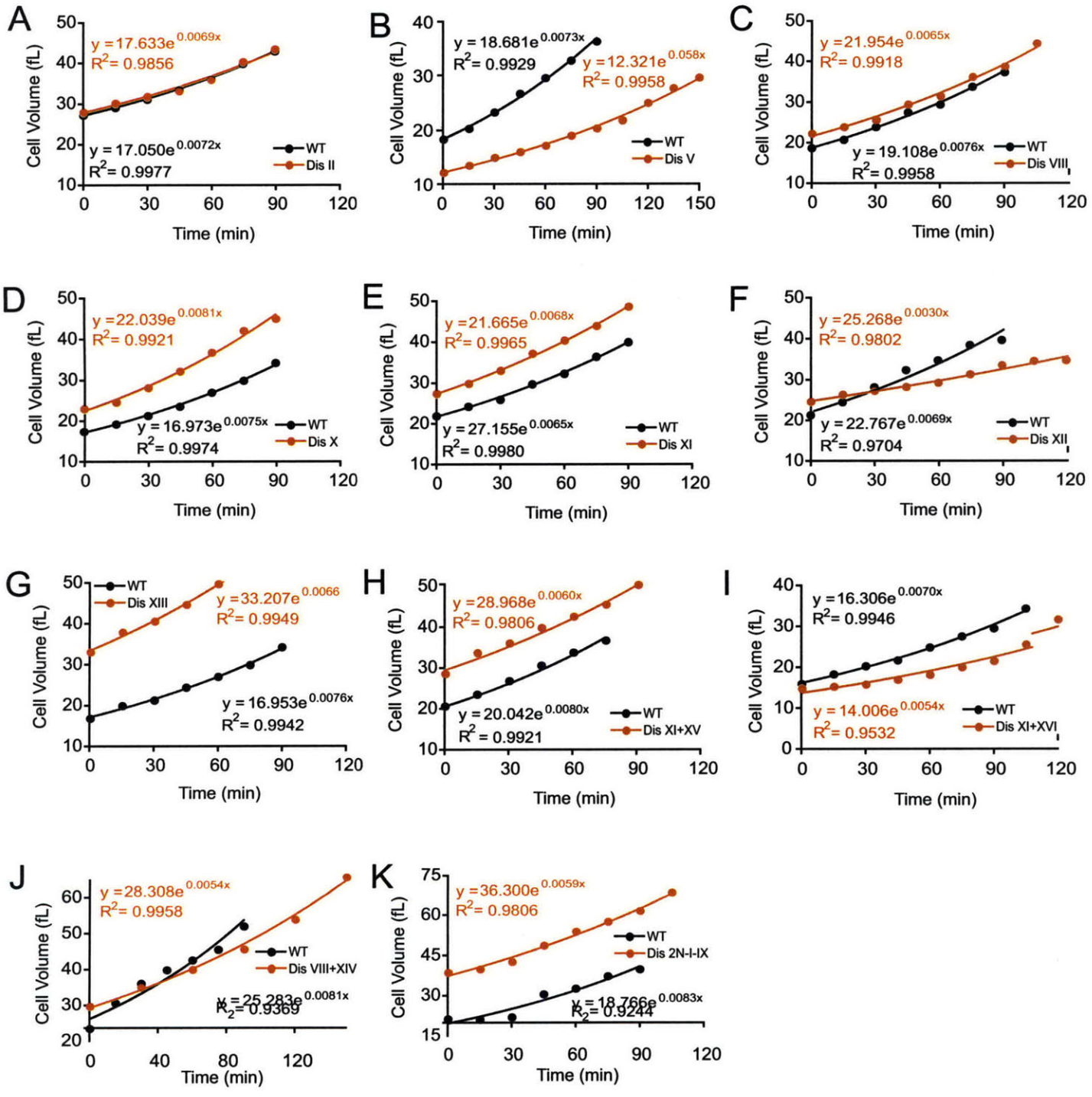
A
y = 17.633e^0.0069x
R²= 0.9856
y = 17.050e^0.0072x
R²= 0.9977
WT
Dis II
B
y = 18.681e^0.0073x
R²= 0.9929
y = 12.321e^0.058x
R²= 0.9958
WT
Dis V
C
y =21.954e^0.0065x
R²= 0.9918
y = 19.108e^0.0076x
R²= 0.9958
WT
Dis VIII
D
y =22.039e^0.0081x
R²= 0.9921
y = 16.973e^0.0075x
R²= 0.9974
WT
Dis X
E
y =21.665e^0.0068x
R²= 0.9965
y = 27.155e^0.0065x
R²= 0.9980
WT
Dis XI
F
y =25.268e^0.0030x
R²= 0.9802
y = 22.767e^0.0069x
R²= 0.9704
WT
Dis XII
G
WT
Dis XIII
y =33.207e^0.0066
R²= 0.9949
y = 16.953e^0.0076x
R²= 0.9942
H
y =28.968e^0.0060x
R²= 0.9806
y = 20.042e^0.0080x
R²= 0.9921
WT
Dis XI+XV
I
y =16.306e^0.0070x
R²= 0.9946
y = 14.006e^0.0054x
R²= 0.9532
WT
Dis XI+XVI
J
y =28.308e^0.0054x
R²= 0.9958
WT
Dis VIII+XIV
y = 25.283e^0.0081x
R²= 0.9369
K
y =36.300e^0.0059x
R²= 0.9806
WT
Dis 2N-I-IX
y = 18.766e^0.0083x
R²= 0.9244
Cell Volume (fL)
Time (min)

Figure 4. Cells carrying an extra chromosome decrease the rate of volume accumulation during the G1 phase of the cell cycle. (A-K) Wild type ([A-K], A11311, black), disome II ([A], A6863, red),), disome V ([B], A14479, red), disome VIII ([C], A13628, red), disome X ([D], A12689, red), disome XI ([E], A15245), disome XII ([F], A15566, red), disome XIII ([G], A15567, red), disome XI + XV ([H], A12691, red), disome XI + XVI ([I], A12699, red), disome VIII + XIV ([J], A15615, red), and disome 2N – I - IX ([K], A15245 red) cells were grown at 30°C in synthetic media supplemented with 2% glucose. Small daughter cells were then isolated by centrifugal elutriation and released into the cell cycle at 30°C in YEP supplemented with 2% glucose. Time points were taken every 15 minutes and cell size measured with a Coulter counter. Curves were fitted to a simple exponential.

Figure 5

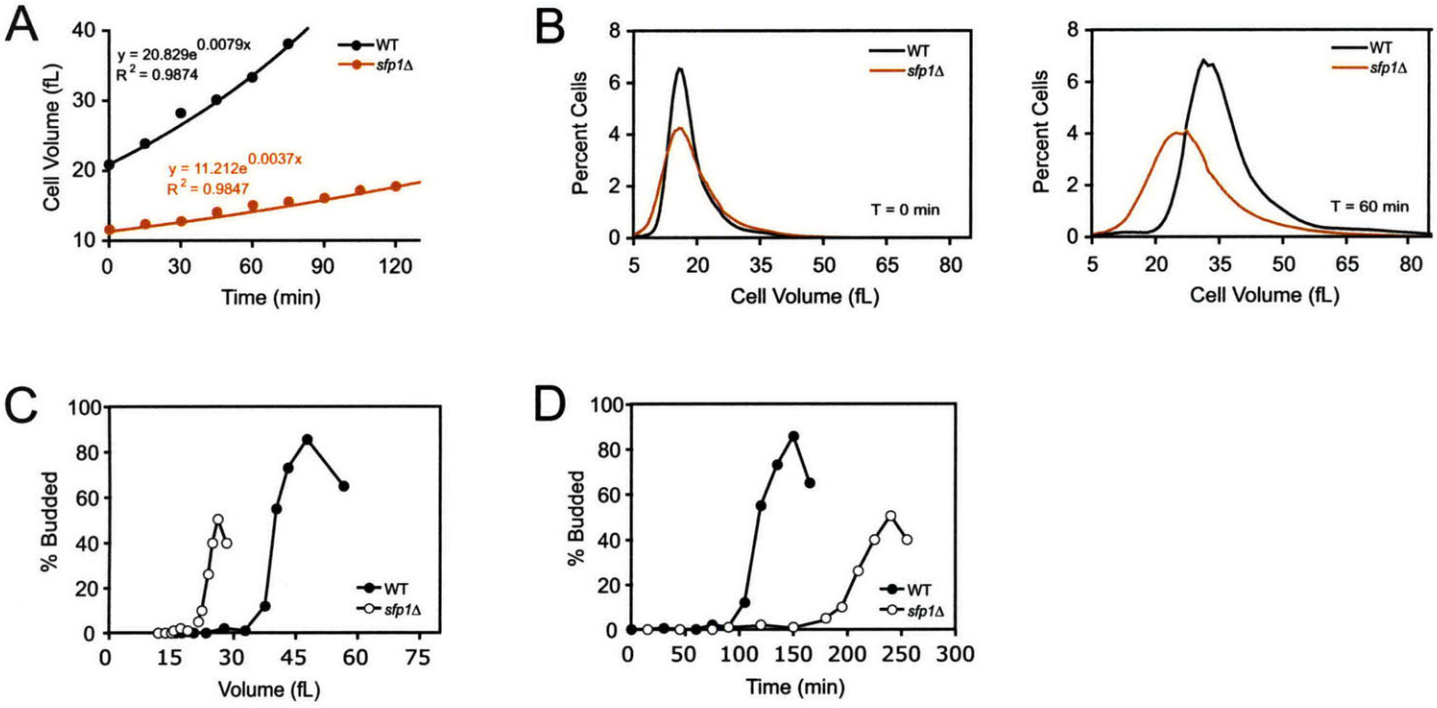
A
y = 20.829e^0.0079x
R^2 = 0.9874
y = 11.212e^0.0037x
R^2 = 0.9847
WT
sfp1Δ
Cell Volume (fL)
Time (min)
B
Percent Cells
T = 0 min
T = 60 min
Cell Volume (fL)
C
% Budded
Volume (fL)
D
% Budded
Time (min)

Figure 5. Deletion of *SFP1* delays entry into the cell cycle by decreasing the rate of volume accumulation.
(A) Deletion of *SFP1* results in slow volume accumulation during G1. (B) Cell size distributions for wild type and *sfp1Δ* cells are different after one hour of growth. (C) *sfp1Δ* cells bud at a smaller volume than wild type cells. (D) *sfp1Δ* cells delay budding.

Figure 6

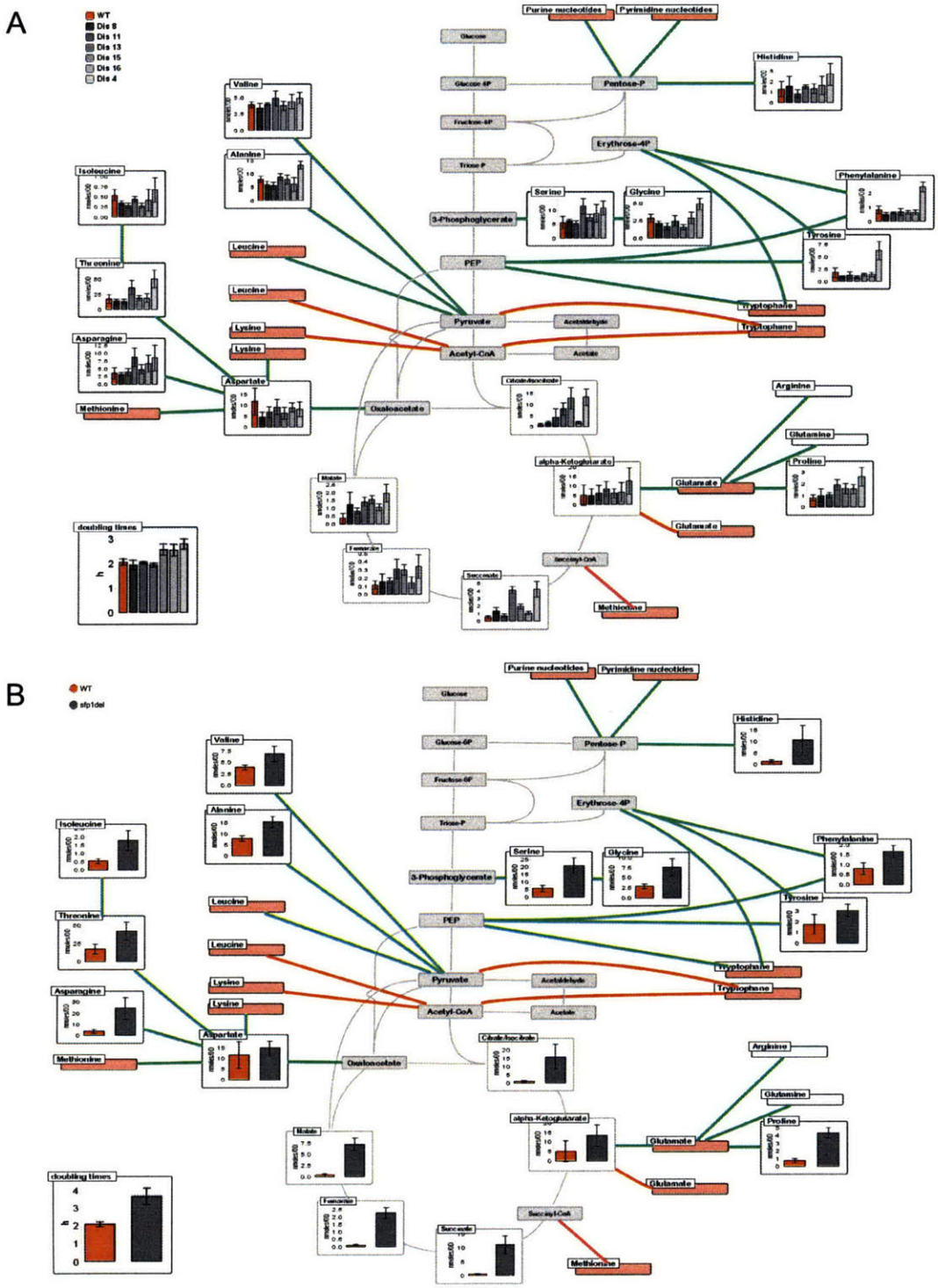
A
WT
Dis 8
Dis 11
Dis 13
Dis 15
Dis 16
Dis 4
Purine nucleotides
Pyrimidine nucleotides
Glucose
Glucose-6P
Pentose-P
Histidine
Fructose-6P
Erythrose-4P
Triose P
Phenylalanine
Serine
Glycine
3-Phosphoglycerate
Tyrosine
Valine
Alanine
Isoleucine
Leucine
PEP
Threonine
Tryptophane
Leucine
Pyruvate
Acetaldehyde
Lysine
Acetyl-CoA
Acetate
Asparagine
Lysine
Aspartate
Arginine
Methionine
Oxaloacetate
Glutamine
Proline
alpha-Ketoglutarate
Glutamate
Malate
Glutamate
doubling times
Fumarate
Succinyl-CoA
Succinate
Methionine
B
WT
sfp1del
Purine nucleotides
Pyrimidine nucleotides
Glucose
Glucose-6P
Pentose-P
Histidine
Fructose-6P
Erythrose-4P
Triose-P
Phenylalanine
Serine
Glycine
3-Phosphoglycerate
Tyrosine
Valine
Alanine
Isoleucine
Leucine
PEP
Threonine
Tryptophane
Leucine
Pyruvate
Acetaldehyde
Lysine
Acetyl-CoA
Acetate
Asparagine
Lysine
Aspartate
Arginine
Methionine
Oxaloacetate
Glutamine
Proline
alpha-Ketoglutarate
Glutamate
Malate
Glutamate
doubling times
Fumarate
Succinyl-CoA
Succinate
Methionine

Figure 6. Metabolomic analysis shows that free amino acid pools are not depleted in aneuploid cells.
(A) Metabolomic analysis of disomes IV, VIII, XI, XIII, XV and XVI. (B) Metabolomic analysis of a *sfp1Δ* strain. Cells were grown in synthetic media supplemented with the minimum amino acids required for growth. Metabolites were extracted, separated by gas chromatography and injected to a ToF spectrometer.

Figure 7

A

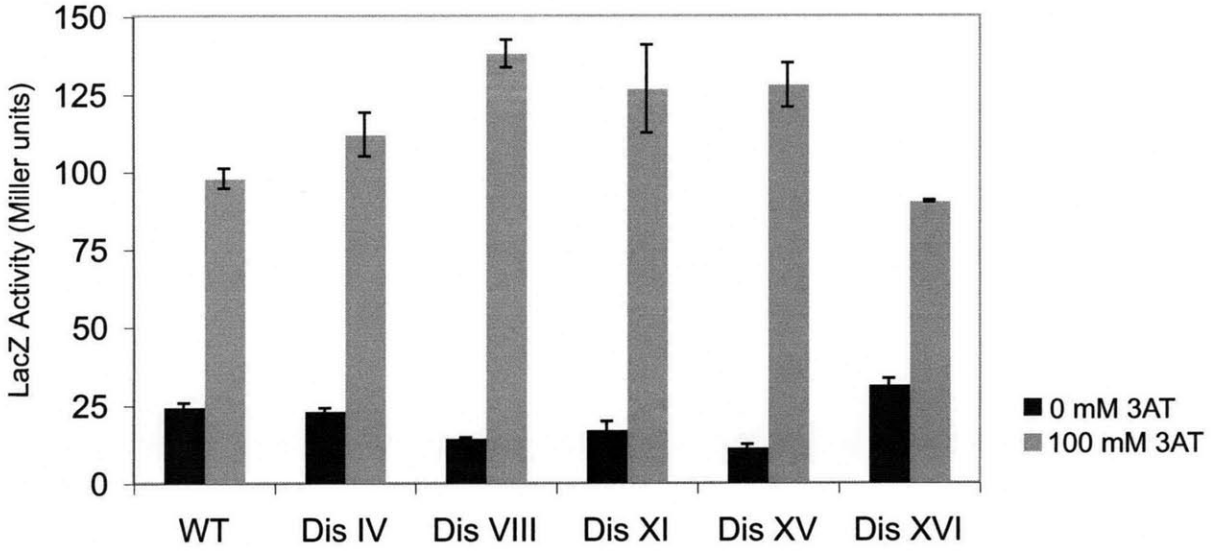
150
125
100
75
50
25
0
LacZ Activity (Miller units)
WT
Dis IV
Dis VIII
Dis XI
Dis XV
Dis XVI
0 mM 3AT
100 mM 3AT

Figure 7. Aneuploidy does not affect the nutritional status of cells nor their response to starvation.
Wild type and aneuploid strains carrying a GCN4-LacZ reporter were starved with 100mM 3-aminotriazole for 5 hours. Cells were then harvested, lysed, and beta-galactosidase activity measures.

Figure 8

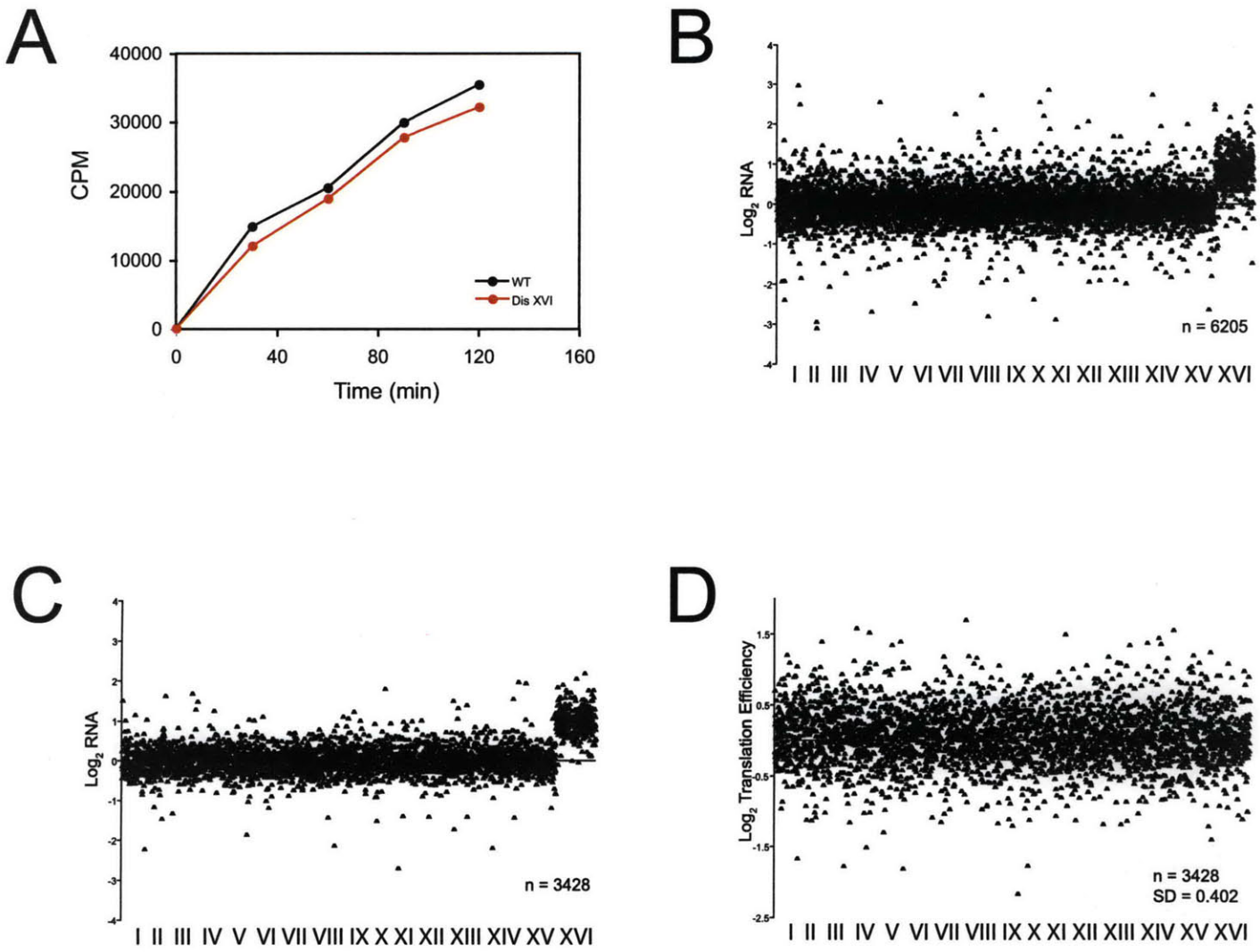
A
40000
30000
20000
10000
0
CPM
0
40
80
120
160
Time (min)
WT
Dis XVI
B
Log2 RNA
n = 6205
I II III IV V VI VII VIII IX X XI XII XIII XIV XV XVI
C
Log2 RNA
n = 3428
I II III IV V VI VII VIII IX X XI XII XIII XIV XV XVI
D
Log2 Translation Efficiency
n = 3428
SD = 0.402
I II III IV V VI VII VIII IX X XI XII XIII XIV XV XVI

Figure 8. Polysomal footprinting analysis reveals no major differences in the translational status of disome XVI and wild type cells.
(A) Protein synthesis rate for wild type and disome XVI cells. Counts were normalized per million cells. (B) Total mRNA levels (C) Ribosome footprint levels. (D) Translation efficiency across chromosomes. The x-axis representes chromosomal position with the very left end being the beginning of chromosome I and the very right the end of chromosome XVI.

Figure 9

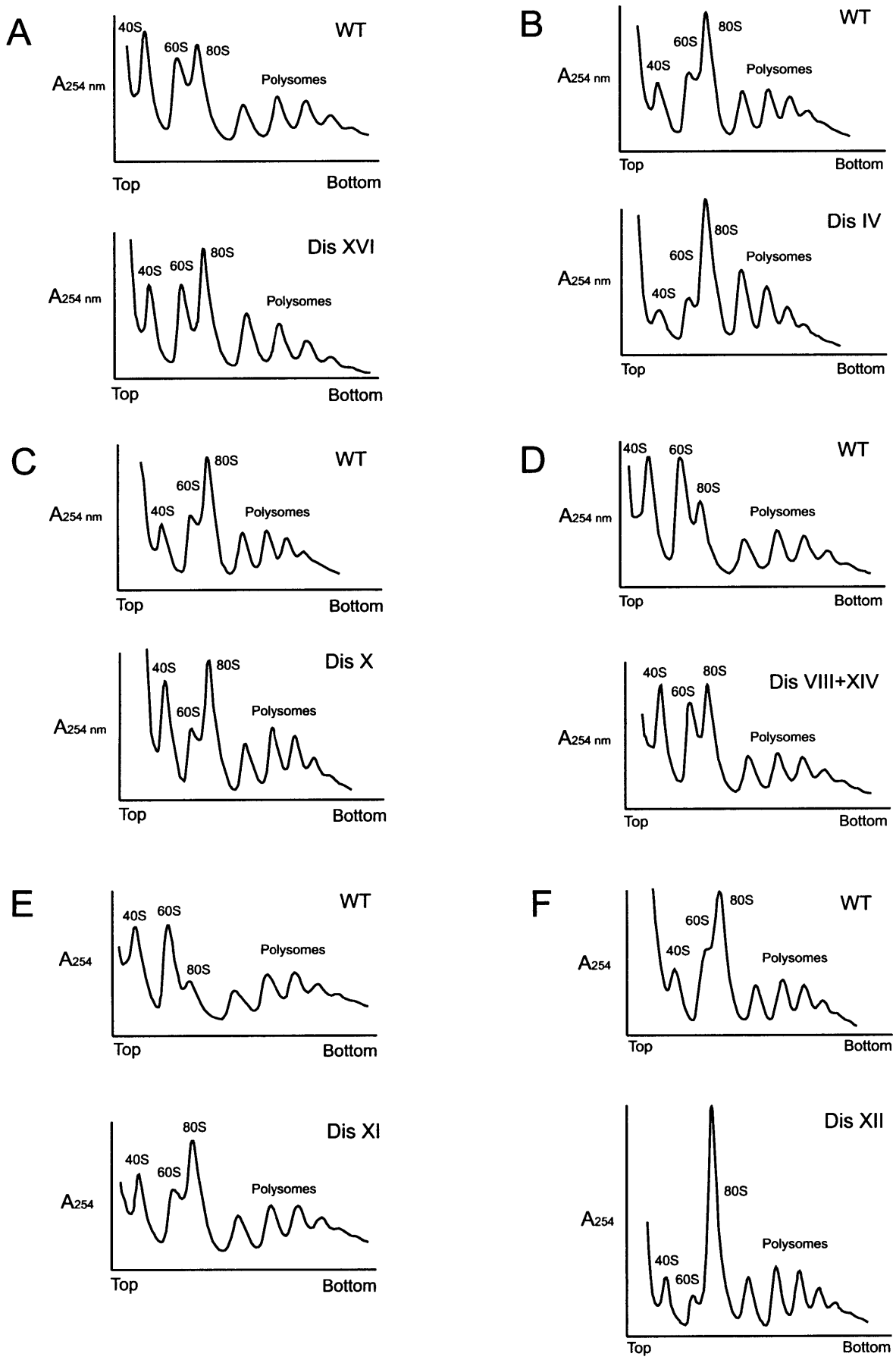
A
WT
40S
60S
80S
Polysomes
A254 nm
Top
Bottom
Dis XVI
B
WT
Dis IV
C
WT
Dis X
D
WT
Dis VIII+XIV
E
WT
Dis XI
F
WT
Dis XII

Figure 9. Polysomal profiles show that aneuploid cells do not have major defects in ribosome synthesis and assembly.
(A-F) Polysomal profiles of wild type ([A-F], top), and disome XVI ([A], A12700, bottom), disome IV ([B], A12687, bottom), disome X ([C], A12689, bottom), disome VIII + XIV ([D], A15615, bottom), disome XI ([E], A13771, bottom), disome XII ([F], A15566, bottom). Extracts from wild type and aneuploid cells were resolved on 10% to 50% sucrose gradients, and the OD_{254} monitored.

Figure 10

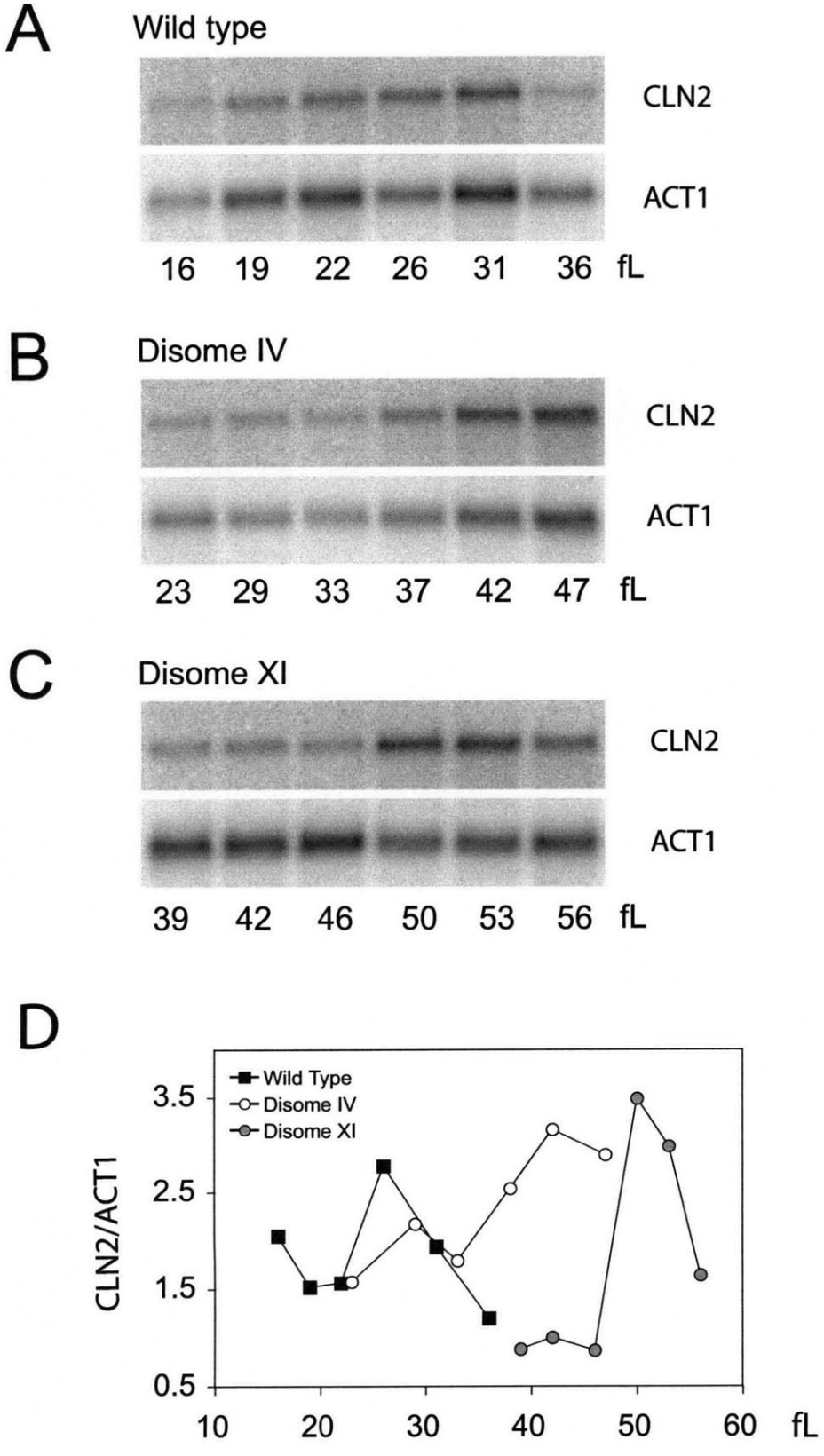
A
Wild type
CLN2
ACT1
16 19 22 26 31 36 fL
B
Disome IV
CLN2
ACT1
23 29 33 37 42 47 fL
C
Disome XI
CLN2
ACT1
39 42 46 50 53 56 fL
D
Wild Type
Disome IV
Disome XI
CLN2/ACT1
3.5
2.5
1.5
0.5
10 20 30 40 50 60 fL

Figure 10. *CLN2* transcription is delayed in aneuploid cells.
Disomic and wild-type cells were grown at 30°C in synthetic media supplemented with 2% raffinose to mid-log phase. Small daughter cells were isolated by centrifugal elutriation at 4°C and then shifted to 30°C in YEP media supplemented with 2% glucose. Cell volume was measured with a Coulter counter. Blots were hybridized with *CLN2* probes. *ACT*1 probes were used as loading controls. (A) Wild-type (A11311). (B) Disome IV (A12687). (C) Disome XI (A13771).

Figure 11

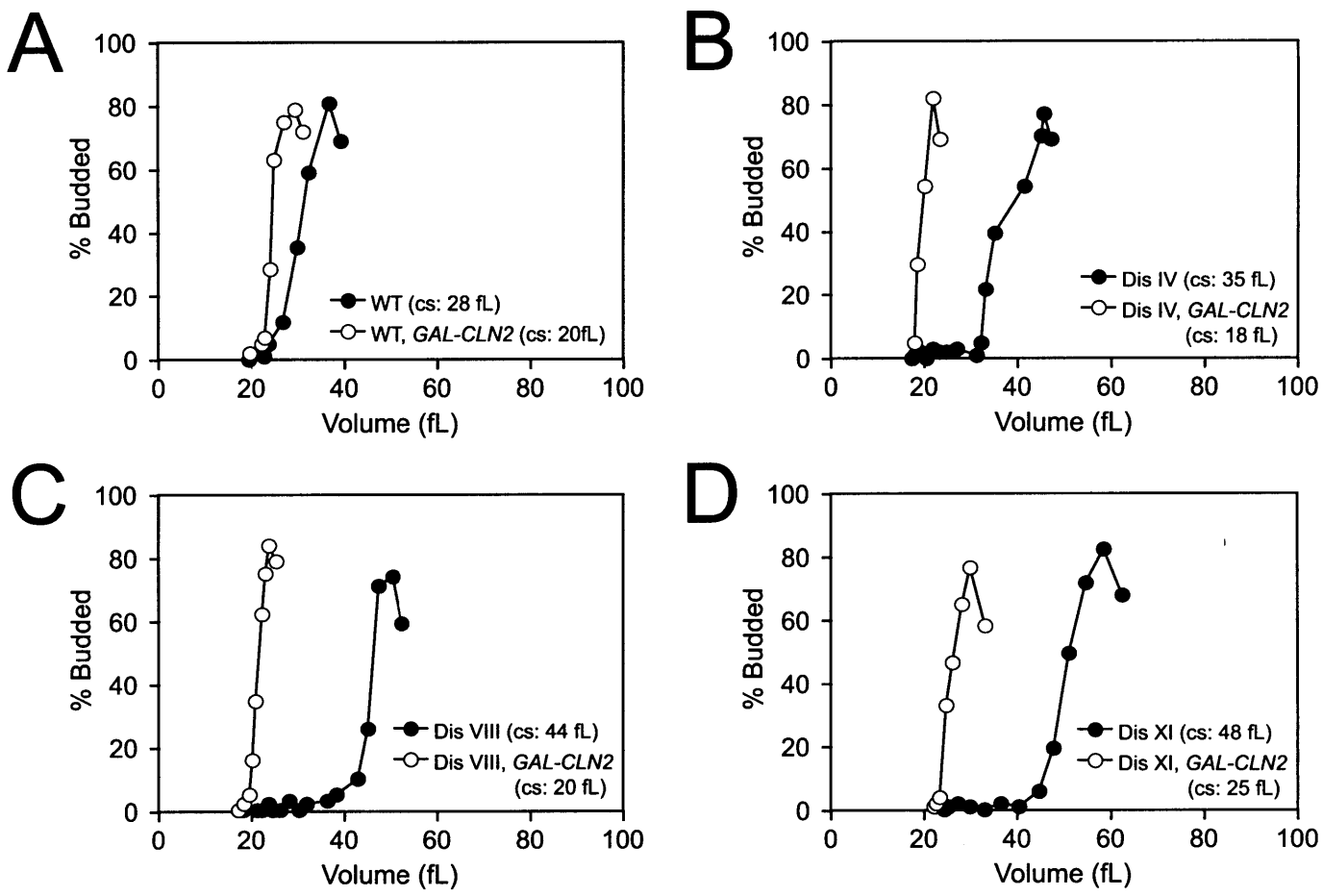
A
B
C
D
% Budded
Volume (fL)
0
20
40
60
80
100
WT (cs: 28 fL)
WT, GAL-CLN2 (cs: 20fL)
Dis IV (cs: 35 fL)
Dis IV, GAL-CLN2 (cs: 18 fL)
Dis VIII (cs: 44 fL)
Dis VIII, GAL-CLN2 (cs: 20 fL)
Dis XI (cs: 48 fL)
Dis XI, GAL-CLN2 (cs: 25 fL)

Figure 11. Overexpression of *CLN2* fully rescues the increase in critical size seen in aneuploid cells.
(A-D) Wild type ([A], A25475, open symbols), disome IV ([B], A25477, open symbols), disome VIII ([C], A25476, open symbols), and disome XI ([D], A25474, open symbols) cells carrying a *GAL-CLN2* construct and wild type ([A], A11311, closed symbols), disome IV ([B], A12687, closed symbols), disome VIII ([C], A13628, closed symbols), and disome XI ([D], A13771, closed symbols) cells without it were grown to mid-log phase in synthetic media supplemented with 2% raffinose. 2% Galactose was then supplemented to the media, and the cultures induced for 1 hour. Small daughter cells were then isolated by centrifugal elutriation at 4°C and then released at 30°C in YEP media containing 2% galactose and 2% raffinose. Time points were taken every 15 minutes, cell size measured with a Coulter counter, and the percentage of budded cells determined

Figure 12

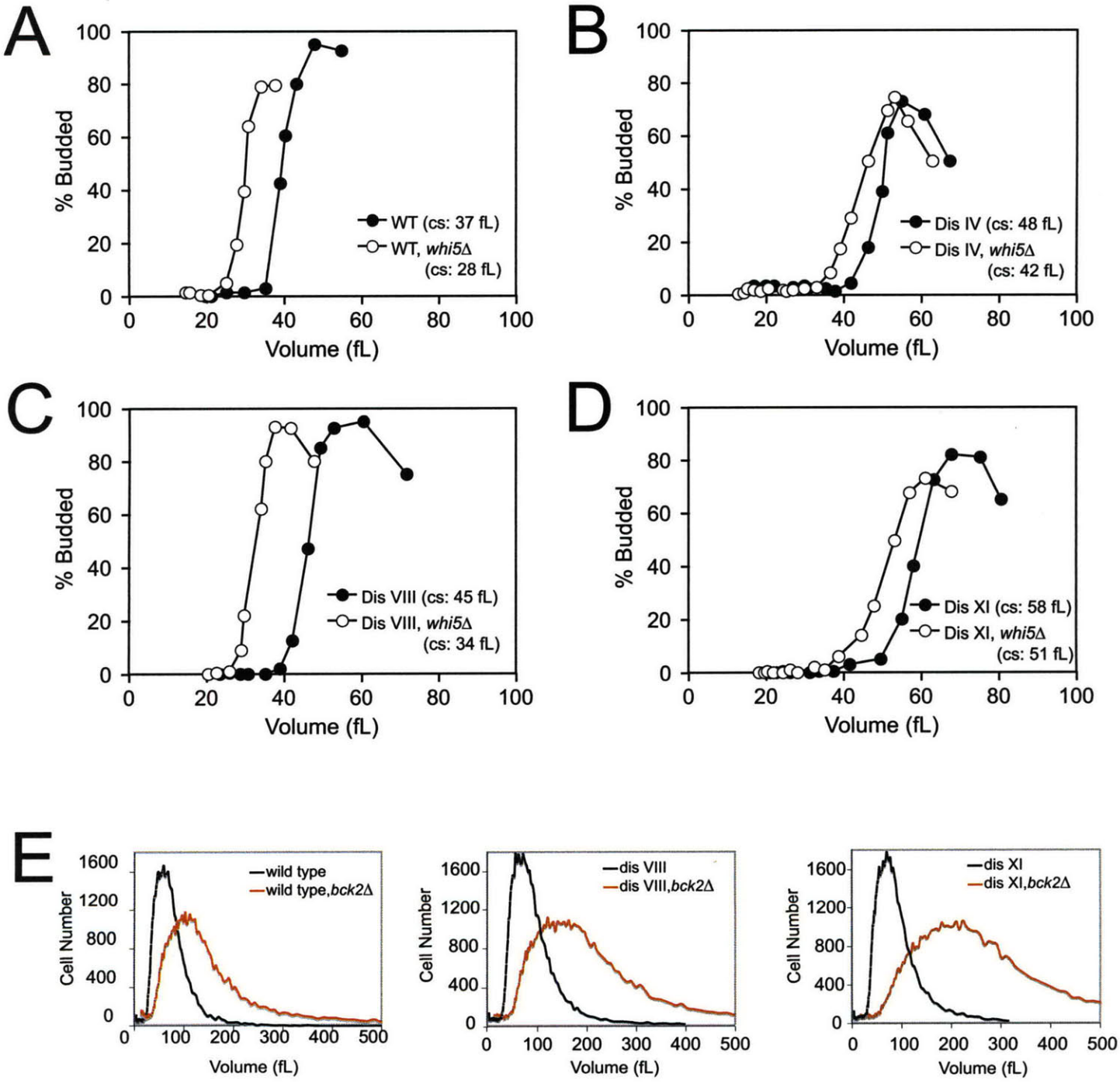
A
% Budded
Volume (fL)
WT (cs: 37 fL)
WT, whi5Δ (cs: 28 fL)
B
% Budded
Volume (fL)
Dis IV (cs: 48 fL)
Dis IV, whi5Δ (cs: 42 fL)
C
% Budded
Volume (fL)
Dis VIII (cs: 45 fL)
Dis VIII, whi5Δ (cs: 34 fL)
D
% Budded
Volume (fL)
Dis XI (cs: 58 fL)
Dis XI, whi5Δ (cs: 51 fL)
E
Cell Number
Volume (fL)
wild type
wild type,bck2Δ
dis VIII
dis VIII,bck2Δ
dis XI
dis XI,bck2Δ

Figure 12. Aneuploidy acts parallel to *WHI5* and *BCK2*.
(A-D) Wild type ([A], A25479, open symbols), disome IV ([B], A25481, open symbols), disome VIII ([C], A25480, open symbols), and disome XI ([D], A25482, open symbols) with WHI5 deleted and wild type ([A], A11311, closed symbols), disome IV ([B], A12687, closed symbols), disome VIII ([C], A13628, closed symbols), and disome XI ([D], A13771, closed symbols) cells without WHI5 deleted were grown to mid-log phase in synthetic media supplemented with 2% raffinose. Small daughter cells were then isolated by centrifugal elutriation at 4°C and then released at 30°C in YEP media containing 2% galactose. Time points were taken every 15 minutes, cell size measured with a Coulter counter, and the percentage of budded cells determined (E) Deletion of *BCK2* in wild type and disomes VIII and XI increases the size of cycling cells. Cells were grown in YEP supplemented with 2% glucose at 30°C. Cell size was measured using a Coulter Counter.

Table 1: Growth rates and critical size in aneuploid cells.

Numbers in parenthesis are wild type results for that particular experiment.

Strain:	Size at 50% budding (fL)	k
WT	38	0.0075 ± 0.0005*
Dis II	38	0.0069 (0.0072)
Dis IV	52	0.0044 (0.0069)
Dis V	33	0.0058 (0.0073)
Dis VIII	46	0.0065 (0.0076)
Dis X	45	0.0081 (0.0075)
Dis XI	56	0.0068 (0.0076)
Dis XII	70	0.0030 (0.0069)
Dis XIII	80	0.0066 (0.0076)
Dis XIV	41	0.0061 (0.0074)
Dis XV	64	0.0059 (0.0076)
Dis XVI	36	0.0053 (0.0079)
Dis XI+XV	62	0.0060 (0.0080)
Dis XI+XVI	55	0.0054 (0.0070)
Dis VIII+XIV	42	0.0054 (0.0081)
2N-I-IX	92	0.0059 (0.0083)
Diploid	72	

* from 16 experiments

Table 2: Top 100 Genes Translationally Upregulated

Gene	Name	Translational Efficiency
YBR115C	LYS2	8.58
YGR138C	TPO2	3.52
YBR054W	YRO2	3.47
YKL163W	PIR3	3.33
YPR184W	GDB1	3.16
YKL161C		3.05
YPL189C-A	COA2	2.48
YPL240C	HSP82	2.42
YCL064C	CHA1	2.37
YDR019C	GCV1	2.33
YEL065W	SIT1	2.31
YPR098C		2.29
YPR158W	CUR1	2.27
YDR270W	CCC2	2.25
YER053C-A		2.24
YOL155C	HPF1	2.24
YDR171W	HSP42	2.20
YPR021C	AGC1	2.20
YHR209W	CRG1	2.19
YNL160W	YGP1	2.16
YPL123C	RNY1	2.10
YJL088W	ARG3	2.08
YKL096W	CWP1	2.08
YPL011C	TAF3	2.08
YNR066C		2.06
YMR189W	GCV2	2.04
YPR111W	DBF20	2.04
YPR149W	NCE102	2.00
YPL067C		1.91
YPL088W		1.91
YOL058W	ARG1	1.90
YPL224C	MMT2	1.90
YPL100W	ATG21	1.89
YPL250C	ICY2	1.86
YPL196W	OXR1	1.84
YPL175W	SPT14	1.82
YDR077W	SED1	1.79
YDR258C	HSP78	1.79
YPL135W	ISU1	1.79
YPL191C		1.77
YPR006C	ICL2	1.77
YPL242C	IQG1	1.75
YPR004C	AIM45	1.75

YMR120C	ADE17	1.74
YPL253C	VIK1	1.73
YPR079W	MRL1	1.73
YPL241C	CIN2	1.72
YOR020W-A		1.71
YPL087W	YDC1	1.71
YPL144W	POC4	1.71
YPR008W	HAA1	1.71
YPR185W	ATG13	1.71
YPR091C		1.70
YPR162C	ORC4	1.70
YPL107W		1.69
YPR141C	KAR3	1.68
YPL154C	PEP4	1.66
YPL221W	FLC1	1.66
YBL064C	PRX1	1.64
YPL179W	PPQ1	1.64
YPL219W	PCL8	1.64
YPL128C	TBF1	1.62
YPL138C	SPP1	1.62
YPL045W	VPS16	1.61
YPL159C	PET20	1.61
YPL203W	TPK2	1.59
YPL208W	RKM1	1.59
YPR028W	YOP1	1.59
YPR122W	AXL1	1.59
YDR096W	GIS1	1.58
YPL078C	ATP4	1.56
YIR034C	LYS1	1.54
YPL115C	BEM3	1.54
YPL016W	SWI1	1.53
YPL069C	BTS1	1.53
YPL110C	GDE1	1.53
YPL132W	COX11	1.52
YPL042C	SSN3	1.51
YPR042C	PUF2	1.51
YDL072C	YET3	1.50
YNL305C		1.50
YPL002C	SNF8	1.50
YPL031C	PHO85	1.50
YPL103C	FMP30	1.50
YPL170W	DAP1	1.50
YPR148C		1.50
YPR155C	NCA2	1.50
YBR169C	SSE2	1.49

YPL152W	RRD2	1.49
YPR180W	AOS1	1.49
YPL153C	RAD53	1.48
YPR047W	MSF1	1.47
YPR067W	ISA2	1.47
YML131W		1.46
YPL116W	HOS3	1.46
YPR106W	ISR1	1.46
YNR065C		1.45
YER069W	ARG5,6	1.43
YLR231C	BNA5	1.43
YPL065W	VPS28	1.43

Table 3: Top 100 Genes Translationally Downregulated

Gene	Name	Translational efficiency
YBR296C	PHO89	-4.18
YBR093C	PHO5	-3.86
YHR215W	PHO12	-3.03
YNL142W	MEP2	-3.03
YJR010W	MET3	-2.98
YJR137C	MET5	-2.66
YKL001C	MET14	-2.61
YKR039W	GAP1	-2.48
YCR098C	GIT1	-2.31
YBR208C	DUR1,2	-2.25
YER081W	SER3	-2.19
YGL255W	ZRT1	-2.01
YNR044W	AGA1	-1.94
YHR136C	SPL2	-1.88
YOR377W	ATF1	-1.85
YFR055W	IRC7	-1.76
YLR452C	SST2	-1.67
YGL135W	RPL1B	-1.61
YLR303W	MET17	-1.56
YDR492W	IZH1	-1.54
YOR315W	SFG1	-1.41
YER042W	MXR1	-1.40
YDR461W	MFA1	-1.31
YFR030W	MET10	-1.31
YDL227C	HO	-1.15
YKR093W	PTR2	-1.14
YIL009W	FAA3	-1.13
YDR044W	HEM13	-1.08
YNL141W	AAH1	-1.08
YGR251W		-1.07
YDR460W	TFB3	-1.05
YBR200W	BEM1	-1.04
YJL157C	FAR1	-1.03
YLL061W	MMP1	-1.02
YLR099C	ICT1	-1.01
YLR257W		-1.00
YDR365C	ESF1	-0.99
YMR011W	HXT2	-0.96
YBR085W	AAC3	-0.93
YOR095C	RKI1	-0.93
YHL020C	OPI1	-0.91
YKL002W	DID4	-0.90
YER056C	FCY2	-0.89

YCL025C	AGP1	-0.88
YMR269W	TMA23	-0.88
YBL028C		-0.87
YBR089C-A	NHP6B	-0.86
YDR075W	PPH3	-0.85
YGL055W	OLE1	-0.85
YDR334W	SWR1	-0.84
YDR384C	ATO3	-0.84
YDL150W	RPC53	-0.83
YBR067C	TIP1	-0.82
YGR177C	ATF2	-0.82
YMR246W	FAA4	-0.82
YLR214W	FRE1	-0.81
YDR083W	RRP8	-0.80
YOR369C	RPS12	-0.80
YIL133C	RPL16A	-0.79
YGR152C	RSR1	-0.77
YGR159C	NSR1	-0.77
YHR128W	FUR1	-0.77
YHR148W	IMP3	-0.77
YNL112W	DBP2	-0.77
YOL093W	TRM10	-0.76
YOR119C	RIO1	-0.76
YOR375C	GDH1	-0.76
YDL043C	PRP11	-0.75
YDL191W	RPL35A	-0.75
YER057C	HMF1	-0.75
YGR118W	RPS23A	-0.75
YJR148W	BAT2	-0.75
YDL085C-A		-0.74
YHL015W	RPS20	-0.74
YJR009C	TDH2	-0.74
YJR123W	RPS5	-0.74
YGR175C	ERG1	-0.73
YMR006C	PLB2	-0.73
YBR181C	RPS6B	-0.72
YKL172W	EBP2	-0.72
YNL302C	RPS19B	-0.72
YOR236W	DFR1	-0.72
YCR087C-A	LUG1	-0.71
YDL136W	RPL35B	-0.71
YMR233W	TRI1	-0.71
YDR502C	SAM2	-0.70
YGR280C	PXR1	-0.70
YNL221C	POP1	-0.70
YML063W	RPS1B	-0.69

YOL040C	RPS15	-0.69
YCR016W		-0.68
YGL099W	LSG1	-0.67
YGR032W	GSC2	-0.67
YIL019W	FAF1	-0.67
YOL125W	TRM13	-0.67
YBR123C	TFC1	-0.66
YER074W	RPS24A	-0.66
YGL164C	YRB30	-0.66
YHR058C	MED6	-0.66
YBR084C-A	RPL19A	-0.65

Table 4: Strains used in this study

Strain	Disomic for Chromosome	
A6865	II	*MATa, lys2::HIS3, lys2::KanMX6*
A12687	IV	*MATa, trp1::HIS3, trp1::KanMX6*
A14479	V	*MATa, can1::HIS3, intergenic region (187520-187620) between YER015W and YER016W::KanMX6*
A13628	VIII	*MATa, intergenic region (119778-119573) between YHR006W and YHR007C::HIS3, intergenic region (119778- 119573) between YHR006W and YHR007C::KanMX6*
A12689	X	*MATa, ura2::HIS3, ura2::KanMX6*
A13771	XI	*MATa, intergenic region (430900-431000) between YKL006C-A and YKL006W::HIS3, intergenic region (430900-431000) between YKL006C-A and YKL006W::KanMX6*
A12693	XII	*MATa, ade16::HIS3, ade16::KanMX6*
A12695	XIII	*MATa, ura5::HIS3, ura5::KanMX6*
A13979	XIV	*MATa, intergenic region (622880-622980) between YNL005C and YNL004W::HIS3, intergenic region (622880- 622980) between YNL005C and YNL004W::KanMX6*
A12697	XV	*MATa, leu9::HIS3, leu9::KanMX6*
A12700	XVI	*MATa, met12::HIS3, met12::KanMX6*
A12691	XI + XV	*MATa, leu9::HIS3, leu9::KanMX6*
A12699	XI + XVI	*MATa, met12::HIS3, met12::KanMX6*
A15615	VIII + XIV	*MATa, intergenic region (119778-119573) between YHR006W and YHR007C::HIS3, intergenic region (119778- 119573) between YHR006W and YHR007C::KanMX6*
A15245	2N - I - IX	*MATa, trp1::KAN, trp1::HIS, cln2::CLN2-3xHA-LEU2*
A25481	IV	*MATa, trp1::HIS3, trp1::KanMX6, WHI5::caURA3*
A25480	VIII	*MATa, intergenic region (119778-119573) between YHR006W and YHR007C::HIS3, intergenic region (119778- 119573) between YHR006W and YHR007C::KanMX6, WHI5::caURA3*

A25482	XI	*MATa, intergenic region (430900-431000) between YKL006C-A and YKL006W::HIS3, intergenic region (430900-431000) between YKL006C-A and YKL006W::KanMX6, WHI5::caURA3*
A25477	IV	*MATa, trp1::HIS3, trp1::KanMX6, GAL-CLN2::URA3*
A25476	VIII	*MATa, intergenic region (119778-119573) between YHR006W and YHR007C::HIS3, intergenic region (119778- 119573) between YHR006W and YHR007C::KanMX6, GAL-CLN2::URA3*
A25474	XI	*MATa, intergenic region (430900-431000) between YKL006C-A and YKL006W::HIS3, intergenic region (430900-431000) between YKL006C-A and YKL006W::KanMX6, GAL-CLN2::URA3*
A25872	IV	*MATa, trp1::HIS3, trp1::KanMX6, GCN4-LacZ::URA3*
A25871	VIII	*MATa, intergenic region (119778-119573) between YHR006W and YHR007C::HIS3, intergenic region (119778- 119573) between YHR006W and YHR007C::KanMX6, GCN4-LacZ::URA3*
A25874	XI	*MATa, intergenic region (430900-431000) between YKL006C-A and YKL006W::HIS3, intergenic region (430900-431000) between YKL006C-A and YKL006W::KanMX6, GCN4-LacZ::URA3*
A25873	XV	*MATa, leu9::HIS3, leu9::KanMX6, GCN4-LacZ::URA3*
A25875	XVI	*MATa, met12::HIS3, met12::KanMX6, GCN4-LacZ::URA3*
A25870	GCN4-LacZ wt control	*MATalpha, ade2-1, leu2-3, ura3, trp1-1, his3-11,15, can1-100, GAL, psi+, ade1::HIS3, lys2::KAN, GCN4-LacZ::URA3.*
A25475	GAL-CLN2 wt control	*MATa, ade1::HIS3, lys2::KAN, GAL-CLN2::URA3*
A25472	WHI5 deletion	*MATa, ade1::HIS3, lys2::KAN, WHI5::caURA3*
A11311	wild type control	*MATa, ade1::HIS3, lys2::KAN*
A3009	*SFP1* deletion	*MATa, SFP1::HIS*

References:

Alberghina L, Rossi RL, Querin L, Wanke V, Vanoni M. 2004. A cell sizer network involving Cln3 and Far1 controls entrance into S phase in the mitotic cycle of budding yeast. J Cell Biol. 167(3):433-43.

Baim SB, Pietras DF, Eustice DC, Sherman F. 1985. A mutation allowing an mRNA secondary structure diminishes translation of Saccharomyces cerevisiae iso-1-cytochrome c. Mol Cell Biol. 5(8):1839-46.

Costanzo M, Nishikawa JL, Tang X, Millman JS, Schub O, Breitkreuz K, Dewar D, Rupes I, Andrews B, Tyers M. CDK activity antagonizes Whi5, an inhibitor of G1/S transcription in yeast. 2004. Cell.;117(7):899-913.

Cross FR, Tinkelenberg AH. 1991. A potential positive feedback loop controlling CLN1 and CLN2 gene expression at the start of the yeast cell cycle. Cell 65:875–883.

de Bruin RA, McDonald WH, Kalashnikova TI, Yates J 3rd, Wittenberg C. 2004. Cln3 activates G1-specific transcription via phosphorylation of the SBF bound repressor Whi5. Cell. 117(7):887-98.

Dever, T. 1997. Using GCN4 as a reporter of eIF2 alpha phosphorylation and translational regulation in yeast. Methods. 11(4):403-17.

Dirick L, Böhm T, Nasmyth K. 1995. Roles and regulation of Cln-Cdc28 kinases at the start of the cell cycle of Saccharomyces cerevisiae. EMBO J. 14(19):4803-13

Epstein CB, Cross FR. 1994. Genes that can bypass the CLN requirement for Saccharomyces cerevisiae cell cycle START. Mol Cell Biol. 14(3):2041-7.

Ewald JC, Heux S, Zamboni N. 2009. High-throughput quantitative metabolomics: workflow for cultivation, quenching, and analysis of yeast in a multiwell format. Anal Chem 81(9):3623-9.

Fingerman I, Nagaraj V, Norris D, Vershon AK. 2003. Sfp1 plays a key role in yeast ribosome biogenesis. Eukaryot Cell. 2(5):1061-8.

Gutherie C, Fink GR. 1991 Guide to yeast genetics and molecular biology. Academic Press, San Diego.

Hanna J, Leggett DS, Finley D. 2003. Ubiquitin depletion as a key mediator of toxicity by translational inhibitors. Mol Cell Biol. 23(24):9251-61.

Hinnebusch AG. 1985. A hierarchy of trans-acting factors modulates translation of an activator of amino acid biosynthetic genes in Saccharomyces cerevisiae .Mol Cell Biol 5(9):2349-60.

Hinnebusch AG. 2005. Translational regulation of GCN4 and the general amino acid control of yeast. Annu Rev Microbiol. 59:407-50.

Hochwagen A, Wrobel G, Cartron M, Demougin P, Niederhauser-Wiederkehr C, Boselli MG, Primig M, Amon A. 2005. Novel response to microtubule perturbation in meiosis. Mol Cell Biol. 25:4767–4781.

Ingolia NT, Ghaemmaghami S, Newman JR, Weissman JS. 2009. Genome-wide analysis in vivo of translation with nucleotide resolution using ribosome profiling. Science. 324(5924):218-23.

Jorgensen P, Tyers M. 2004. How cells coordinate growth and division. Curr Biol. 14(23):R1014-27.

Li X, Cai M. 1999. Recovery of the yeast cell cycle from heat shock-induced G(1) arrest involves a positive regulation of G(1) cyclin expression by the S phase cyclin Clb5. J Biol Chem. 274(34):24220-31.

Morgan DO. 1997. Cyclin-dependent kinases: engines, clocks, and microprocessors. Annu Rev Cell Dev Biol. 1997;13:261-91.

Niwa O, Tange Y, Kurabayashi A. 2006. Growth arrest and chromosome instability in aneuploid yeast. Yeast. 23(13):937-50.

Polymenis M, Schmidt EV. 1997. Coupling of cell division to cell growth by translational control of the G1 cyclin CLN3 in yeast. Genes Dev.11(19):2522-31.

Rupes I. 2002. Checking cell size in yeast. Trends Genet. 18(9):479-85.

Torres EM, Sokolsky T, Tucker CM, Chan LY, Boselli M, Dunham MJ, Amon A. 2007.Effects of aneuploidy on cellular physiology and cell division in haploid yeast. Science. 317:916-24.

Torres EM, Williams BR, Amon A. Aneuploidy: cells losing their balance. Genetics. 179(2):737-46

Tyers M, Tokiwa G, Futcher B. 1993. Comparison of the Saccharomyces cerevisiae G1 cyclins: Cln3 may be an upstream activator of Cln1, Cln2 and other cyclins. EMBO J. 12(5):1955-68.

Verduyn C, Postma E, Scheffers WA, Van Dijken JP.1992 Effect of benzoic acid on metabolic fluxes in yeasts: a continuous-culture study on the regulation of respiration and alcoholic fermentation.Yeast 8 (7):501-517.

White MA, Riles L, Cohen BA. 2009. A systematic screen for transcriptional regulators of the yeast cell cycle. Genetics. 181(2):435-46.

Williams BR, Prabhu VR, Hunter KE, Glazier CM, Whittaker CA, Housman DE, Amon A. 2008. Aneuploidy affects proliferation and spontaneous immortalization in mammalian cells. Science. 322(5902):703-9.

Chapter 3: Key Conclusions and Future Directions

Previous work by Torres et al. (2007) shows that aneuploidy delays cell cycle progression in yeast cells arrested by mating factor. Not only that, but aneuploidy also increases the time it takes a cell to double and it makes them more sensitive to translational inhibitors. Aneuploidy also alters cellular morphology and almost all of the aneuploid strains studied are actually larger than wild type cells. In this thesis I studied the effects that aneuploidy has specifically on cell cycle entry. I find that during the G1 phase of the cell cycle aneuploid cells accumulate volume more slowly than wild type cells and that they also increase the critical size for budding.

Aneuploidy and the cell cycle

As shown in Chapter 2 of this thesis, aneuploid cells delay cell cycle entry by increasing the critical size for budding. What this means is that disomic cells for reasons that are at this point unclear grow more than their wild type counterpart before they can bud. This observation points to the fact that aneuploidy affects the timing of the G1 phase cycling program. I set out to characterize how aneuploidy is interfering with the cycling program.

As described in Chapter 1, the molecular events that lead to budding have been well characterized in yeast. First, I looked at the timing of *CLN2* transcription in wild type and aneuploid cells. The data show that indeed expression of *CLN2* is delayed in disomes IV and XI when compared to wild type. Next, I expressed *CLN2* at a volume much smaller than that of the critical size to determine whether aneuploidy could

interfere with cell cycle events after *CLN2* expression. All disomes overexpressing *CLN2* budded at nearly the same volume as wild type cells also overexpressing *CLN2* thus indicating that aneuploidy is acting at the level of *CLN2* transcription or acting on other factors that activate *CLN2* transcription.

Next, I deleted *WHI5* to see if aneuploidy is interfering with Whi5 inactivation. The data in Chapter 2 show that disomes IV, VIII, and XI all budded earlier when WHI5 was deleted. This shows that deletion of *WHI5* partially suppresses the cell cycle entry defect seen in aneuploid cells. In addition, all these strains, including wild type, decreased the critical size by the same amount, close to 10 fL. These observations can be interpreted in two ways: either aneuploidy is not interfering with Cln3 activation and thus Whi5 inactivation or is doing so but the effect is not severe (i.e. aneuploidy could be delaying Cln3 activation in such a way that the net result would not have an increase in the critical size of more than 10 fL). Nevertheless, it is clear that aneuploidy is interfering most likely with events at the level of SBF-dependent transcription (Figure 1).

Further evidence that aneuploidy interferes with the cycling program is demonstrated by the fact that these strains also delay cell cycle entry from an α-factor arrest (Torres et al. 2007). It is important to note that cells arrested with α-factor grow beyond their critical size therefore size no longer affects cell cycle entry. The set of experiments presented in Appendix I show that Whi5 nuclear exit is delayed in aneuploid strains released from an α-factor block and that this delay can be rescued by

overexpression of Cln3. α-factor then seems to be interfering with the activation of Cln3. Exactly how this could be is unclear at this point. Moore (1998) has shown that protein synthesis is required for recovery from pheromone block. Cells arrested with α-factor and treated with sublethal doses of cycloheximide delayed entry into the cell cycle once released from the block. The delay seen in aneuploid cells recovering from pheromone block would be consistent with them having defects in protein synthesis. Another possibility could be that aneuploidy is somehow interfering with the binding of Far1 to the G1 cyclins. Tyers and Futcher (1993) have shown that Far1 physically associates with the three Cln-CDK complexes thereby inhibiting them. Upon pheromone block release this inhibition must be relieved and aneuploidy might be interfering with it thus delaying cell cycle entry. These data together with what was shown in Chapter 2 seem to indicate that aneuploidy can affect both cyclin activity and SBF-dependent transcription.

Future work should try to address exactly how is that being in an aneuploid state affects SBF-dependent transcription and cyclin activity. An important aspect to be explored is the regulation of the Swi4/Swi6 transcription factor. Exactly how Swi4 and Swi6 are regulated is still not fully understood. It has been shown that the abundance of *SWI4* mRNA is cell cycle regulated, however, the accumulation of de novo synthesized Swi4 is not necessarily the main cause for transcriptional activation (Marini and Reed 1992, Koch et al. 1996). Furthermore, Taba et al. (1991) showed that the DNA-binding activity of SBF is detectable throughout the cell cycle. Furthermore, Koch et al (1996) showed that SCB elements are occupied in cells arrested prior to START as well as in small daughter cells. What then activates SBF-dependent transcription? As already

mentioned, a negative regulator of Sw4/Swi6, Whi5, has already been characterized (Costanzo et al. 2004, de Bruin et al. 2004). Since deletion of Whi5 does not fully rescue the increase in critical size, it is possible that additional factors are inhibiting SBF-dependent transcription in aneuploid cells. It will be important to identify any other factors that may or may not be aneuploidy-specific that regulate Swi4/Swi6 and Cln2 transcription. It would be interesting to perform an analysis similar to the one performed here on the collection of *Lge* mutants described by Jorgensen et al. (2002). This would identify factors that could potentially directly or indirectly affect Cln2 transcription. It will then be important to assess whether these same factors are being misregulated in aneuploid cells. Additionally, it might be also important to look at the timing of SBF loading. Despite the fact that in wild-type cells SBF –elements are already occupied in G1, it is formally possible that aneuploidy is interfering with the loading of these factors. For this experiment, however, cells will have to be synchronized at the very end of mitosis (perhaps using a Cdc15-ts allele) and then released. This synchronization will take away the contributions of size to the activation of these factor but will reveal whether or not there are any in defects in occupying SBF-elements.

Aneuploidy and growth

Work by Torres et al. (2007) has shown that aneuploidy increases a cell's doubling time. This increase in doubling time is due to a decrease in the cell's ability to grow and proliferate. In the work presented I have shown that aneuploidy affects volume accumulation during the G1 phase of the cell cycle. This effect was clearly evident in

disome XVI, which delayed cell cycle entry only because it grew more slowly and not because it increased its critical size.

Protein synthesis is a very important component of growth. There are two main reasons why protein synthesis might be affected in a cell under certain conditions: lack of nutrients (amino acids or sugars) or a defective translational machinery. For instance, Kraft et al. (2008) showed that when cells are starved for nitrogen they selectively degrade mature ribosomes. The cell is using this mechanism to produce amino acids by autophagy. Similarly, cells defective in ribosome biogenesis are impaired in growth. One of the most extreme cases, as already mentioned in Chapter 1, is deletion of *SFP1*, a transcription factor that turns on ribosomal protein gene expression (Fingerman et al. 2003). These cells display lower level of individual ribosomal subunits as well as polysomes.

The nutritional status of disomic cells was investigated in two different ways. A metabolomic approach looked at intracellular amino acid levels. The analysis for disomes IV, VIII, XI, XIII, XV, and XVI revealed that these cells do not have low levels of intracellular amino acids. In addition, disomes IV, VIII, XI, XV and XVI also did not increase translation of the *GCN4* gene. This is consistent with the fact that these cells are not starved for amino acids. With these observations it can be concluded that aneuploidy does not exhaust the amino acid pools inside the cell.

To investigate the status of the translational machinery in aneuploid cells I examined radioactive methionine incorporation and ribosomal assembly in these cells and compared them to wild type cells. The results presented in Chapter 2 showed that there seems to be no severe defects in global translation as the rate of S^{35}-methionine incorporation in disome XVI and wild type was nearly identical. In addition, ribosomal assembly and polysome assembly for disomes IV, X,XI, XVI, VIII+XIV did not seem severely impaired as judged by their polysomal profiles obtained from sucrose gradients. These data indicates that aneuploidy does not grossly affect the translational machinery and that the experimental techniques used here are not sensitive enough to detect any small changes in translation capacity or in ribosome levels or defects in their assembly.

The results summarized until now show that aneuploidy does not have a severe impact on the translational machinery of the cell. Why then are these cells growing slower than wild type? It is important to note that aneuploidy increases the mRNA levels of the genes present on an entire chromosome. This raises several questions: Are these mRNAs being translated? Is the translational machinery limiting? Are there any global changes in ribosomal association? Can these changes explain the slow growth seen?

To answer these questions we turned to a recently developed technique called ribosomal footprinting (Ingolia et al. 2009). This technique allowed us to see exactly where along mRNAs ribosomes are binding. As mentioned in Chapter 2, we find that for disome XVI there is a number of genes that show a decreased translation efficiency, some that showed an increase in translation efficiency and others that displayed no

change. These data, however, do not show whether translation is limiting or not. Instead the data shows that the cell is able to respond to the mRNA imbalance introduced by being aneuploid and that it accordingly alters the translational efficiency of several genes. Interestingly, and as mentioned in Chapter 2, some of these genes were involved in ribosome biogenesis and others, when deleted, produced a slow growth phenotype.

Why are aneuploid cells growing slowly then? It seems that the slow growth phenotype seen in aneuploid cells is just a sum of subtle changes in protein levels and stoichiometry. In effect, having an extra chromosome imbalances the cell's mRNAs and in turn the cell responds by rearranging ribosomal association and decreasing or increasing the translation efficiency of certain genes. These changes are not large changes – not as severe as a deletion. However, these changes when taken together could be significant. The fact that some ribosomal proteins are not being translated as efficiently as in wild type could cause a subtle defect in the translation machinery. Also, it is important to take note that while translation of some genes goes down, translation of others go up, so it is possible that global translation is not being severely affected and this would explain why the rate of S^{35}-methionine incorporation is the same in wild type and aneuploid cells. The possibility exists also that the proteins with increased translation are not essential and are therefore degraded with no net contribution to growth.

Aneuploidy thus seems to be producing a global response with a net result of slow growth. What exactly triggers this response? Is it the nature of the genes along the chromosome? Is it just having extra mRNAs to translate? Is there a threshold for this

effect? These are questions that need to be addressed in the future. It would be interesting to be able to express a large set of non-toxic proteins (using several YACS containing these genes under the *GAL1-10* promoter) and see if a translational and growth defect ensues. Alternatively, it would also be interesting to create yeast strains containing chromosomal fragments (perhaps using multiple YACS) instead of whole chromosomes to determine whether or not there is a minimum chromosomal size required for the observed effects.

Aneuploidy and cancer

The work presented in this thesis shows clearly that aneuploidy affects the ability of a cell to proliferate. It shows that carrying an extra chromosome actually imposes a burden on the cell and impairs growth and proliferation. As a result, cells get larger and accumulate volume more slowly.

The work presented here favors the idea that aneuploidy is not necessarily what causes cancer. While it might be a contributing factor, it does not have to necessarily be a cause behind tumorigenesis. Indeed the work presented in this thesis suggests that when a cell undergoes a defective mitosis and acquires an extra chromosome it does not acquire any concomitant growth advantage. On the contrary, aneuploid cells have a greater proliferative disadvantage. For a cell then to become tumorigenic and acquire any growth

advantages it will have to overcome the stress induced by being aneuploid and most likely acquire additional mutations that will enhance its proliferative capacity.

The fact that cells carrying an extra chromosome divide more slowly than wild type cells could have important implications for cancer therapy. If the results presented here also hold true for human cells, and assuming that there are no other spontaneous suppressor mutations that could increase the capacity of a cell to proliferate, then it would contradict the logic of some current chemotherapeutic therapies. For instance, 5-fluorouracil, a pyrimide analog, has been used for decades for the treatment of colorectal and pancreatic cancer (Heidelberger et al. 1983, Li et al. 2009). Once metabolized, it is incorporated into DNA and RNA and leads to cell cycle arrest and apoptosis (Li et al. 2009). The selectivity of the drug depends on cellular metabolism and proliferative capacity – cells that divide faster uptake the drug and die. If aneuploid cancer cells are actually under the proliferative burden seen in yeast cells, using this drug might not be the best therapy.

Concluding Remarks

The work presented here shows that aneuploidy affects cellular proliferation in two ways: it increases the critical size for budding and it decreases the rate of volume accumulation during the G1 phase of the cell cycle. Furthermore, aneuploidy seems to be interfering directly with Swi4/Swi6. Aneuploidy affects growth but it does not cause gross defects in the cell's translational machinery.

Figure 1

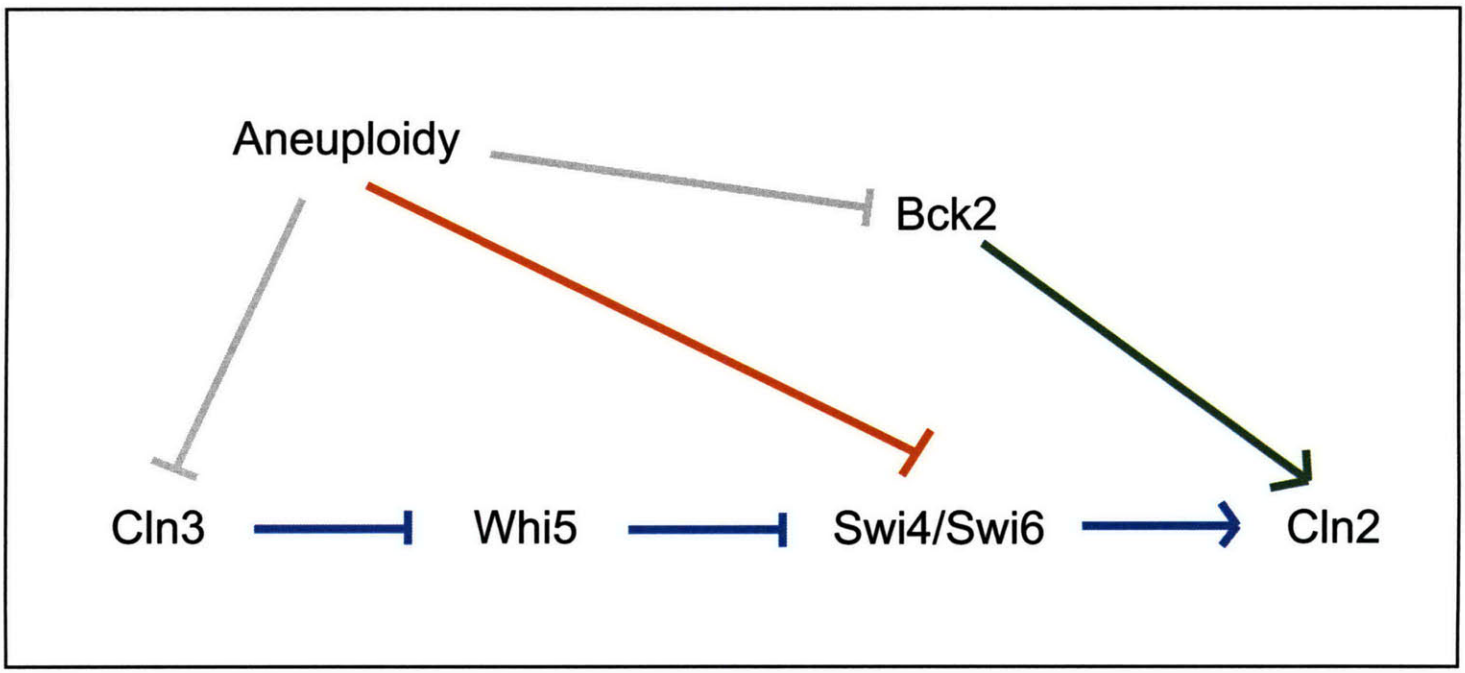

Figure 1: G1 phase progression in yeast and aneuploidy.
The data presented in this work supports a model in which aneuploidy is interfering through a pathway parallel to Cln3 and Bck2 with Swi4 and Swi6 transcription. The nature of this inhibitory activity is at this point unknown.

References:

Costanzo M, Nishikawa JL, Tang X, Millman JS, Schub O, Breitkreuz K, Dewar D, Rupes I, Andrews B, Tyers M. CDK activity antagonizes Whi5, an inhibitor of G1/S transcription in yeast. 2004. Cell.;117(7):899-913.

de Bruin RA, McDonald WH, Kalashnikova TI, Yates J 3rd, Wittenberg C. 2004. Cln3 activates G1-specific transcription via phosphorylation of the SBF bound repressor Whi5. Cell. 117(7):887-98.

Fingerman I, Nagaraj V, Norris D, Vershon AK. 2003. Sfp1 plays a key role in yeast ribosome biogenesis. Eukaryot Cell. 2(5):1061-8.

Heidelberger C, Danenberg PV, Moran RG. 1983. Fluorinated pyrimidines and their nucleosides. Adv Enzymol Relat Areas Mol Biol. 54: 58–119.

Ingolia NT, Ghaemmaghami S, Newman JR, Weissman JS. 2009. Genome-wide analysis in vivo of translation with nucleotide resolution using ribosome profiling. Science. 324(5924):218-23.

Jorgensen P, Nishikawa JL, Breitkreutz BJ, Tyers M. 2002. Systematic identification of pathways that couple cell growth and division in yeast. Science. 297(5580):395-400.

Koch C, Schleiffer A, Ammerer G, Nasmyth K. 1996. Switching transcription on and off during the yeast cell cycle: Cln/Cdc28 kinases activate bound transcription factor SBF (Swi4/Swi6) at start, whereas Clb/Cdc28 kinases displace it from the promoter in G2. Genes Dev. 10(2):129-41.

Kraft C, Deplazes A, Sohrmann M, Peter M. 2008. Mature ribosomes are selectively degraded upon starvation by an autophagy pathway requiring the Ubp3p/Bre5p ubiquitin protease. Nat Cell Biol. 10(5):602-10.

Li LS, Morales JC, Veigl M, Sedwick D, Greer S, Meyers M, Wagner M, Fishel R, Boothman DA.. 2009. DNA mismatch repair (MMR)-dependent 5-fluorouracil cytotoxicity and the potential for new therapeutic targets. Br J Pharmacol. 158(3):679-92.

Marini NJ, Reed SI. 1992. Direct induction of G1-specific transcripts following reactivation of the Cdc28 kinase in the absence of de novo protein synthesis. Genes Dev. 6(4):557-67.

Moore SA. 1988. Kinetic evidence for a critical rate of protein synthesis in the Saccharomyces cerevisiae yeast cell cycle. J Biol Chem. 263(20):9674-81.

Taba MR, Muroff I, Lydall D, Tebb G, Nasmyth K. Changes in a SWI4,6-DNA-binding complex occur at the time of HO gene activation in yeast. Genes Dev. 5(11):2000-13.

Torres EM, Sokolsky T, Tucker CM, Chan LY, Boselli M, Dunham MJ, Amon A. 2007.Effects of aneuploidy on cellular physiology and cell division in haploid yeast. Science. 317:916-24.

Tyers M, Futcher B. 1993. Far1 and Fus3 link the mating pheromone signal transduction pathway to three G1-phase Cdc28 kinase complexes. Mol Cell Biol. 13(9):5659-69.

Appendix I: Aneuploidy and Cell Cycle Entry

Aneuploidy delays cell cycle entry after release from α-factor arrest.

Aneuploidy, a condition characterized by having an uneven number of chromosomes, has profound effects on cellular physiology and cell cycle progression. Torres et al. (2007) showed that when yeast cells become aneuploid they increase in size, grow more slowly, and become more sensitive to translational inhibitors and temperature. Interestingly, these cells delay cell cycle entry upon treatment with α-factor. Indeed, aneuploidy seems to be interfering with the Cln-CDK activity necessary for cell cycle entry.

Under most circumstances, yeast cells do not require extracellular mitogens to stimulate growth and proliferation. However, when yeast cells mate they must do so while in the G1 phase of the cell cycle (Chang and Herskowitz 1990). A secreted peptide, or pheromone, that arrests cells at this stage. Mating factors induce cell cycle arrest by causing the inhibition of all three Cln-Cdc28 complexes. It also produces profound morphological changes such as the development of mating projections also known as shmoos.

The molecular events that lead to cell cycle arrest in G1 by mating factor have been well characterized. Inhibition is primarily carried out by Far1, a protein present only in G1 that binds to cycling-Cdc28 complexes only in the presence of mating factor. Far1 needs to be phosphorylated for it to bind to cyclin-Cdc28 complexes. This phosphorylation is carried out by the kinase Fus3 (Elion et al. 1993). The signaling

process that results in the activation of Fus3 and subsequent phosphorylation of Far1 involves the mating receptor, a heterotrimeric G protein-coupled receptor. The G protein associated with the mating receptor has three subunits: an α subunit that binds guanine nucleotides and a βγ subunit. Upon binding of mating factor to the mating receptor, GDP is exchanged for GTP in the α subunit and the βγ subunit pair then gets released. The released βγ subunit then activates a cascade of kinase activities that results in the activation of Fus3. Once Fus3 is phosphorylated, it translocates to the nucleus and phosphorylates and activates Far1. (Chang and Herskowitz 1992, Dohlman and Slessareva 2006).

Here I explore the delay that aneuploidy causes upon release from α-factor induced G1 arrest. First I show that Whi5 (described in Chapter 1) nuclear exit is delayed in aneuploid cells and that this correlates with budding. I also show that overexpression of the G1 cyclin Cln3 can accelerate cell cycle entry after release from an α-factor block. Finally, I arrested cells by two different method: just growing them to stationary phase and by arresting them with α-factor and letting them escape. I showed that in both cases cell cycle entry is also delayed. Aneuploidy thus disrupts the ability of a cell to reenter the cell cycle when arrested by at least two different methods.

Results

Torres et al (2007) previously showed that aneuploidy delays cell cycle entry upon an α-factor block and release. The delays ranged from between 5 to 10 minutes for

disomes XI and XII to almost an hour for disome IV. These data shows that aneuploidy is interfering with the program required for recovery from mating factor block. The data below further characterize this delay.

Aneuploidy delays Whi5 nuclear exit.

As already described in Chapter 1, Whi5 is a G1-S transcription inhibitor. It binds the transcription factors Swi4 and Swi6 and its inhibitory activity is relieved by Cln3-Cdc28 phosphorylation. Once phosphorylated, Whi5 exits the nucleus and transcription of G1-S genes follows. Cln3-Cdc28 kinase activity is very difficult to measure so tracking the localization of Whi5 provides a useful way to measure the activity status of the Cln3-Cdc28 complex. I tagged Whi5 with green fluorescent protein and looked at its localization during mating factor block and after release (Figure 1). As reported by Costanzo et al. and Wittenberg et al., during an α-factor block, Whi5 is nuclear (Figure 1A). In cycling cells we see both: nuclear Whi5 in cells that have not gone through Start and cytoplasmic for cells that have already gone through Start (Figure 1A, B). I also tracked the localization of Whi5 as a function of time in cells released from an α-factor block (Figure 2A-C). In brief, the data show that release from α-factor block delays budding for disomes XV and IV, and XVI as previously reported and that there is a similar delay in Whi5 nuclear exit. When compared to wild type, disome XV cells delay budding by around 15 minutes. In this aneuploid strain the delay in Whi5 exit from the nucleus is of similar magnitude. Disome IV cells also delay budding by around 45 minutes and Whi5 nuclear exit by around 40 min. Disome XVI delays budding by around 45 minutes and Whi5 nuclear exit by around 40 minutes. The delay in Whi5

nuclear exit suggests that aneuploidy is interfering with the activation of the Cln3-Cdc28 complex.

Overexpression of Cln3 accelerates cell cycle entry in aneuploid cells.

Next I asked whether overexpression of the G1 cyclin Cln3 could suppress the cell cycle entry delay seen in aneuploid cells upon release from a mating factor block. To do this I placed the *CLN3* gene under control of the GAL promoter. Cells were then arrested with α-factor for three hours and preinduced with galactose for one hour and DNA content followed by FACS analysis upon release in the presence of galactose (Figure 3A,B). Wild type cells overexpressing *CLN3* replicated their DNA 30 minutes after release from the block whereas wild type cells not overexpressing *CLN3* did so at 45 minutes (Figure 3A). Overexpression of Cln3 in wild type cells accelerated cell cycle entry by 15 minutes. Disome XVI cells overexpressing *CLN3* replicated their DNA 30 minutes after release from the block whereas disome XVI cells not overexpressing *CLN3* did so at 60 minutes (Figure 3A). Overexpression of Cln3 in wild type cells accelerated cell cycle entry by 30 minutes. Our data is consistent with the idea that aneuploidy is interfering with Cln3 activation after release from pheromone block.

Aneuploidy confers no advantage in reentering the cell cycle from two different kinds of arrests.

Next I wanted to observe the kinetics of aneuploid cells as they escaped from a mating factor block or how they entered the cell cycle after a different kind of arrest such

as that caused by growth to stationary phase. Arresting the cells by growing them to saturation is another way to arrest them with a size larger than their critical size for budding. This type of arrest also does not involve the changes induced by pheromone block. For the mating factor experiment, cells were grown to exponential phase and mating factor added to the culture – there was no release step. Budding index was then monitored as a function of time. For the stationary phase escape, cells were grown overnight to saturation and then diluted. Aneuploid cells delayed exit from the mating factor block (Figure 4). Wild type escaped around 100 minutes after full arrest while disomes IV, VIII, XI, and XVI escaped around 160, 140, 125, and 155 minutes respectively. Aneuploid cells also delayed exit from stationary phase. Both wild type and disome II, a not so sick disome, reached 50% buds at around 90 minutes while disomes IV, XII, and XII at 140, 100, and 135 minutes respectively. These data show that aneuploidy confers no proliferative advantage to cells and that in fact aneuploidy has a negative impact on cell cycle reentry.

Discussion

Aneuploidy delays Cln3-Cdc28 activation after mating factor block and release

In agreement with Torres et el. (2007), the results presented here show that aneuploidy delays cell cycle entry after a mating pheromone block. Furthermore, the data show that aneuploidy is delaying the activation of the Cln3-Cdc28 complex. As described in Chapter 1 of this thesis, activation of the Cln3-Cdc28 complex leads to

phosphorylation of Whi5, a G1-S transcriptional inhibitor and its subsequent nuclear exit. Relative to wild type, disomes IV, XVI, and VIII+XIV delayed Whi5 nuclear exit. This results is consistent with a delay in Cln3-Cdc28 activation.

It is interesting to note the differences between the results presented here and the results presented in Chapter 2 of this thesis. Here I show that aneuploidy acts by interfering with Cln3-Cdc28 activity and in Chapter 2 I show that aneuploidy acts at the level of *CLN2* transcription. The discrepancy between these two results lies in the synchronization methods used. While elutriation yields small daughters cells that have yet to reach their critical size, synchronization using α-factor yields cells that have grown beyond their critical size. Also, α-factor inhibits the G1 cyclin program, Cln3 included, while elutriation leaves it intact. In other words, the activation of G1 cyclins in elutriated cell is under control of the size requirement for budding whereas in a release from a cell cycle block it is not.

Aneuploidy confers no advantage in escaping a cell cycle block

To see if aneuploid cells acquired the ability to enter the cell cycle under conditions in which wild type cells would not, I arrested cells using mating factor or by growing them to saturation. Cells arrested in α-factor were allowed to escape from the block. Cells arrested by growing them to saturation were diluted and allowed to enter the cell cycle. In these two instances aneuploid cells delayed cell cycle entry. This result

agrees with the conclusions from Chapter 2 of this thesis that aneuploidy imposes a proliferative disadvantage in cells.

The data presented thus far shows that aneuploidy inhibits cell cycle entry as shown by three different methods. In Chapter 2 cells were synchronized by centrifugal elutriation and I showed that they increased the critical size for budding and decreased the volume accumulation during the G1 phase of the cell cycle. Arresting the cell using a pheromone block and then releasing them also shows that aneuploidy delays entry into the cell cycle. In this case the cells get to grow beyond the critical size so cell cycle entry is only due to a delayed activation of the G1 cyclins. Cells arrested by growing to saturation also delayed entry into the cell cycle. In this arrest, the cell cycle machinery is not directly inhibited by an external factor such as α-factor so any artifacts introduced by pheromone treatment are eliminated. Aneuploidy has a striking effect on the cell cycle machinery and growth with the net result that cell cycle entry is delayed and the proliferative capacity of these cells diminished.

Materials and Methods

Yeast strains, plasmids, and growth conditions

All yeast strains are derivatives of W303. Yeast strains were generated and manipulated as described previously (Gutherie and Fink 1991). Cells were grown at 30°C in either YEP supplemented with 2% raffinose or glucose and synthetic media containing G418.

Elutriation

Elutriations were performed as described (Amon 2002). Cells were grown in 1 or 2 L of synthetic media supplemented with 2% raffinose at 30°C to an OD_{600} less than 2. Cells were collected by centrifugation and resuspended in 30 ml of cold YEP. The resuspended cells were then sonicated and kept at 4°C for the duration of the elutriation. A Beckman elutriation rotor JE 5.0 was chilled to 4°C and equilibrated with YEP at 4000 rpm. Cells were then loaded at a pump speed of around 20 ml/min and allowed to equilibrate for 15-20 minutes. Pump speed was then increased until small unbudded cells exited the elutriation chamber. Cells were then concentrated and resuspended in YEP supplemented with glucose at 30°C.

α-factor synchronization

Cells were grown overnight and diluted to an OD_{600} of 0.2. Alpha factor was first added to a final concentration of 0.5 ug/ml. After one hour and thirty minutes, 2.5 ug/ml of α-factor was readded to all cultures to prevent escape from the arrest. Cells were released by washing by filtration using ten times the volume of culture.

Microscopy

Fixed cells were briefly sonicated and five microliters spotted on a slide. Cells were imaged using a Zeiss Axioplan 2 microscope equipped with Hamamatsu ORCA-ER C4742-80 digital CCD camera and processed with Openlab (Improvision) software.

Other techniques

For synchronization at stationary phase cells were grown overnight until no buds were seen. Cells were then diluted to an OD_{600} of 0.2 and grown at 30°C. FACS was performed as described previously (Torres et al. 2007).

Figure 1

A

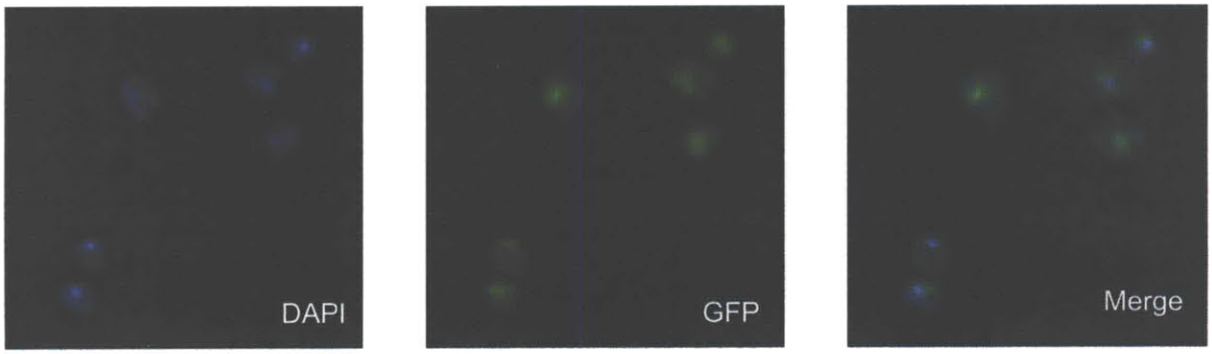

Wild type, arrested

B

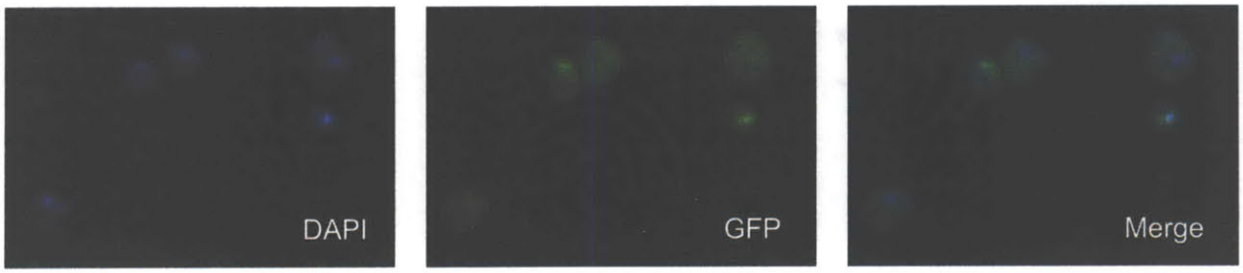

Wild type, cycling

C

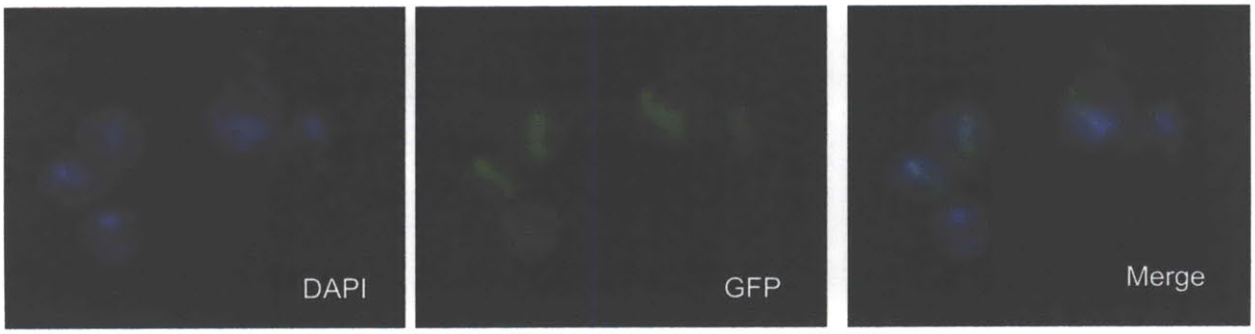

Disome XV, arrested

Figure 1. The localization of Whi5 changes with cell cycle stage.
(A) Whi5 localizes to the nucleus in wild type cells arrested with α-factor. (B) In wild type cycling cells, Whi5 localized to the nucleus only in cells at the G1 stage of the cell cycle while it is cytoplasmic at all other stages. (C) Whi5 localizes to the nucleus in disome XV cells arrested with α-factor.

Figure 2

A

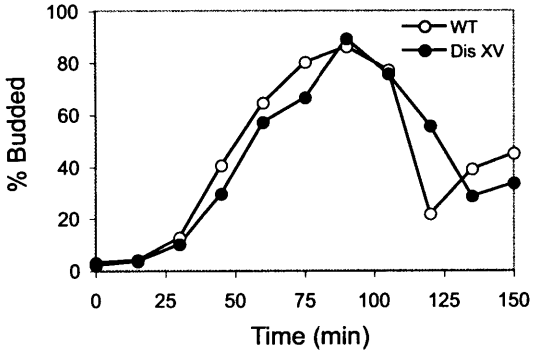
% Budded
Time (min)
WT
Dis XV

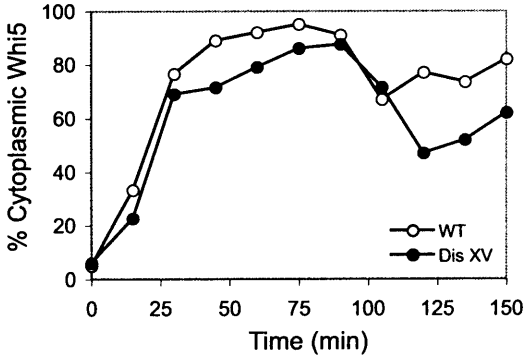
% Cytoplasmic Whi5
Time (min)
WT
Dis XV

B

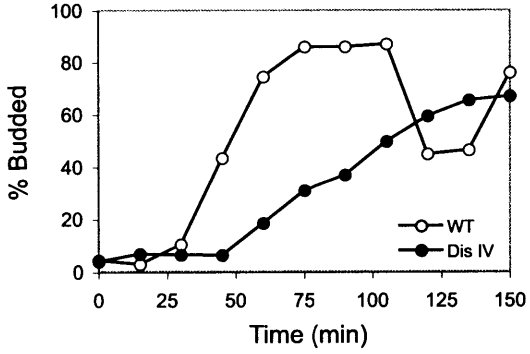
% Budded
Time (min)
WT
Dis IV

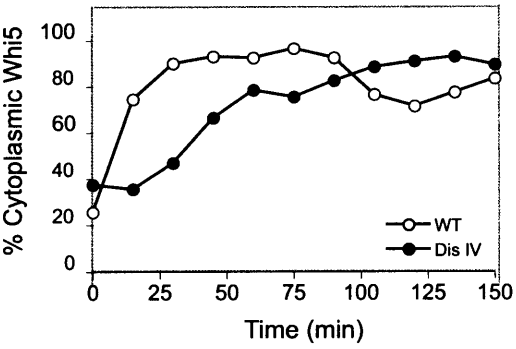
% Cytoplasmic Whi5
Time (min)
WT
Dis IV

C

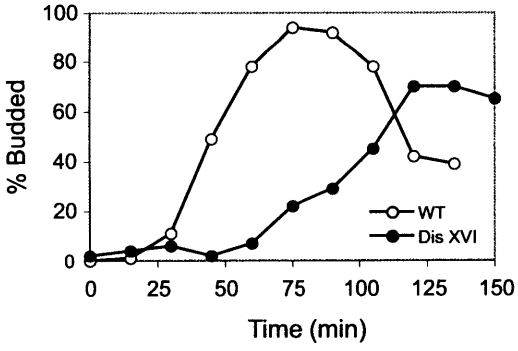
% Budded
Time (min)
WT
Dis XVI

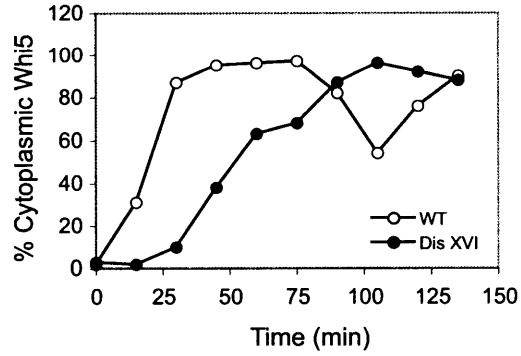
% Cytoplasmic Whi5
Time (min)
WT
Dis XVI

Figure 2. Whi5 nuclear exit is delayed in aneuploid cells released from mating factor block.

(A-C) Wild type ([A-C], A11311, open symbols), disome XV ([A], A12695, closed symbols), disome IV ([B], A12687, closed symbols), disome XVI ([C], A12700, closed symbols). Cells were grown to an OD_{600} of 0.2 at 25°C. 5 ug/ml α-factor was added and 2.5 ug/ml readded an hour and a half later. Cells were then washed by filtration with 10X the culture volume. Time points were taken every 15 minutes. Budding and localization of Whi5 was assessed as a function of time.

Figure 3

A

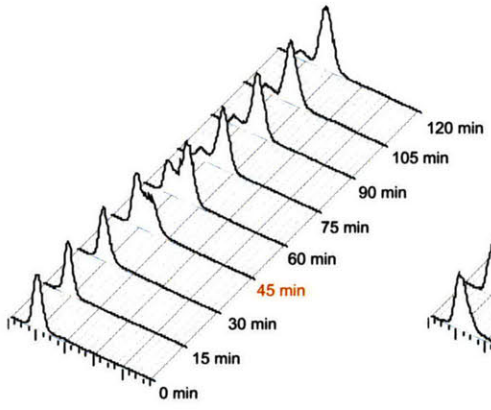

wild type

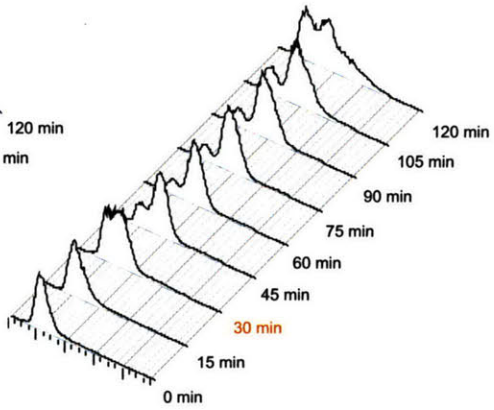

wild type, *GAL-CLN3*

B

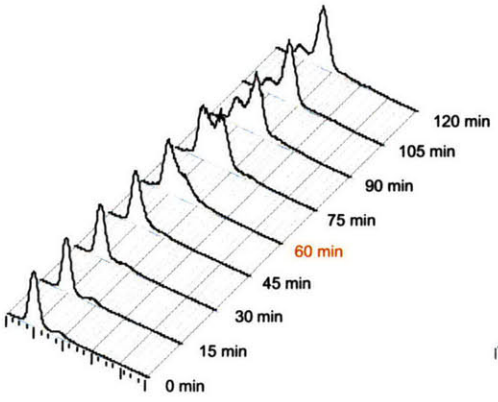

disome XVI

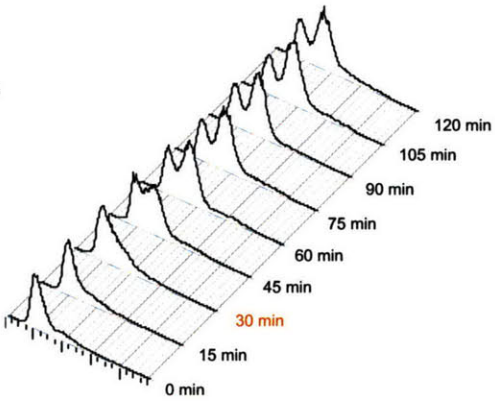

disome XVI, *GAL-CLN3*

Figure 3. Overexpression of *CLN3* accelerates cell cycle entry in both wild type and disome XVI cells.
(A) Wild type cells. (B) Disome XVI. Cells were arrested in YEP media supplemented with 2% raffinose with α-factor as described previously. 2% galactose was added one hour prior to release. Time points for FACS were taken every 15 minutes.

Figure 4

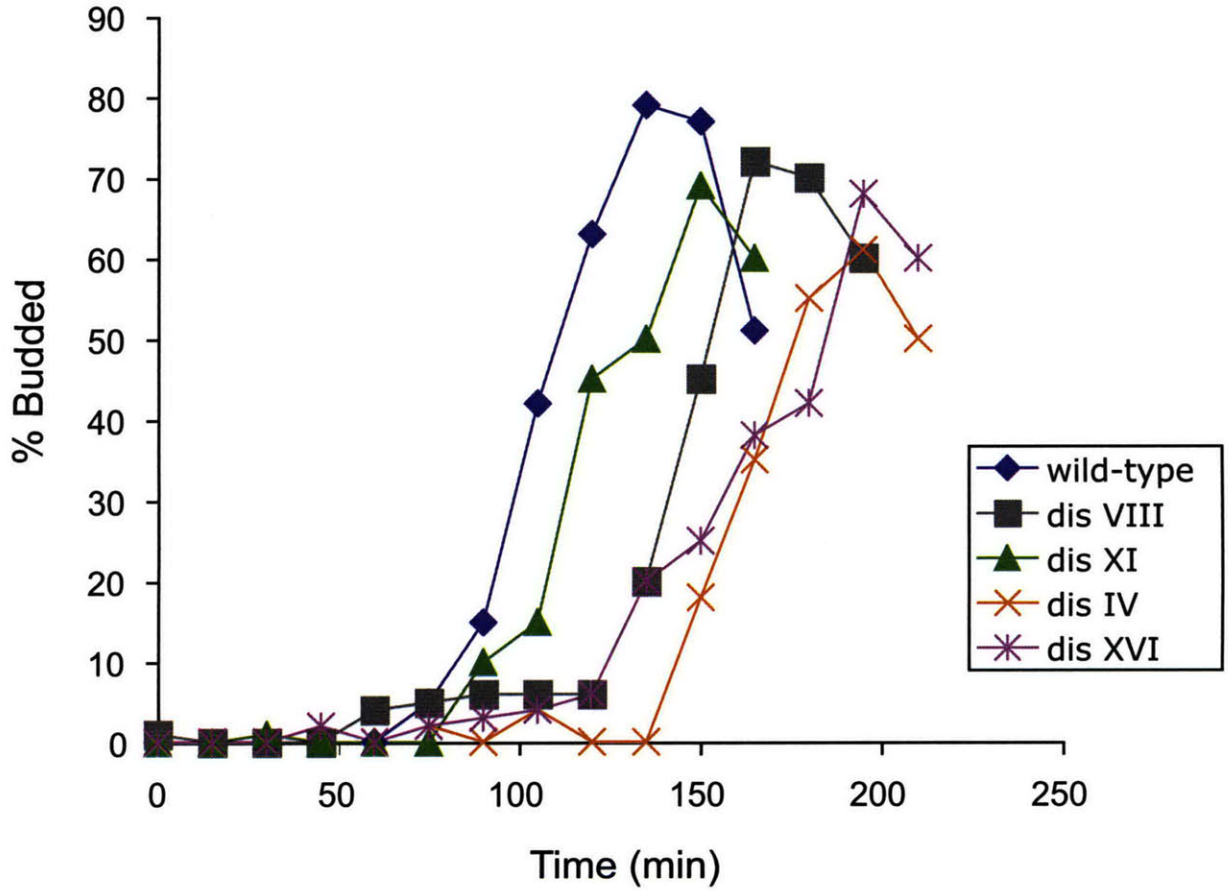
90
80
70
60
50
40
30
20
10
0
% Budded
0
50
100
150
200
250
Time (min)
wild-type
dis VIII
dis XI
dis IV
dis XVI

Figure 4. Aneuploid cells delay escape from α-factor arrest.
Cells were arrested with 5 ug/ml α-factor. 2.5 ug/ml were readded 90 minutes later. Cells were then grown at 25°C and samples taken every 15 minutes. Wild type is in blue, disome VIII in black, disome XI in green, disome IV in orange and disome XVI in purple.

Figure 5

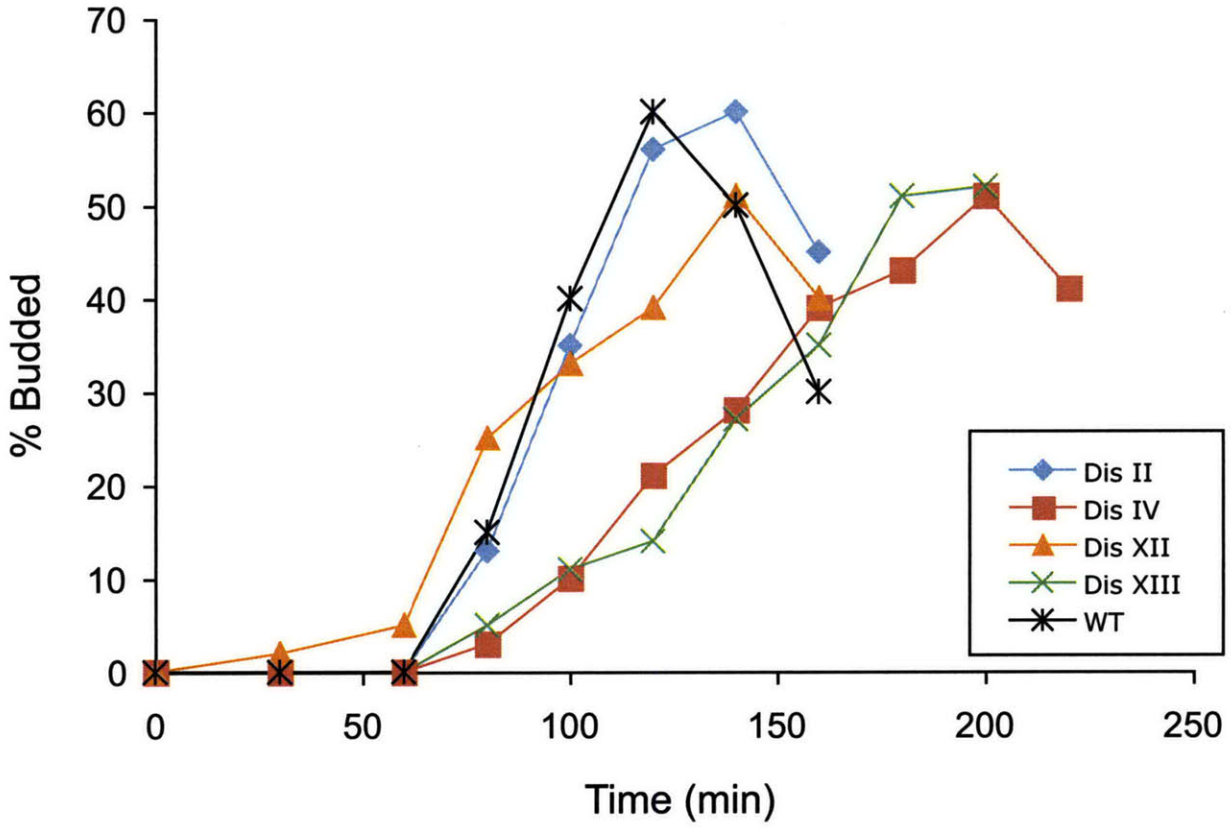
70
60
50
40
30
20
10
0
% Budded
0
50
100
150
200
250
Time (min)
Dis II
Dis IV
Dis XII
Dis XIII
WT

Figure 5. Aneuploid cells delay cell cycle reentry when arrested at G0.
Cells were grown in YEP supplemented with 2% glucose to saturation overnight. Cells were then diluted to OD_{600} of 0.1 and allowed to reenter the cell cycle. Times points were taken and the budding index determined.

Table 1: Strains used in this study

Strain	Disomic for Chromosome	
A6865	II	*MATa, lys2::HIS3, lys2::KanMX6*
A12687	IV	*MATa, trp1::HIS3, trp1::KanMX6*
A13628	VIII	*MATa, intergenic region (119778-119573) between YHR006W and YHR007C::HIS3, intergenic region (119778- 119573) between YHR006W and YHR007C::KanMX6*
A13771	XI	*MATa, intergenic region (430900-431000) between YKL006C-A and YKL006W::HIS3, intergenic region (430900-431000) between YKL006C-A and YKL006W::KanMX6*
A12693	XII	*MATa, ade16::HIS3, ade16::KanMX6*
A12695	XIII	*MATa, ura5::HIS3, ura5::KanMX6*
A12700	XVI	*MATa, met12::HIS3, met12::KanMX6*
A25879	IV	*MATa, trp1::HIS3, trp1::KanMX6, WHI5-GFP::URA3*
A25878	XV	*MATa, leu9::HIS3, leu9::KanMX6, WHI5-GFP::URA3*
A25880	XVI	*MATa, met12::HIS3, met12::KanMX6, WHI5-GFP::URA3*
A25883	XVI	*MATa, met12::HIS3, met12::KanMX6, GAL-CLN3::URA3*
A11311	wild type control	*MATa, ade1::HIS3, lys2::KAN*
A25882	GAL-CLN3, wt	*MATa, ade1::HIS3, lys2::KAN, GAL-CLN3::URA3*
A25877	WHI5-GFP	*MATa, ade1::HIS3, lys2::KAN, WHI5-GFP::URA3*

References:

Chang F, Herskowitz I. 1990. Identification of a gene necessary for cell cycle arrest by a negative growth factor of yeast: FAR1 is an inhibitor of a G1 cyclin, CLN2. Cell. 63(5):999-1011.

Chang F, Herskowitz I. 1992 Phosphorylation of FAR1 in response to alpha-factor: a possible requirement for cell-cycle arrest. Mol Biol Cell. 3(4):445-50

Dohlman HG, Slessareva JE. 2006. Pheromone signaling pathways in yeast. Sci STKE. 2006(364):cm6.

Elion EA, Satterberg B, Kranz JE. 1993. FUS3 phosphorylates multiple components of the mating signal transduction cascade: evidence for STE12 and FAR1. Mol Biol Cell. 4(5):495-510.

Gutherie C, Fink GR. 1991 Guide to yeast genetics and molecular biology. Academic Press, San Diego.

Torres EM, Sokolsky T, Tucker CM, Chan LY, Boselli M, Dunham MJ, Amon A. 2007.Effects of aneuploidy on cellular physiology and cell division in haploid yeast. Science. 317:916-24.